KTH ROYAL INSTITUTE
OF TECHNOLOGY

Doctoral Thesis in Biotechnology

The application of microfluidic devices and multifunctional fibers in cancer diagnostics

THARAGAN KUMAR

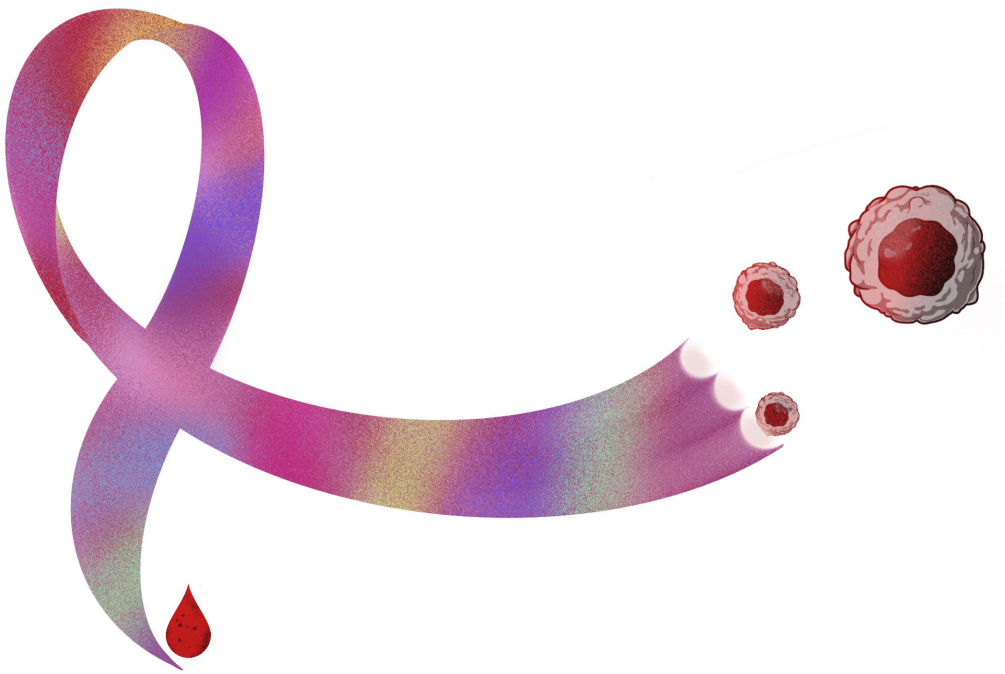

Stockholm, Sweden 2022

The application of microfluidic devices and multifunctional fibers in cancer diagnostics

THARAGAN KUMAR

Academic Dissertation which, with due permission of the KTH Royal Institute of Technology, is submitted for public defence for the Degree of Doctor of Philosophy on Friday the 1st April 2022, at 10:00 a.m. in David at Widerströmska huset, Tomtebodavägen 18a, Solna.

Doctoral Thesis in Biotechnology
KTH Royal Institute of Technology
Stockholm, Sweden 2022

ISBN 978-91-8040-141-8
TRITA-CBH-FOU-2022:14

Printed by: Universitetsservice US-AB, Sweden 2022

Public defense of dissertation

Academic dissertation which, with due permission from KTH Royal Institute of Technology, is submitted for public defense for the degree of Doctor of Philosophy on 1st of April 2022 at 10:00 a.m. in the room 'David' at Widerströmska huset, Tomtebodavägen 18a, Solna.

Respondent:
Tharagan Kumar
KTH- Royal Institute of Technology

Faculty Opponent:
Assoc. Prof. Johan Kreuger
Uppsala University

Evaluation Committee:
Prof. Nicole Pamme
Stockholm University

Prof. Masood Kamali- Moghaddam
Uppsala University

Assoc. Prof. Linda Sofie Lindström
Karolinska Institutet

Chairman:
Prof. Jochen Schwenk
KTH- Royal Institute of Technology

Main Supervisor:
Prof. Aman Russom
KTH- Royal Institute of Technology

Co-Supervisors:
Prof. Fredrik Laurell
KTH- Royal Institute of Technology

Dr. Gustaf Mårtensson
KTH- Royal Institute of Technology

Mentor:
Prof. Matthias Löhr
KI- Karolinska Institute

I dedicate this work to my uncle
Mr. Kanapathy Maruthamuthu

எந்நன்றி கொன்றார்க்கும் உய்வுண்டாம் உய்வில்லை
செய்ந்நன்றி கொன்ற மகற்கு.

திருவள்ளுவர்
Thiruvalluvar

Explanation: He who has killed every virtue may yet escape; there is no escape for him who has killed a benefit.

Abstract

Efficient separation and detection of rare cells in a mixed population is important in many biomedical applications. For instance, isolating and detecting circulating tumor cells (CTCs) from whole blood samples could allow for early cancer diagnosis and prognosis during treatment. CTCs are rare cells circulating in blood detached from the primary tumor site, carrying important information such as the origin of cancer and metastatic information. The detection of CTC from blood samples, besides being a minimally invasive procedure, could be vital in case of difficulty to access the tumor site via traditional biopsies, such as colon and pancreatic cancer.
Microfluidics is a research field with great promise towards the development of methods to isolate and separate cells for clinical applications. Microfluidic based cell separation has been demonstrated using biological approaches using cell surface markers, and biophysical approaches using cell size, shape, and deformability. This thesis will focus on developing passive strategy using inertial microfluidics (biophysical, paper 1-4) and affinity biomarker (biochemical, paper 5) based strategy to isolate and analyze CTCs. Inertial microfluidics relies on inherent hydrodynamic forces, inertial forces, in flow through the microfluidic channel. Depending on the geometry of the channel, inertial forces drive the particles and cells to a specific streamline position, allowing for focusing and separation. In contrast, affinity-based isolation relies on biomarkers expressed on the surface of the targeted cells, which is highly specific. In paper 1, using the elasto inertial microfluidic technique, high throughput particle focusing and separation was achieved in a curved rectangular channel with a separation efficiency of 89% for 10 μm and 99% for the 15 μm particles at a high volumetric flow rate (1 mL/min). In paper 2, a detailed analysis of particle focusing was studied experimentally and numerically in a circular cross-section. Using the FENE-P model simulating non-Newtonian fluid and an immersed boundary method to account for the particles, it was observed that a combination of inertia and elasticity leads to several intermediate focusing positions. In paper 3, we developed a portable microflow cytometer using fiberoptics capillaries. By combining elasto inertial microfluidics and optical fibers, we focused particles and cells and demonstrated particle counting at a throughput of 2500 particles/second. In paper 4, we built an all-fiber separation and detection component and demonstrated a separation efficiency of 100% for the 10 μm and 97% for the 1 μm particles as a proof of principle. In addition, the separated 10 μm particles could be

quantified in the all-fiber component. In paper 5, an affinity-based separation approach was carried out to utilize the surface markers to capture and release viable CTCs for downstream analysis. A novel layer-by-layer nanofilm coating strategy was developed using cellulose nanofibril (CNF) built into multiple layers and functionalized with antibodies to capture the cells. After capture, the CNF were enzymatically degraded to release the CTCs. HCT116 colon cancer cells were captured with an efficiency of more than 97%, and when spiked in whole blood, an approximately 200 fold average enrichment was achieved compared to white blood cells. 80% of the cancer cells spiked in whole blood were recovered with 97% viability in less than 30 minutes.

In summary, this thesis presents different microfluidics-based separation of cancer cells based on biophysical and biochemical properties. Using elasto inertial microfluidics, we developed several approaches to separate and detect cells and particles. Using layer-by-layer coating of CNF, we successfully demonstrated capture and release of cancer cells with maintained high viability. While the thesis has focused on different properties of cells for separation and analysis, combining these methods will be important for efficient isolation and characterization of CTCs for improved diagnostics.

Keywords: Circulating tumor cells, microfluidics, point of care, inertial microfluidics, elasto inertial microfluidics, nano-cellulose, layer-by-layer, optical fiber, microflow cytometer.

Populärvetenskaplig sammanfatning

Separationen och detektionen av specifika celler i en blandad population av celler är viktig i många biomedicinska tillämpningar. Som exempel, möjligheten att isolera och detektera cirkulerande tumörceller (CTC) från helblod skulle kunna tillåta tidig cancer diagnos och prognos under behandling. CTC är sällsynta celler som cirkulerar i blodet och bär med sig viktig information, som den specifika cancerns ursprung och metastatiska information. Att kunna detektera CTC med hjälp av blodprover, förutom att erbjuda en minimalt invasiv metod, skulle kunna vara viktig i fall där tumörområdet är svårtillgänglig för traditionell provtagning via biopsier, såsom kolon- och bukspottkörtel-cancer.

Mikrofluidik är ett forskningsfält med betydande potential att möjliggöra utvecklingen av metoder för att isolera och separera celler för kliniska tillämpningar. Separation av celler baserad på mikrofluidik har demonstrerats med olika angreppssätt så som biologiska med hjälp av affinitetsmarkörer, och biofysiska metoder där man utnyttjar storlek, form, och deformerbarhet för att separera celler. Denna avhandling fokuserar på att utveckla en passiv strategi som utnyttjar tröghets-baserade mikrofluidik som domineras av tröghetskrafter (papper 1-4) och strategier med affinitetsbiomarkörer (paper 5) med målet att isolera och analysera CTC. Tröghetsfokusering i mikroflöden baseras på hydrodynamiska krafter, tröghetskrafter, som utvecklas i vätskeflöden i mikrokanaler. Beroende på mikrokanalens geometriska utformning och vätskans flödes hastighet kommer tröghetskrafterna att driva partiklar eller celler till specifika positioner i strömningsfältet och i sin tur möjliggöra fokusering och separation. Å andra sidan, affinitetsbaserad isolering är beroende på biomarkörer som uttrycks på ytan av specifika celler och är därmed mycket specifik. I papper 1 utnyttjas mikrofluidisk metod med tröghetskrafter med elastiska bidrag för att möjliggöra partikel fokusering och separation vid höga volymsflöden. I papper 2, en detaljerad analys av partikelfokusering i en circulärt tvärsnitt genomfördes experimentellt och numeriskt. I papper 3, en portabel mikroflödescytometer utvecklades med hjälp av fiberoptiska kapillärer. Med hjälp av mikrofluidik som utnyttjar elastiska och tröghetskrafter tillsammans med optiska fibrer, fokuserades partiklar och celler och demonstrerade möjligheten att räkna partiklar och celler. I papper 4 beskrivs en fiber-baserad komponent för separation och detektion som demonstrerade en

separationseffektivitet av 100% för 10 μm-partiklar och 97% för 1 μm-partiklar som ett bevis på principen. I papper 5, en affinitetsbaserad separationsmetod utvecklades för att utnyttja ytmarkörer som finns på cirkulerande tumörceller. En beläggningsstrategi med hjälp av nanocellulosa utvecklades för att först fånga in och och sedan frigöra levande CTC för vidare analys. Den nya nanocellulosa-baserade ytbeläggningen fångar och frigör celler med hjälp av en enzym för analys nedströms. Sammanfattningsvis, denna avhandling presenterar mikrofluidik-baserad separation av cancerceller som utnyttjar biofysiska och biokemiska egenskaper. Med hjälp av tröghetsfokusering i mikrofluidik utvecklades flera metoder för att separera och detektera celler och partiklar. Dessutom utvecklades en original metod som bygger på att ytbehandla chip med nanocellulosa för infångning och frigörande av CTCs. I avhandlingen har vi undersökt olika metoder för isolering and analys av cancer celler. Medan varje metod har sin fördel och svaga punkter, kommer det att vara viktigt att kombinera dessa metoder och andra för att bidra till bätter cancer diagnostik i framtiden.

Preface

The work presented in this thesis concern the development of microfluidics based methods to isolate cells from peripheral blood for cancer diagnostics. The thesis is presented in five chapters according to the following description.

Chapter 1 talks about how cancer originates, the process of metastases, the role of circulating tumor cells, existing diagnostic tools to detect cancer, a new generation of liquid biopsy-based diagnosis, and state-of-the-art technologies in detecting circulating tumor cells. Chapter 2 gives a detailed insight into microfluidic techniques used in cancer diagnostics and different separation methods that rely on either biophysical or biochemical properties of a cell. Chapter 3 briefly discusses the biomaterials used in the field of microfluidics to do surface enhancements for the capturing and release of circulating tumor cells. Chapter 4 summarizes all the techniques used in this thesis to target circulating tumor cell isolation. Finally, chapter 5 specifies the conclusion and prospects of the technologies used in this thesis.

Stockholm, March 2022
Tharagan Kumar

List of appended papers

Paper 1

High throughput viscoelastic particle focusing and separation in spiral microchannels. *SciRep* 11, 8467, doi:10.1038/s41598-021-88047-4 (2021)

Tharagan Kumar*, Harisha Ramachandraiah*, Sharath Narayana Iyengar, Indradumna Banerjee, Gustaf Mårtensson & Aman Russom

Paper 2

Analogue tuning of particle focusing in elasto-inertial flow. *Meccanica* 56, 1739-1749, doi:10.1007/s11012-021-01329-z (2021).

Banerjee, I., Rosti, M. E., **Kumar, T**., Brandt, L. & Russom, A.

Paper 3

High performance micro-flow cytometer based on optical fibres. *Scientific Reports* 7, doi:10.1038/s41598-017-05843-7 (2017).

S. Etcheverry, A. Faridi, H. Ramachandraiah, **T. Kumar**, W. Margulis, F. Laurell & A. Russom

Paper 4

Lab-in-a-fiber based particle separation and counting. *bioRxiv*, 2021.2004.2013.439593, doi:10.1101/2021.04.13.439593 (2021). Manuscrpit-Submitted

T. Kumar; A.V. Harish; S. Etcheverry; W. Margulis; F. Laurell; A. Russom

Paper 5

Multi-layer assembly of cellulose nanofibrils in a microfluidic device for the selective capture and release of viable tumor cells from whole blood. *Nanoscale* **12**, 21788-21797, doi:10.1039/d0nr05375a (2020).

Tharagan Kumar*, Ruben R. G. Soares*, Leyla Ali Dholey, Harisha Ramachandraiah, Negar Abbasi Aval, Zenib Aljadi, Torbjörn Pettersson and Aman Russom.

Paper not included in this thesis

High resolution and rapid separation of bacteria from blood using elasto-inertial microfluidics. Electrophoresis 2021**,** 00, 1-14. DOI: 10.1002/elps.202100140.

S.N Iyengar, **T. Kumar**, G. Mårtensson, A. Russom.

Respondent's contribution to appended papers

Paper 1

Major part in experiment, data analysis and manuscript writing.

Paper 2

Major part in experiment, minor contribution in data analysis.

Paper 3

Major part in experiment, minor part in data analysis and manuscript writing.

Paper 4

Major part in experiment, data analysis and manuscript writing.

Paper 5

Major part in experiment, data analysis and manuscript writing.

Table of Contents

Chapter 1: Introduction

1.1 Beginning of a life

Life begins with a single cell. The cell is the basic building block of all living organisms. Breathing, digesting, energy generation, and reproduction are just a few of its many duties performed with the help of organs. Organs, bones, and skin are formed due to cell division, called the cell cycle. DNA damage repair, tissue hyperplasia in response to injury, and diseases like cancer are all impacted by the cell cycle, which is an all-pervasive and intricate process[1]. The eukaryotic cell cycle contains four phases: G1, S, G2, and M. (Figure 1). During G1 a cell's DNA replication process begins. At this point in the cell cycle, the cell chooses whether or not to continue, stop, or terminate the cycle. The G1 phase of mammalian cells has a crucial checkpoint. Replication of DNA and the conclusion of a cell cycle are both signified by the term "restriction point" in mammalian cells. DNA synthesis occurs during the S phase of mitosis. Cells begin preparing for division during G2. The chromosomes are copied and then divided into discrete nuclei by cytokinesis to produce two daughter cells during the mitotic phase. In addition to G1, S, G2, and M, the term G0 is used to identify cells that have finished the cell cycle and are now quiescent[2-7].

One or more of the three billion nucleotide bases or the phosphodiester backbone to which they are linked are continually under assault in every mammalian cell's DNA (Figure 2). An organism is exposed to external sources of ionizing radiation in the environment where free oxygen radicals, for example, are produced due to regular cell metabolism. DNA and base damage both maybe induced by them. When it comes to DNA repair, life on Earth has developed a remarkable ability to cope with internal and external threats[8]. Cells have created several elegant but flawed DNA-repair methods to cope with the attack on their DNA. This is partly due to the wide variety of DNA damages that may be repaired[9,10].

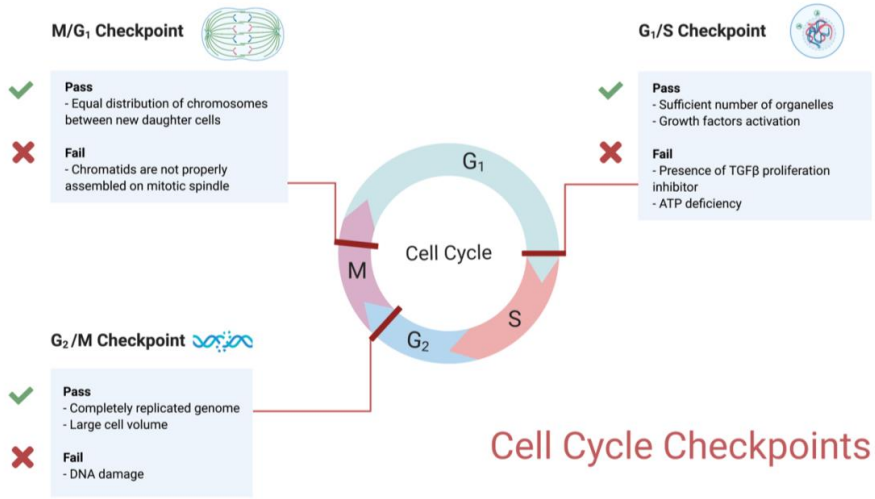

Figure 1: Checkpoints in the cell cycle. The cell is tested during the second growth phase (G2) to see whether it is large enough for the synthesis phase and has produced sufficient proteins. S/G2 phase (DNA synthesis) occurs throughout the synthesis process (S). Cell cycle verifies whether DNA has been appropriately replicated before being cloned. If this is the case, mitosis will succeed (M). The cell cycle's mitotic phase occurs during the M phase. Checks to see whether mitosis has been completed. If this happens, the cell divides, and the cycle is restarted. Created with BioRender.com

In addition to actively repairing DNA breaks or adducts, cells react to DNA damage by stopping cell-cycle advancement or suffering programmed cell death. Even though we are just beginning to understand how cell-cycle arrest or death and DNA repair are coordinated, this coordination is essential to the cell's or organism's outcome.[11,12] In addition to DNA damage, other stressors, such as intermittent or prolonged exposure to low levels of oxygen or nutrients, must be addressed. Although cells employ different parts of their signaling pathways to deal with these kinds of alterations in their microenvironment, the measures taken by cells to deal with DNA damage are similar[13-15]. People's risk of developing cancer is influenced by their level of exposure to certain chemicals and their cells' response to DNA damage, among other things.

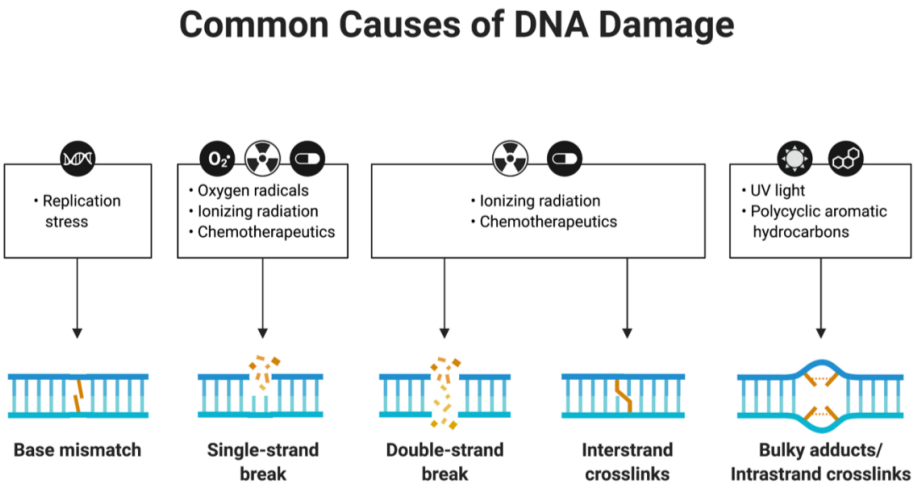

Figure 2: Eukaryotic DNA damage may be caused by a wide range of factors, and it can be repaired in many ways. DNA lesions may take on a variety of shapes and sizes depending on the substances used to damage the molecule. Genome repair processes include mismatch repair, base-excision repair, homologous recombination repair, non-homologous end-joining, nucleotide excision repair, and direct damage reversal. Created with BioRender.com

1.2 Cancer and Metastases

GLOBOCAN 2020 predicted (figure 3) that in 2020, 19.3 million new cases of cancer will be diagnosed, and about 10 million people will die as a result of cancer. The illness is a significant source of death and morbidity around the globe, affecting people of all socioeconomic levels. In high-income nations in Europe and North America, men and women will have about identical cancer-related mortality rates in 2020. It is thus vital for global cancer control efforts to develop a sustainable infrastructure for the spread of proven cancer prevention strategies and the provision of cancer care in transitional nations. The global cancer burden is expected to rise by 47% from 2020 to 28.4 million cases in 2040, with a more considerable increase in transitioning countries (64% to 95%) than transitioned countries (32% to 56%) due to demographic changes[16].

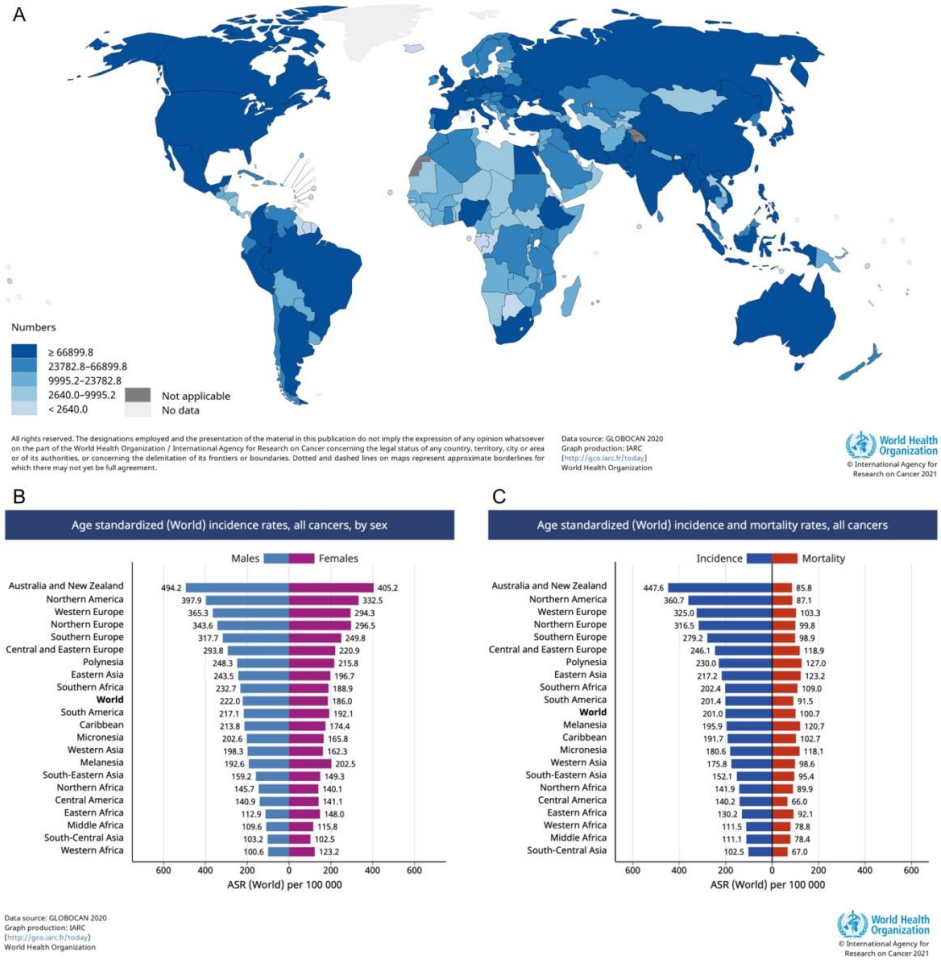

Figure 3: A) Predicted new cancer cases in 2020 to be the same for men and women of all ages and every form of cancer. B) Age-standardized incidence rates, regardless of cancer type or sex, based on the age at which the disease is diagnosed. C) Regardless of cancer, age-standardized incidence and death rates are grouped.

Cancer is a disease that includes different side effects. Cancer can develop in every tissue in the body, and some tissues may do so in several ways. Malignant tumors have distinct traits, as well. Nevertheless, the underlying processes that lead to these different malignancies seem to be identical[12,17]. An initial precancerous lesion may become a malignant tumor via a multi-stage process that converts normal cells into tumors. External stimuli interact with a person's hereditary factors to cause these changes (Figure 4). For example, UV and ionizing radiation are physical carcinogens, while asbestos, tobacco smoke components, aflatoxin, and arsenic are chemical carcinogens. Biological carcinogens include infections from viruses, bacteria, or parasites[18].

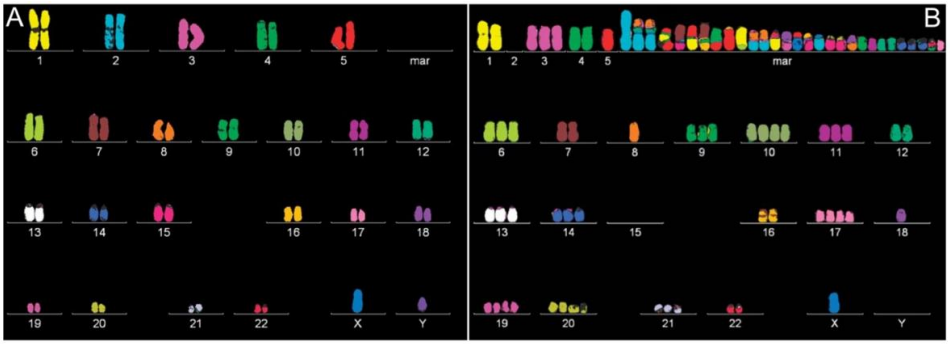

Figure 4: Comparison between a normal cell and cancer cell chromosomes. A) Karyotype of a normal cell from a male. B) Breast cancer cell line MDA 231. Marker (mar) chromosomes are architecturally aberrant, and they are either inter- or intra-chromosomally altered to generate diverse hybrid chromosomes. Copyright © 2005 Hindawi Publishing Corporation and the authors[19].

The 30 trillion cells that make up an average human body live in a complex, interdependent ecosystem where they regulate one another's development. Normal cells only divide when instructed by other cells in the vicinity. Each tissue's size and architecture are tailored to the body's needs because of this ongoing partnership. On the other hand, cancer cells reject this system by becoming mute to the usual limitations on proliferation and instead pursuing their reproduction plans[20,21]. They may also spread to other places of the body from where they originated, infecting the tissues around them and forming masses. There is a gradual increase in the aggressiveness of tumors generated by these malignant cells over time, which finally leads to the patient death[22-24].

It's not uncommon for healthy cells to undergo a sequence of changes known as hallmarks (Figure 5) before becoming cancerous. To facilitate tumor formation and malignancy, cancer cells may adopt certain features. Several problems exist in the systems that control how frequently cancer cells divide and the feedback networks that regulate them. However, normal cells are subject to several limitations in their development. For them to grow, they need growth factors. A molecular brake stops them from separating if damaged until they are restored. If they can't be saved, they'll die due to programmed cell death called apoptosis[25-27]. They can only divide a set number of times until they are done. They are a part of the tissue structure and don't move. They need blood to grow. All of these mechanisms must be beaten to transform a cell into cancer. A different set of proteins controls each route. A crucial protein must obstruct each of these routes. Somatic mutations that alter the DNA sequence of these proteins result in their inability to function correctly. Hanahan and Weinberg's characteristics describe this progression[28].

It used to be that cancer's hallmarks consisted of six biological capabilities, but they have now been enlarged to include eight biological capabilities and two additional supporting capabilities (Figure 5). The Hallmarks of Cancer[28], written by Douglas Hanahan and Robert Weinberg, introduced the idea. These qualities serve as a unifying framework for comprehending the complexities of cancer. Replicative immortality and angiogenesis are two of the most critical aspects of cancer's ability to proliferate and spread. Genome instability, which promotes genetic variety, and inflammation, which supports numerous hallmark activities, are the foundation of these hallmarks' acquisition speed[29-31].

A significant factor in cancer's fatality is metastasis or the spread of the disease throughout the body. Surgery is no longer an option when cancer has gone beyond the tumor's original site and formed metastases in other organs. Because of this, the hallmarks of cancer include metastasis and malignant cells entering normal tissue[32,33]. The cells that make up these so-called benign tumors proliferate, but they do not infiltrate or spread, unlike malignant cancer cells. As a result, the ability of cancer cells to spread to new tissues is a crucial phase in their development. To properly metastasize, cancer cells must leave their original site, enter the blood or lymphatic vessels, travel through the circulatory system, and establish a new cellular colony in a new location[34-36].

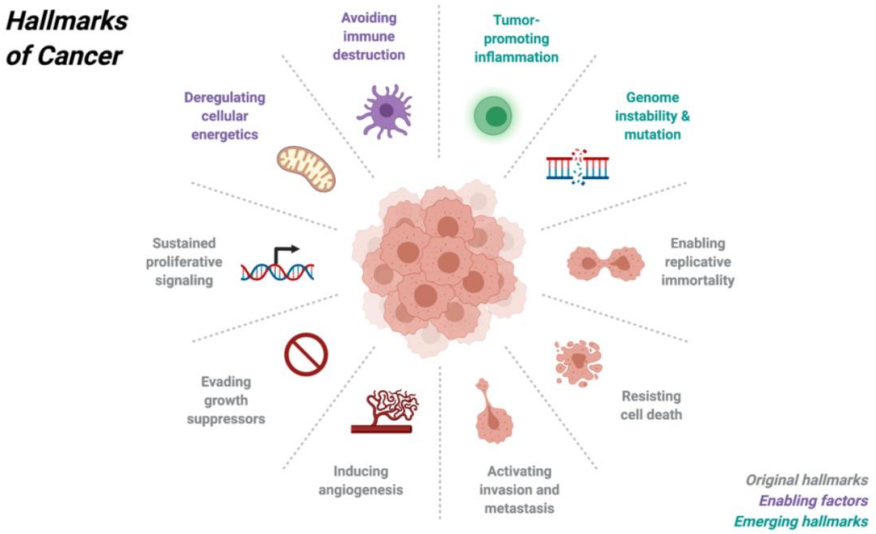

Figure 5: Tumor cell secretory activities impact the characteristics of cancer. The graphic by Hanahan and Weinberg shows how the secretory pathway is linked to many cancer hallmarks. Created with BioRender.com

When cancer cells expand throughout the body, they rely on processes of invasion and metastasis to do it. Breaking through the basement membrane, which separates cancer cells from the rest of the body, is the first step in the process. Some of these invading cells can penetrate the basement membrane and the endothelial cells that line blood vessels. After that, the cells are free to move throughout the circulation as they like (Figure 6). A cancerous cell may one day find its way into a blood vessel. If it adheres to and penetrates the capillary wall again, it might develop into a secondary tumor[37,38]. One out of every ten thousand cancer cells will spread from the primary tumor to an adjacent organ. For cell migration to proceed smoothly, adhesion between cells is essential. More than half of all human cells contain cell-cell adhesion and extracellular matrix adhesion. Without adhering to neighboring cells, a cell may spread across the matrix and become more invasive[39,40]. If a cell does not attach to the extracellular matrix, it may separate from its original tissue. It is

possible for a cell to underdo apoptosis if it does not link to the extracellular matrix or adheres to the wrong kind of matrix (cellular suicide). On the other hand, cancer cells may remain even if they are not adherent to the body[41,42].

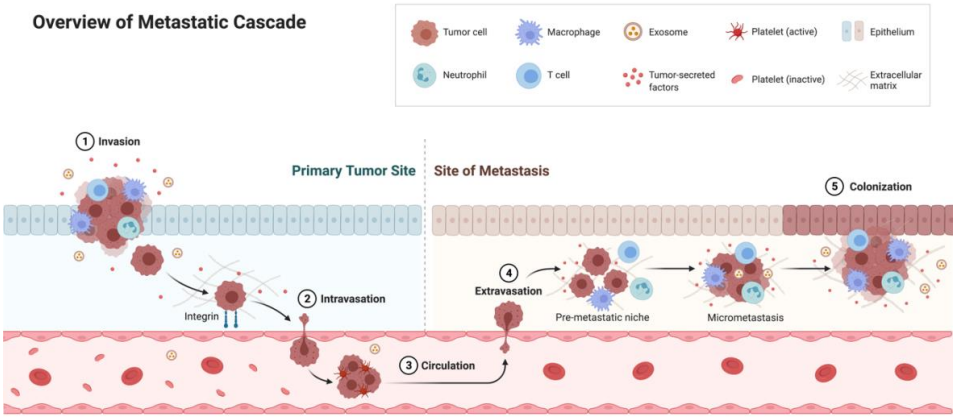

Figure 6: In a nutshell, the five critical processes in metastasis are invasion, intravasation, circulation, extravasation, and colonization. Created with BioRender.com

An essential aspect of a person's circulatory system may help explain how they get cancer. Tumors in the skin and many other tissues often spread to the lungs first because the lungs contain the first capillary bed "downstream" of most organs. Colorectal cancers typically spread to the liver since the intestines first send blood. In addition, prostate cancer commonly spreads to the bones, making circulation a secondary problem. Prostate cancer cells have receptors comparable to bone tissue, which may explain this tendency[43-45].

If cancer cells reach circulation, new tumors are not an inevitable conclusion. Circulating cells face several challenges. At this new location, it must first attach itself to the inside of an artery's wall before moving on to infiltrate and proliferate in the tissues below the basement membrane (Figure 6)[41,42]. Each of these problems put a higher burden on the tumor cell than it had to bear in its natural environment. Another obstacle to the spread of cancer is that it may not wholly defeat the defense mechanisms that keep our cells in the right places. Most cancer cells that enter the circulation do not survive long enough to develop new tumors elsewhere. The

reasons for this apparent brittleness in the circulation are unclear; it is possible that the anchorage independence of tumor cells is not flawless, and they sometimes die via apoptosis. However, scientists think the cells must swiftly stick to a small blood vessel's inner lining. Certain metastatic tumors prefer to spread to specific locations which attributes to differences in blood flow.

In many cases, the first capillary bed (or network of capillaries, the tiniest blood vessels) that circulating tumor cells (CTCs) encounter "downstream" of their origin confines them[46,47]. Only the intestines deliver blood to the liver first before it passes via the lungs and into the rest of the circulatory system. Consequently, the lungs and liver are the most common sites of metastasis[48].

1.3 Circulating tumor cells (CTCs)

One million WBCs and one billion RBCs are found in every milliliter of peripheral blood, making the number of circulating tumor cell(s) an insignificant proportion of that total. During cancer invasion, the goal is to gain control of the territory and ultimately destroy cells[46,49]. Figure 7 shows an example of how CTCs invade through blood vessels from one organ to the other. These mechanisms and the identification of CTCs and leukocytes in the blood have gained the attention of many people throughout the years. Knowing the importance of CTC in a cancer patient's long-term survival is thus crucial. Cell type enumeration and subsequent medication delivery are critical for cancer patient care, as are CTC collection and identification procedures[50-55].

CTCs, despite their low concentration such as 1-10 CTCs in 1 mL of whole blood, may provide diagnostic, prognostic, and therapeutic response monitoring information. As a result, CTCs are essential biomarkers in cancer patients' targeted molecular treatment and preclinical models for characterizing CTC features. The modest concentration of CTCs makes it challenging to isolate, count, and identify them in peripheral blood samples. CTCs may also be damaged during the separation technique due to the required purification phase for their characterisation[53,56].

There are two types of CTCs: single cells and clusters. While circulating clusters are more susceptible to metastasis, they are not that common. Invading cancer cells

coexist with stromal cells and immune system components in clusters, all of which contribute to the heterogeneity and longevity of the cluster. The ability of neutrophils to form clusters and limit the activation of leukocytes increases the survival of CTCs. CTCs engage with platelets to form a platelet coating barrier, which prevents immune cells from identifying cancer cells and provides the structural support needed to endure the physical rigors of circulation[54,57].

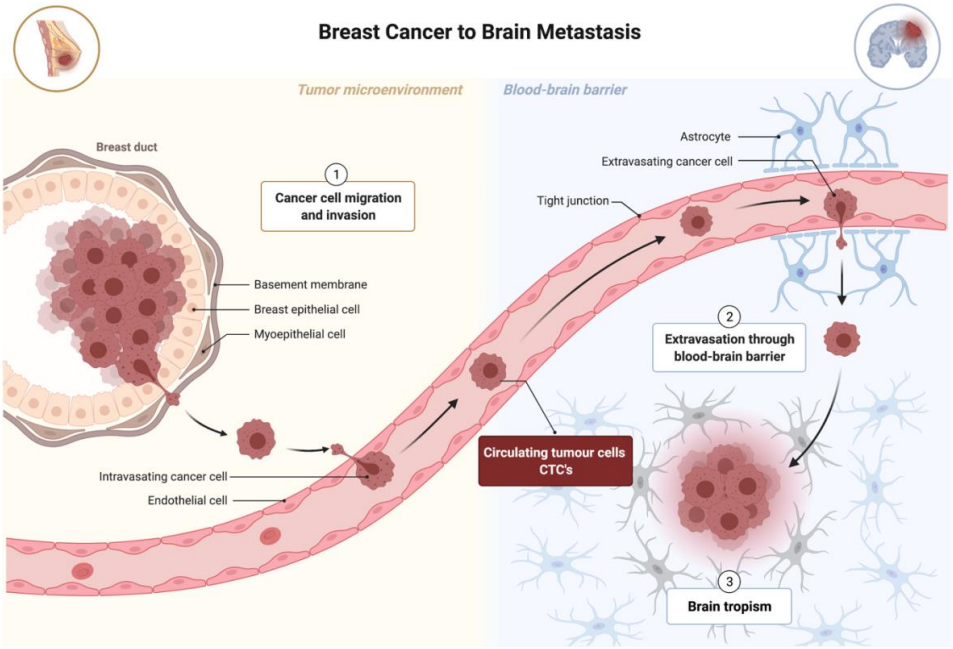

Figure 7: Cancer cell migration and invasion from primary tumor site (Breast) to a secondary site (Brain) via metastases process. Tumor cells that invade the blood vessel and circulate in the bloodstream can be seen in the figure shown as circulating tumor cells (CTCs). Created with BioRender.com

1.4 Conventional diagnostics tools to detect cancer

Imaging-based diagnostics:
Depending on cancer's location in the body, various imaging technologies may be used to detect it. It is possible to detect malignant changes in the throat or the esophagus using a barium swallow, commonly known as a barium enema test. X-rays are acquired when a barium solution is taken orally. Another usage for barium is for checking the colon and rectal area [58,59]. It is possible to apply radioactive dye intravenously before nuclear imaging is utilized to investigate the bone for malignant changes to identify cancer that has spread. Computed tomography (CT) scans are among the most frequently used imaging technologies for cancer diagnosis. It is possible to identify cancer and locate its specific location using CT scans, creating very detailed images. The DEXA scan (dual-energy X-ray absorptiometry) measures the bone mineral density to estimate the overall bone health and function[60,61]. By employing radiofrequency radiation to make images of the inside organs, magnetic resonance imaging (MRI) may be used to diagnose disease. For detecting malignant tissue, MRI is routinely used[62,63]. If the doctor suspects anything is wrong with the breast tissue, a mammogram might be done to find out [64,65]. Ultrasounds, which utilize high-frequency sound waves to produce images of the inside organs, commonly detect cancer. Using this technology, the doctor can see inside the body in real-time and monitor how various organs are funtioning[66,67]. X-rays are often employed to diagnose, stage, and treat multiple types of cancer. X-ray images are formed utilizing electromagnetic radiation with a high level of energy[68,69].

Invasive procedures based diagnostics:
Cancer may be detected with the following procedures, which analyze tissue or blood samples (Figure 8). To detect anomalies or collect a sample, an anoscopy is performed. The rectum and anus may be seen using an anoscope to help rule out cancer. The physician may remove a piece of tissue or fluid from the patient body to detect malignant cells. The only way to know whether you have cancer is to have a biopsy[70,71]. A thin instrument with a lit camera is entered via the nose or mouth to assess aberrant areas and collect a biopsy to assist in diagnosing lung or oesophageal cancer. One of the most popular ways to detect colon and rectal cancer is a colonoscopy[72]. In the course of the process, a colonoscopy, a thin, lighted tube will be put into the intestine to check for and remove any abnormal growths. As the name

suggests, a spinal tap involves taking a sample of cerebrospinal fluid from the patient to check for cancers of the brain, spine, or leukemia[73,74]. Cervical cancer screening tests like the Pap-smear enable the doctor to obtain a sample of cells from the cervix and examine them under a microscope in a lab[75].

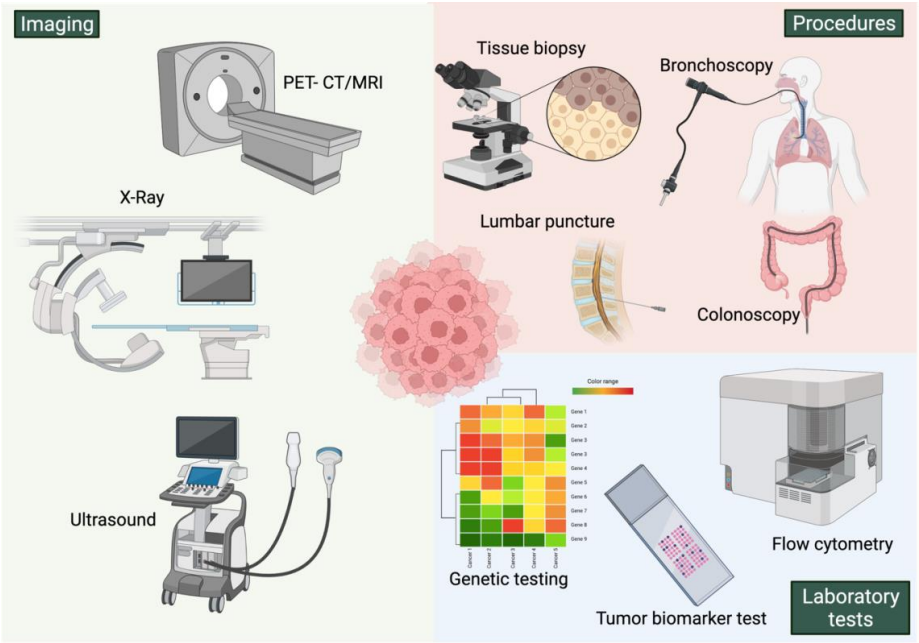

Figure 8: Conventional diagnostic tools and methods available in the market today. Cancer can be diagnosed by imaging techniques, extensive invasive procedures, and analyzing samples in a laboratory or combining all of these techniques to provide an accurate diagnostic report. Created with BioRender.com

Genetics and genomics-based diagnostics:

Changes in the DNA, known as gene mutations, may increase the cancer risk. Inheritance or acquisition might be the source of specific genetic abnormalities. BRCA1 and BRCA2 are two instances of hereditary gene mutations that increase the risk of breast and ovarian cancer[76,77]. Some tests may help determine whether you are genetically susceptible to certain cancers. The most advanced kind of genomic

analysis is when a biopsy sample cell is collected, and their DNA is sequenced in a lab to check for mutation-like features. The doctor will be able to make better treatment decisions with this information. A blood or mouthwash sample is taken to identify gene changes that may raise the risk of cancer[78,79]. To find tumor markers or abnormal cells, laboratory tests may be used to examine blood, urine, and other fluid samples. CellSearch®'s Circulating Tumor Cell (CTC) Test is used to detect and monitor the metastatic cancers of the breast, prostate, and colorectal organs, which identifies circulating tumor cells[80-82].

1.5 Liquid biopsy— A new era

Liquid biopsy is a non-invasive method to detect cancer. Liquid biopsy components may be investigated, including tumor cells, tumor-derived extracellular vesicles, circulating tumor nucleic acids, and other components of a circulating tumor[83] (Figure 9). Tracking tumor development and recognizing the start of therapeutic resistance and tumor recurrence early on is the primary goal of investigating these components. Blood-based liquid biopsy with increased sensitivity and specificity has been developed in recent decades[84,85], thanks to significant developments in nanotechnology.
CTCs may be enriched and identified using a variety of approaches that make use of their physical and biological characteristics [50]. In the eyes of cancer patients, CTC tests are similar to a "liquid biopsy" that occurs in real-time. A patient's prognosis is influenced by the spread of cancerous cells from the primary tumor site to distant organs such as the bone marrow (BM), liver, lungs, or brain, and the subsequent proliferation of these cells in their new microenvironment. Disseminated tumor cells (DTCs) and micro-metastases may remain dormant for years after the primary tumor has been surgically removed[86-88], but they may eventually manifest as visible metastases. Secondary metastases may occur from the spread of DTCs generated by such metastases[89].

DTCs may now be discovered in the bone marrow, lymph nodes, or circulating blood utilizing sensitive and specific testing. However, high-resolution imaging methods cannot identify the minimal residual illness. Needle aspiration via the iliac crest provides easy access to the BM. It has performed the most crucial role in indicating little residual sickness as far as distant organs are concerned. For DTCs from a wide

range of cancers, the BM seems to be a frequent destination, as well as a source of DTCs that may re-emerge in distant organs. Cancer patients need to be followed up regularly, and sequential analysis is essential. For prognosis estimation and drug monitoring[90,91], researchers are currently exploring the clinical relevance of testing for tumor cells in the blood rather than the BM aspiration since it is much more intrusive than collecting peripheral blood.

In recent years, various new approaches have been developed to detect CTCs in cancer patients' peripheral blood. However, detecting CTCs is still a technical problem to this day. One tumor cell in a sea of millions of blood cells is what's needed to detect CTCs[83]. To identify and characterize them, we need highly sensitive and specialized analytical techniques that often combine enrichment and detection methods[92-97].

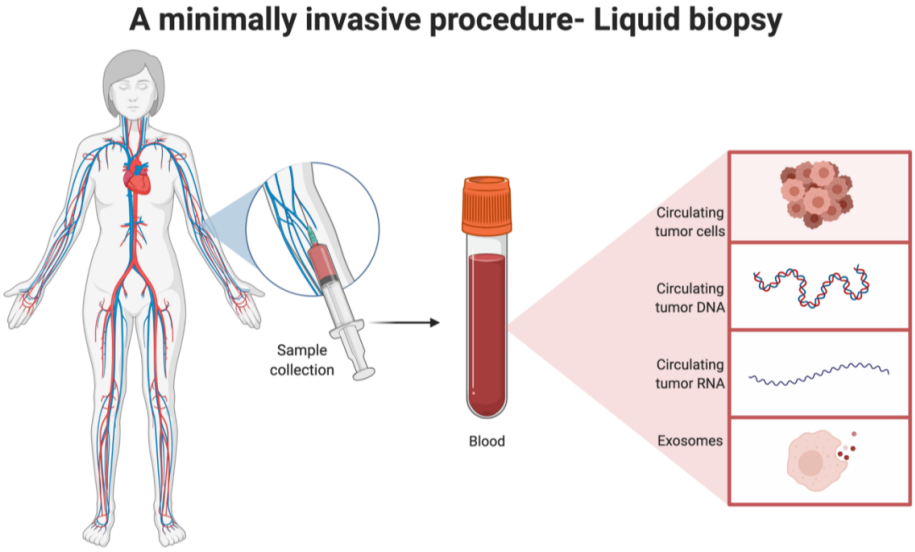

Figure 9: Liquid biopsy— a minimally invasive procedure: Blood withdrawn from a patient can have vital information such as circulating tumor cells (CTCs), circulating tumor DNA, RNA and exosomes. Created with BioRender.com

1.6 State of the art to detect CTCs

Biophysical marker-based technologies:

Physical features have the benefit of allowing CTC separation without labeling (Figure 10). In addition to density gradient centrifugation, filtration through a special three-dimensional microfilter, a new versatile label-free biochip that exploits the unique differences in size and deformability of cancer cells that is larger and stiffer than blood cells, a flow cytometer, microfluidic devices that combine hydrodynamic forces and the dielectrophoresis (DEP) cell separation technique, and a DEP field-flow fractionation device are a few examples that allows for the separation of cancer cells from healthy cells[98,99].

Microfiltration technology has shown the most promise for the continuous processing of enormous quantities of blood. Since its invention in the 1960s, track-etched polymer filters have been extensively employed for cell enrichment in biological research and therapeutic treatment[100]. The smaller size of contaminated leukocytes is exploited to enrich CTCs utilizing either adequately sized holes or particular 3D geometries in microfiltration techniques, which are among the most prevalent nonepithelial-based enrichment procedures for CTC separation[101]. Rarecells Diagnostics (Paris, France) developed the commercially available ISET® (Isolation by Tumor Cell Size) technology. Vacuum filtration is used to pass diluted whole blood through a filter with an 8-micrometer pore width. In contrast to leukocytes, which pass through the pores at random, larger CTCs retained by the filter. The assay's sensitivity has been reported to be 1 CTC per 1mL of blood. To enrich and evaluate CTCs in different malignancies, track-etched filters have been effectively employed with success[102,103].

Separation of CTCs by dielectrophoresis relies on the distinct electrical signatures of CTCs compared to contaminated leukocytes. The size, density, conductivity, and volume of the cells affect these electrical fingerprints. An electrode on the device chamber floor attracts CTCs, whereas leukocytes are flushed out as trash. The platform uses these features to its advantage. When cells are exposed to an AC electric field, they become electrically polarized. In an non-homogeneous field, cells are subject to a lateral dielectrophoretic (DEP) force whose frequency response is determined by the underlying electrical characteristics of the cells[104,105]. A cell's

composition and structure, as well as its shape and phenotype, influence these traits. As a result of the non-homogeneous electric field, cells with varying electrical polarizabilities may experience various forces. According to this, DEP gives the means to distinguish between distinct cell types and a physical force for separating them.

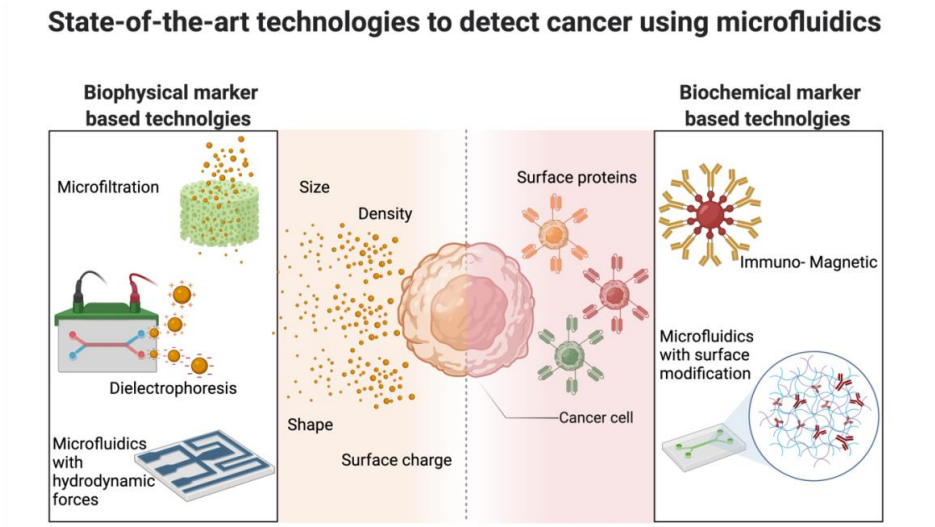

Figure 10: State of the art technologies used to detect cancer using microfluidic techniques. It is mainly categorized into two properties of cell— Biophysical properties such as size, shape, density, and charge. Biochemical properties rely on the surface protein expressed on the cell's surface. Created with BioRender.com

Microfluidics provides unprecedented control and manipulation of very small amount/volume of fluids. Increasingly innovative methods for sorting and studying biological cells on microchips have been presented during the last decade. For microfluidic enrichment of tumor cells, inertial flow fractionation uses hydrodynamic forces to select tumor cells of various sizes[106]. To arrange tumor cells and confine tumor cells in micro-scale vortices[107,108], microfluidic tubes integrating contraction and expansion reservoirs were created[109]. Compared to prior microfluidic techniques, these devices provide substantially greater throughput.

However, there may be losses in the cell recovery rate and enrichment against leukocytes. This thesis will discuss in detail about inertial focusing in chapter 2.

Biochemical marker-based technologies:

CTC enrichment techniques based on epithelial cells depend on positive selection procedures that use antibodies specific to CTCs (Figure 10). EpCAM, a transmembrane glycoprotein expressed by normal epithelial cells, has traditionally been the principal marker for immunoaffinity-based enrichment. Even though this antigen is present in up to 70% of all primary carcinoma tumor types, it is not present in the hematopoietic cells that usually circulate in the bloodstream of healthy persons[110,111].

Immunomagnetic methods, which depend on antibodies conjugated to the modified surface of magnetic particles, targeted antibodies to differentiate antibody-labeled CTCs from unlabeled contaminating leukocytes, are becoming more popular. One of the most extensively utilized CTC immunomagnetic enrichment technologies is the CellSearch® system, previously mentioned as being FDA-approved[112,113]. Several factors have contributed to the growth of microfluidic chip-based techniques in the CTC area, including their small size and relative cost efficiency, their versatility in research applications, their capacity to collect live CTCs, and their potential for high sample purity. However, in contrast to immunomagnetic methods, these procedures depend on antibodies that are not iron attached; hence, they are not as effective as immunomagnetic techniques. Instead, these systems use fixed antibody-coated surfaces for CTC enrichment, which may be achieved directly on the chip surface or by coated microposts[114-116].

Chapter 2: Separation of CTCs using microfluidics

2.1 Introduction of microfluidics and optofluidics

Microfluidics is the manipulation and control of small quantities of liquid or fluids, down to femtoliters, and provides precise control of the environment around biomedical or environmental samples ranging from individual cells to complete tissues (Figure 11)[117,118]. Microfluidics has the potential to revolutionize future healthcare technologies by addressing significant challenges such as drug discovery, diagnosis, and novel treatments. Microfluidics also allows real-time, continuous measurements and manipulation at the level of individual cells as well as facilitating automation at high throughput screening, and multiplexing[119,120]. The main notion of microfluidics is to combine in small millimeter-sized device processes that would typically need a whole laboratory[121-123].

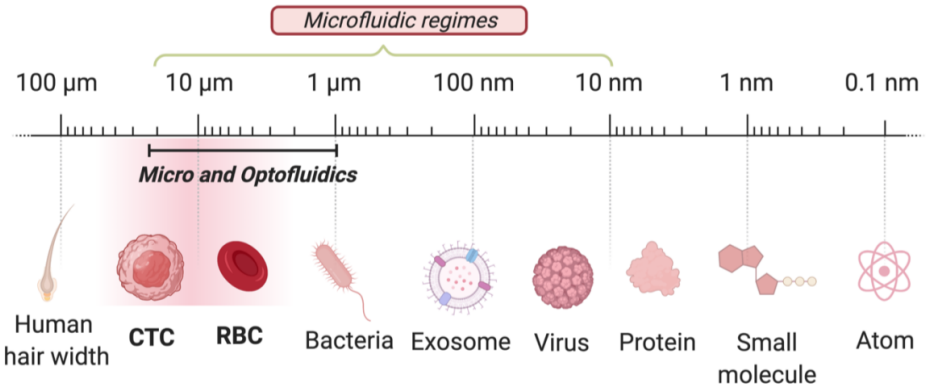

Figure 11: A schematic representation of size comparison of a human hair to an atom. Microfluidics and Optofluidcs lies within a range of 20 micrometers and down to a protein of 10 nanometers. This thesis discusses a size range between 20 and 1 micrometer. Created with BioRender.com

In biomedical analysis, the two primary components of bioanalysis are biological system analysis and the detection of biomolecular compounds. Most recently, scientists have been concentrating on three main topics: point-of-care (POC) testing[124,125], examining single cells or molecules at the molecular level to learn about the genetic heterogeneity of a particular population[126-128], and high-throughput

screening for large-scale research[129-131]. Microfluidic methods, which can revolutionize sampling, sample separation, mixing, chemical reaction, and detection, are rapidly being developed to address these issues. 'Lab on a chip' (LOC) is one of the important tool which takes benefits of the microfluidic technology[132]. Microfluidic technologies have transformed experimental biology and biomedical research and made significant advances in chemical synthesis, biofabrication, drug screening, and organ/tissue modeling since they were developed. With microfluidics, POC testing is able to attain great sensitivity, portability, and specificity[133-135]. Recent advances in bioanalytical microfluidic devices, such as "sample-in/result-out" analysis mode, precise nanoparticle size and pattern control for drug delivery, and discovery of novel chemical entities, have led to a surge in their use in the bioanalytical sector. Faster response times, improved analytical sensitivity, improved temperature control, and portability are just some of the advantages of microfluidics. Due to the lack of expensive equipment to operate, it is considered an affordable low-cost option[136,137].

A new branch of study known as optofluidics has emerged due to the convergence of microphotonics, optics, and microfluidics. Using a laser, photons are transported in a particular sequence known as microphotonics[138,139]. In optics, light and its interactions with other components are studied, and devices that use or detect light are manufactured. Fluid waveguides, microdroplets lasers, displays, biosensors, optical switches, or molecular imaging tools are all examples of optofluidics applications[140-142]. This thesis has put a substantial effort into miniaturizing tools that require a functional laboratory into portable lab-in-a-fiber devices. With the help of optofluidics, we were able to detect and count particles[143], which can replace the flow cytometer and separate them based on size[144].

2.2 Microfluidic based separation methods

2.2.1 Biophysical marker-based separation (Label-free sorting)

Many diagnostic and therapeutic applications rely on cell sorting as a primary research tool. Methods that do not identify cells biochemically are in great demand, and this is especially true for cell sorting. For example, several microfluidic approaches take advantage of cell features such as their size, shape, electrical

polarity, or hydrodynamic qualities to solve this problem[145-147]. Physical approaches, like size-based enrichment, are independent of antigen expression on a cell's surface. They prevent the inaccuracy of CTC antigen expression. These techniques leverage physical and mechanical distinctions between CTCs and other blood cells. Microfluidic-based approaches have also been reported[148-150]. These techniques output label-free, unmodified, and viable cells with high capture efficiency and enrichment, allowing application of subsequent downstream methods, such as next-generation sequencing (NGS), to gain insight from one sample and improve the comprehensive study of a particular cancer type and cancer development. Since no biochemical alterations are required, size-based approaches are projected to be less costly and take less time to enrich samples[106,151-154].

Microfluidics based filtration

Because of microfabrication processes, thin polycarbonate sheets with regulated nano to micron-sized holes are now accessible for use in microfiltration. A flexible micro spring array (FMSA) microfilter (Figure 12 (C)) is a high-throughput device with a fast-processing speed to separate CTCs based on size and deformity[155-157]. A parylene diaphragm with an effective surface area of 0.5 cm^2 is etched with micro spring structures that are highly porous and flexible. Large amounts of blood may be processed within 10 minutes with this system. Capture efficiency is 90%, and viability is over 80%. Another size-based CTC collection method has been made possible by a separable bilayer (SB) microfilter which was recently developed[158]. The SB microfilter (Figure 12 (A)) has a unique design and filtering principles. The SB microfilter's top and bottom porous membranes are separated by a gap that serves as a capture mechanism. Cell viability is better preserved because of the biocompatible polymer parylene-C used to make the membranes. Another technique that has recently been reported is a fluid-assisted separation technique (FAST), which has recently been developed and commercialized by Clinomics to isolate CTCs with reasonably high purity from the whole blood[159-161]. Track-etched polycarbonate membranes with 8-micron holes are used to isolate CTCs, and the membrane pores are filled with liquid to limit the amount of clogging and the amount of time it takes to separate them. CTCs can be extracted from whole blood with a spin of the disc, and this process takes less than a minute for 3 ml of whole blood. At a spinning velocity of 600 rpm, the capture efficiency was $95.9 \pm 3.1\%$. The purity was more than 2.5 log depletion, and the recovery rate was $96.2 \pm 2.6\%$.

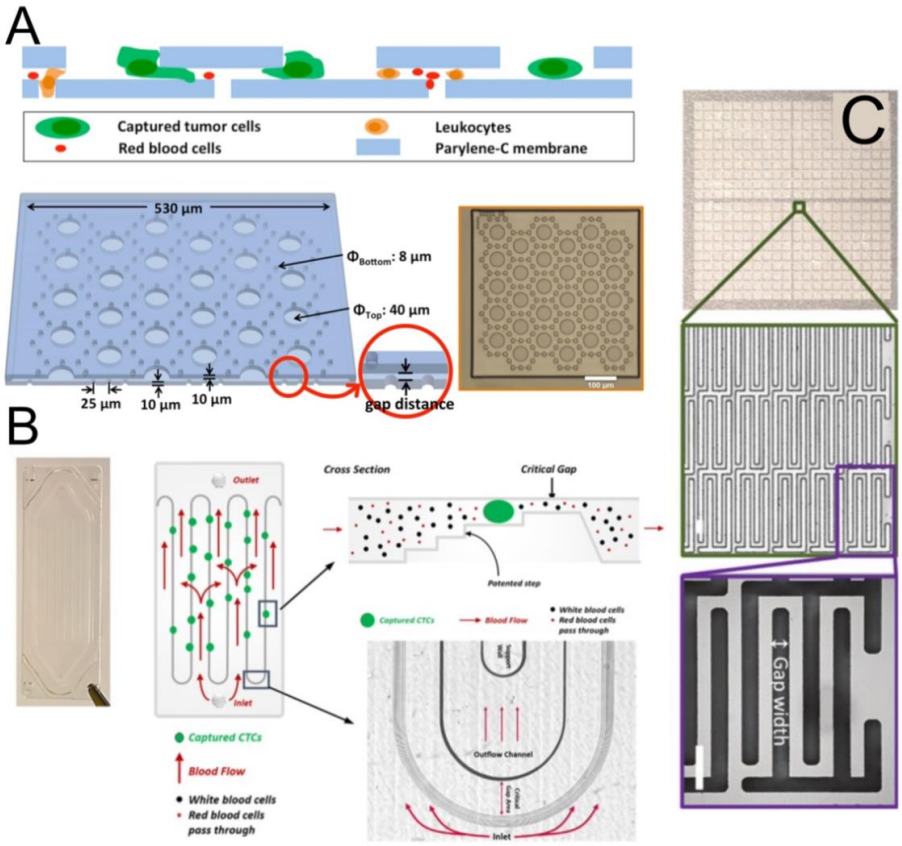

Figure 12: Images showing different technologies involved in microfluidics-based filtration. A) Separable bilayer (SB) microfilter[158] B) Parasortix[162] C) Flexible micro spinning array (FMSA)[155]. Reproduced with permission from ref [155] [158] [162] under the terms of the Creative Commons Attribution License.

A typical issue with mechanical microfilters is sample blockage and adherence. Increased fluid-driving pressure resulting from cell buildup on the filter increases the possibility of harming trapped cells. ANGLE invented the Parsortix disposable microfluidic cassette, which enables the collection and harvesting of CTCs through reverse flow[162-165]. This device utilizes a microscale graduated separation structure with a cross-sectional gap that progressively reduces the dimension of the

fluid channel and keeps CTCs due to their minor deformable nature and size while allowing other blood particles to flow through, as shown in figure 12 (B). For early validation of the device, 4 ml of spiked blood samples containing several cancer cell lines with varying cell counts were examined, with capture rates ranging from 42–70 percent for individual cell types. The harvesting efficiency was also determined in the same experiment, ranging between 54% and 69%. A microcavity array (MCA)[166-168] is another microfluidic device that separates tumor cells depending on their size to achieve highly efficient and repeatable cell recovery. The MCA system is comprised of a blood reservoir, a filter-included cartridge, and individual tubes. It filters blood using electroformed nickel and gold metal filters. The filtering cartridge is made of polymethyl methacrylate (PMMA). It incorporates a metal filter with precisely regulated pore shape, size, and density, eliminating the frequent issues associated with track-etched polycarbonate filters. 96% detection efficiency was reported in a 1-ml blood sample treated with 10–100 cells. Additionally, the MCA method separated CTC clusters that immunomagnetic separation technologies such as CellSearch could not accomplish[153,166].

Deterministic lateral displacement (DLD)

This technique was initially published by Huang et al. in 2004[169], and it was used in a continuous flow to segregate particles based on size with an accuracy down to 10 nm. It has been employed for a variety of applications since its introdcution, including the separation of white blood cells (WBCs), red blood cells (RBCs), circulating tumor cells (CTCs), and platelets from the blood[170-173]. This technique uses a channel's exact post arrangement to separate particles based on their relative sizes above and below a predetermined critical diameter (D_c). Separate flow laminae are formed in the device when successive rows of a constriction are pushed laterally apart by a predetermined distance, as shown in figure 13. When a particle is encountering a post and its center is beyond the breadth of the first streamline, it is displaced into the second streamline, which is how DLD's separation mechanism works. Geometric characteristics in DLD are altered and combined with external forces to separate particles based on additional factors beyond size, such as the shape and deformability of the particles and the dielectric properties of the particles.

Every time a particle bigger than D_c passes through a post and moves to the next streamline, the operation repeats. On the other hand, particles smaller than D_c stay

inside the initial streamline and follow their prescribed path through the device. Along the length of a device, particles smaller and bigger than D_c may be segregated from one another. Cell viability was reported to be 87% for cells isolated from CTC clusters in a study by Au et al. using a two-stage DLD separation array[174]. With high flow rates and the deformability parameter, Xavier et al. could boost the purity of the human osteosarcoma cell lines MG-63 and HL-60 during separation[175]. A ccording to Liu et al.'s work another innovative integrated DLD array was developed and has two DLD modules, one for blood cell removal and another for the separation of CTCs. Depending on their size and deformability, more than 90% of the CTCs are captured by this device, with a purity of more than 50%[176].

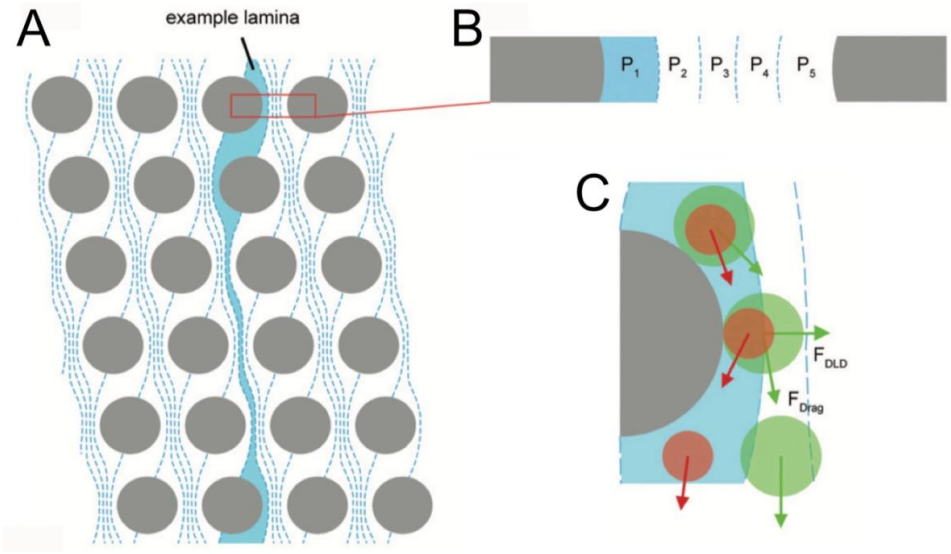

Figure 13: Fundamental principle behind DLD based separation. A) Schematics explain how the post arranged at an angle defines the trajectory of the fluid. B and C) The particles suspended in the fluid follow the trajectory and either stay or move away from it depending on the size. Reproduced from Ref [173] with permission from the Royal Society of Chemistry[173].

Acoustophoresis

Acoustophoresis, another microfluidic cell handling technology, provides label-free and continuous cell separation that enables high throughput and excellent separation performance for bioanalytical or medicinal applications[147,177-180]. There are two ways acoustic radiation forces might drive suspended cells or particles. One way is to have the particles in the pressure nodes at the center of the microchannel. The second way is to place towards the anti-pressure node, which is closer to the sidewalls of the microchannel, as shown in figure 14 (B). The radiation force depends on the cells' size, density, and compressibility with the surrounding medium to determine its magnitude and direction. More dense particles like cells tend to gravitate toward the pressure node in an aqueous environment, while less dense particles like lipids tend to gravitate toward the pressure anti-node[179,181,182].

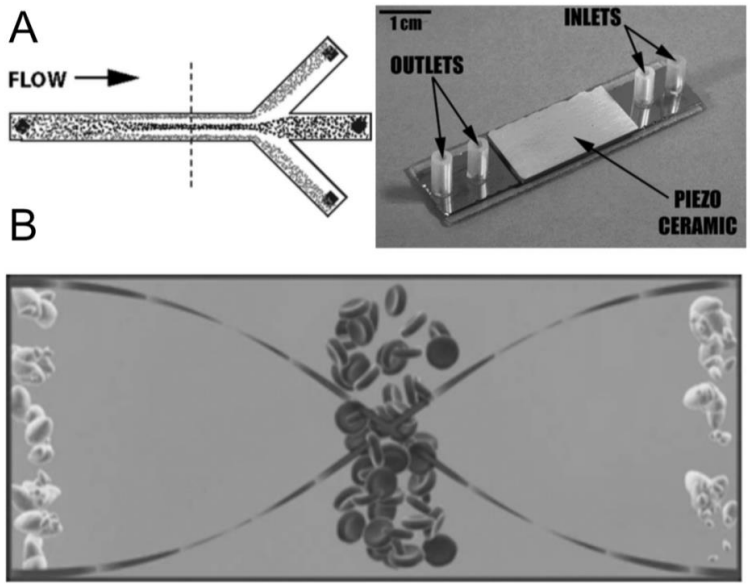

Figure 14: Illustration showing how particles based on acoustic contrast factor are separated. A) The separation of different particle size performed using a silicon chip is shown. B) The pressure antinodes (towards the side walls) collects all the negative acoustic contrast factor particles, whereas the pressure nodes (at the center) collects all the positive acoustic contrast factor particles. Reproduced from Ref [183] with permission from the Royal Society of Chemistry [183].

The acoustic radiation force scales with particle volume; thus, bigger particles travel faster than smaller particles with the same acoustic characteristics. Separation of lymphocytes from granulocytes, the isolation of tumor cells, the separation of WBCs from platelets, the synchronization of cell cycle phases in mammalian cells, and the isolation of bacteria in blood from sepsis patients have all been successfully demonstrated using size-based separation[184-186]. The viability and proliferation capability of acoustically-separated cells are unaffected by acoustophoresis. A high-accuracy acoustic sorting setup was presented by Ding et al. More than 86% of CTCs were isolated from WBCs at a flow rate of 7.5 mL/min[187]. The two-stage acoustophoresis-based device presented by Antfolk et al. successfully separated DU145 prostate cancer cells from WBCs with a capture efficiency of 86.5% ± 6.7% and a throughput rate of 100 μL min^{-1}.[182] Cell-free media inlet for laminating pre-aligned cells close to the channel sidewalls enables high-accuracy cell sorting, as performed by Magnusson et al. with their two-stage acoustic platform for CTC sorting[181].

Magnetophoresis

Non-uniform magnetic fields are used in magnetophoresis to manipulate microparticles and cells. Materials for microfluidic device fabrication such as glass and polymers may be made from a wide variety of sources due to the ability of magnetic fields to pass through them[188-190]. It is also one of the method for separating cells that does not damage the biophysical integrity of live cells and may be utilized directly with raw biological materials in a few easy steps. It is also a stronger force compared to other active manipulation methods[191]. The magnetic characteristics of CTCs and WBCs are often identical, making it difficult to separate the two cell types.

According to some studies, cells of varying sizes have been shown to suffer varied magnetic buoyancy forces in a continuous ferrofluid flow. To sort CTCs in biocompatible ferrofluids, Zhao et al. created a ferrohydrodynamic cell separation (FCS) apparatus microfilter (Figure 15). Patients with non-small cell lung cancer (NSCLC) had their CTCs effectively separated using this technology, with an overall capture rate of 88.3%[192].

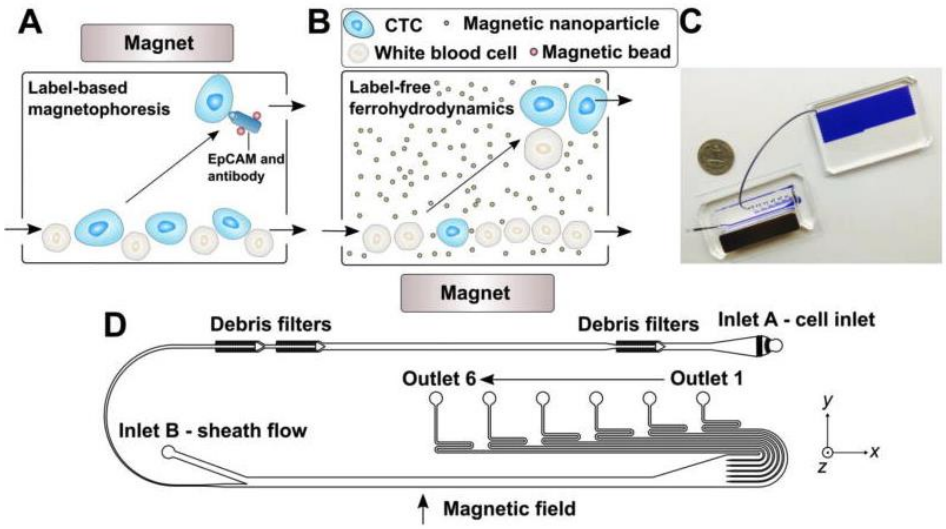

Figure 15: Label-free ferrohydrodynamic cell separation for CTCs. A) Traditional antibody conjugated magnetic bead based magnetophoresis. B) Label-free isolation of CTC using ferrohydrodynamics. C) Actual working device. D) Schematic of the overall design. Reproduced from Ref [192] with permission from the Royal Society of Chemistry [192].

Inertial microfluidics

Inertial microfluidics is a branch of fluid dynamics study where fluid is contained in devices with dimensions smaller than a millimeter in width, length, or depth. As the dimension get to smaller size, the fluid encounter forces distinct from those at larger scales and flows often display features that may benefit microfluidic applications[193,194].

For an incompressible fluid, the Navier-Stokes equations (Equation (1)) may be used to obtain the velocity field (u), which includes the fluid's kinetic viscosity (η) and density (ρ) as well as the pressure field (p). Boundary conditions are not indicated here, although they are still relevant.

$$\rho\left(\frac{\partial u}{\partial t} + (u.\nabla)u\right) = -\nabla p + \eta\nabla^2 u + F \quad (1)$$

These equations explain how the velocity field changes across time and space in a given domain. With the assumption of uniform viscosity and incompressibility, the

conservation principles of momentum and mass may be applied to the fluids in question to get the corresponding quantities. Non-dimensional metrics, such as the hydraulic diameter in a microchannel's hydraulic length, the fluid's typical velocity, and its typical density, all have the same order of magnitude.

Equation 1 may also be expressed in the non-dimensional form shown below as the Reynolds number (Re). Reynolds number is the ratio of inertia to viscosity. To take full advantage of a microfluidic regime we need to reduce Re.

$$\mathrm{Re} = \left(\frac{\rho\, U\, D_h}{\mu}\right) = \frac{Inertial\ force}{Viscous\ force} \quad (2)$$

Equation (2) shows that the amount of the Reynolds number determines the kind of flow regime. It is possible to reduce the size and speed of the flow, which is considered one of the best indicators of flow patterns. Fluid density(ρ), flow velocity(U), hydraulic diameter (D_h), and dynamic viscosity (μ) are all variables in this equation. The Stokes equation governs the flow at low Re because the right side of equation (2) dominates. Because of the inherent regularity of this equation, it leads to a flow with parallel streamlines, as shown in figure 16. Laminar flow occurs when the viscous forces outweigh the inertial forces. Microfluidics often uses a regime exactly to this. The boundary between turbulent and laminar flows may be shown experimentally. The flow is laminar if the Re is less than 2300. Turbulent flow occurs if the Re is greater than 2300. In able to control the fluid in a confined channel it is possible to manipulate both the fluid and particle present in it. Because of it, inertial microfluidics has received greater attention. These include ease of operation, simple construction, gentle to cells, and high throughput. Using inertial microfluidics, particles and cells may be controlled while having a significantly greater throughput than was previously not possible with traditional microfluidics. Inertial microfluidics has been used to manage particles and cells for a variety of applications, including flow cytometry, size-dependent cell separation, high-throughput cell concentration, and selective cell capture, to name a few. In the field of fluid mechanics, research has been done on particles inertial lateral migration in channel flows. At 0.3 times the diameter of the centimeter-scale pipe cross-section, Segre and Silberberg found particles moving through circular pipes aligned in the annulus[195]. Di Carlo was the first to adapt the macroscale inertial effect to the

microscale. Particles in straight and symmetric/asymmetric curved microchannels continuously self-focus and organize[193].
With Newtonian Poiseuille flow in a straight rectangular microchannel, the balance between shear-induced lift force $\boldsymbol{F_{LS}} \sim \frac{\boldsymbol{U^2 a^3 \rho}}{\boldsymbol{D_h}}$ and wall-induced lift force $\boldsymbol{F_W} \sim \frac{\boldsymbol{U^2 a^6 \rho}}{\boldsymbol{D_h^4}}$ actuates the particles to two equilibrium locations. By modifying the aspect ratio of the microchannel, these two focusing positions are modified. Inertial microfluidics has been used to concentrate and separate bigger particles because of the high correlation between inertial lift forces and particle size. The secondary cross-sectional flow is generated in curvilinear channels due to the difference in pressure gradient between the inner and outer walls. Dean vortices above and below the channel symmetry plane are responsible for this secondary flow. Dean drag forces $\boldsymbol{F_D} \sim \frac{\boldsymbol{4\, U^2 a\, \rho}}{\boldsymbol{R\,(w+h)^2}}$ and inertial lift forces drive particles to move and establish their equilibrium places. Inertial microfluidics can achieve exceptionally high volumetric flow rates. However, it is challenging to separate tiny particles. Flow cytometry applications are hindered because particles concentrate on the walls' center faces[196-198]. Non-Newtonian fluids have recently been hypothesized and are receiving considerable attention in particle migration, which will be examined in further depth in the next section.

Kuntaegowdanahalli et al.[194] used a 5-loop Archimedean spiral channel to separate three polystyrene beads with diameters of 10, 15, and 20 μm with a 90% efficiency. With an efficiency of 80%, high vitality of >90%, and throughput of 1 million cells/min, their device separated the SH-SY5Y neuroblastoma cells from the smaller C6 glioma cells. Using an improved Archimedean spiral device with a compact footprint, Nivedita et al. demonstrated 95.3% separation efficiency at a throughput of 1.8 mL/min while sorting RBCs and WBCs from diluted blood[199]. Huang et al. suggested a 99.04% removal rate for blood cells to separate spiked MCF-7 cells from diluted whole blood. A recovery rate of 89.78% was also attained for the spiked MCF-7 cells from the lysed blood[200]. 88.5% tumor recovery rate and 3.33 $\times 10^7$ cells/min throughput were reached by using the double spiral channel to separate spiked MCF-7 and Hela cells from dilutions of whole blood, according to Sun et al. [201]. CTCs were isolated from blood samples of cancer patients using a slanted spiral channel by Warkiani et al. [202]. Over 80% of MCF-7, T24, and MDA-MB-231 cancer cells were

recovered in 8 minutes with a very high purity of 400–680 WBCs/mL and a 4 log WBC depletion.

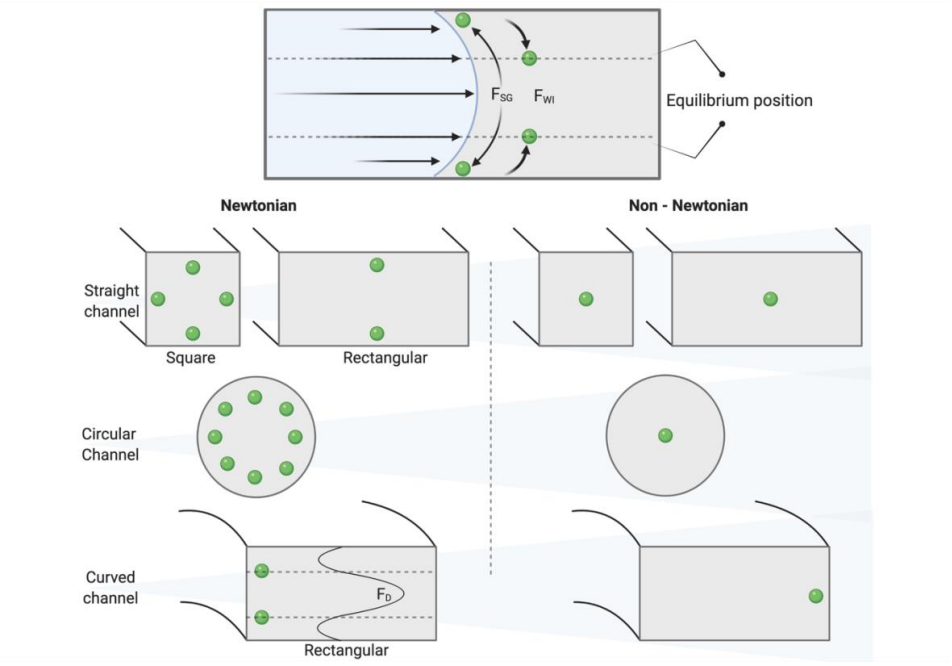

Figure 16: Behavior of particles in Newtonian and non-Newtonian fluids in different geometries. Schematic illustrations showing different inertial lift forces acting on a particle in a microfluidic channel. Different geometries have unique focusing positions depending on which fluid the particles are flowing in. F_{SG} – shear gradient lift force pushes the particle away from the center, while F_{WI}- wall induced lift force pushes particle away from the wall. The equilibrium position is where the particle settles down in a balance between these two forces. F_D- Dean drag force is higher at the center and act towards the outer wall which is not a stable position for the particle to settle down.

A substantial inertial lift force caused big cancer cells to concentrate at the inner wall of a sheath-assisted spiral channel. In contrast, tiny blood cells which did not meet the condition $a_p/D_h > 0.07$, flowed along the Dean vortex and returned to the outer wall. Before CTC enumeration in all clinical samples from patients with metastatic lung cancer (n = 5–20; 5–88 CTCs/mL), the device performance was optimized using cancer cell lines with a >85% recovery ratio. A recovery of 85% for spiked cells

across several cancer cell lines and a 99.99% depletion of WBCs in whole blood were achieved by Warkiani[203]. It was shown by Zhang et al. that an automated microfluidic apparatus with a flow-regulating chip and eight spiral channels can be used to separate CTCs without using labels. Automated MCF-7 cell sorting from diluted human blood with a recovery rate of 85% was achieved within a processing time of 23 minutes using the equipment[146].

Di Carlo originally developed the serpentine channel (Figure 17 (A)) for inertial microfluidics for the continuous focusing and arranging of polystyrene particles in 2007[204]. With a flow rate of 1.5 mL/min and a throughput of 15 000 cells, it is possible to focus blood cells and separate 4 and 7 μm polystyrene particles. Even sub-micrometer particles might be precisely focused to stable equilibrium locations in a sinusoidal channel, as proven by Wang et al. [205]. Particle focusing is possible by utilizing a serpentine channel. The novel focusing idea used secondary flow drag and particle centrifugal force. Polystyrene particles as small as 3 μm and as large as 10 μm have been successfully separated, with separation efficiencies of above 90%, which is more than 97.5% for 10 μm particles 92.8 percent for 3 μm particles[206].

An efficient vortex chip (Vortex HT) developed by Di Carlo's team has been launched for the separation and trapping of CTCs[207]. There are sixteen parallel channels on the Vortex HT processor, each with 12 serial reservoirs. Large cancer cells in each reservoir can travel across the fluid stream and into the vortex, while the smaller blood cells can flow out of the chip and into the surrounding environment. Using a wash solution to remove the remaining blood cells and reduce the flow rate to dissipate the vortices was part of the four-step processing procedure. The priming wash was followed by sample infusion and size-based capture of target cells. In a recent study, CTCs were isolated in less than an hour from 22 patients with advanced prostate cancer, with a purity ranging from 1.74 to 37.59% and a high efficiency ranging from 1.88 to 93.75 CTCs/7.5 mL of blood. In addition to the fact that the Vortex HT chip has a limited capacity in reservoirs, there are two downsides such as its not a continuous process of separation and the capture efficiency drastically reduces due to that. To continually siphon big particles, Wang et al. devised a new design (Figure 17 (B)) with side outputs in each chamber to alleviate these drawbacks. Continuous separation of polystyrene particles with a high size-

selectivity of 2 μm, an efficiency of >90%, and purity of >90% were made possible with this modification[208].

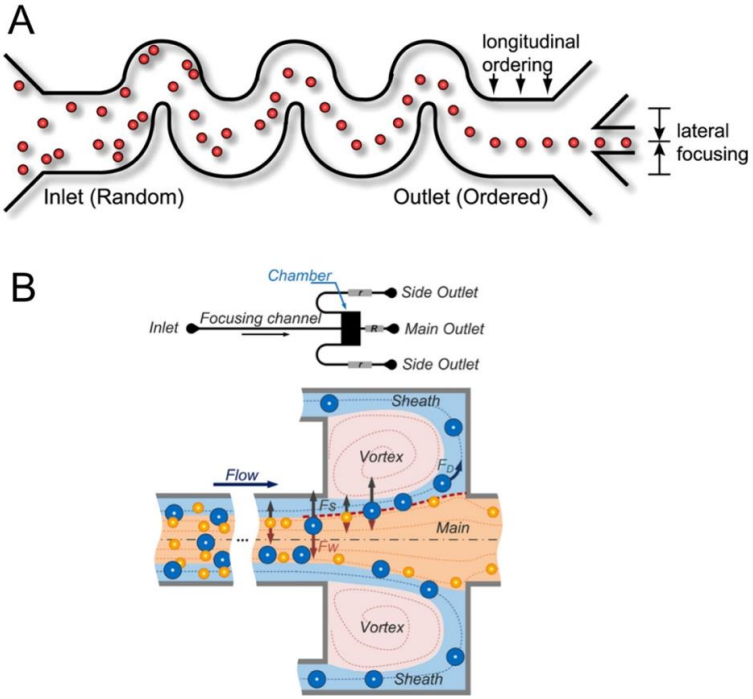

Figure 17: A) Serpentine channel for continuous particle focusing. Copyright (2007) National Academy of Sciences[204]. B) A vortex aided inertial microfluidic device. Trapped particles are siphoned using side outlets improving the overall separation efficiency[208]. Reproduced with permission from ref [207] under the terms of the Creative Commons Attribution License.

Elasto Inertial microfluidics

Due to an uneven distribution of the initial normal stress along the microchannel's centerline and walls, particles in a pressure-driven, viscoelastic flow gravitate toward the centerline. Non-negligible inertial effects are added to the primarily elastic forces[209,210]. The nonlinear effects of fluid inertia and fluid elasticity generated by the non-uniform distribution of normal stress cause the particles in

rectangular geometries to migrate towards the channel's center and corners while performing 3D focusing under identical circumstances. Fluid elasticity and inertia work together to concentrate particles in three dimensions in microchannels with a rectangular cross-section[211-214]. The Weissenberg number describes the relative ratio of elastic to viscous properties, Weissenberg number Wi = $(\frac{2\lambda Q}{h w^2})$, where λ is the relaxation time of the polymer additives. Elastic and inertial contributions are related by the elasticity number El = $(\frac{W_i}{Re})$, calculated as the ratio of Weissenberg and Reynolds numbers. We previously demonstrated robust single-stream particle focusing in viscoelastic fluid at high Reynolds numbers with circular cross-section straight channels by eliminating corner effects in rectangular geometries (Re up to 100)[143]. Non-Newtonian viscoelastic fluid particle migration in curved channels is more complicated and relies on inertial, elastic, and Dean drag forces. The so-called nonlinear viscoelasticity property of non-Newtonian viscoelastic fluids is achieved by simply adding a small amount of macromolecule polymers, such as polyvinylpyrrolidone (PVP), polyacrylamide (PAA), and polyethylene oxide (PEO), to Newtonian fluids. This results in a synthesis of liquid-like viscous and solid-like elastic properties[215,216].

In contrast to the frequently utilized basic straight channels, relatively few studies in the field of elasto-inertial microfluidics have attempted to comprehend or use particle focusing in complex shaped or curved channels. For example, in typical pinched flow fractionation (PFF) channels, Lu et al. exploited elasto-inertial phenomena to augment the displacement of focused particle arrays and achieved continuous shape or size-based particle separation[217]. Using a straight channel with side wells, Kim et al. created an inertialess viscoelastic flow hoop stress inducer[218]. An asymmetrical expansion-contraction channel was devised by Yuan et al. to allow 3D focusing at high throughput while maintaining high efficiency[219]. Lee et al.[211] recently observed an "Elasto-inertial focus band" between 1.5 and 10-micrometer beads at low Reynolds numbers, which they called "Dean-coupled Elasto-inertial focus band." Yinning et al.[220] have shown size-tunable elasto inertial sorting of five distinct particles at a flow rate of 160 µl/min using a method developed by the group. Nan Xiang reported particles focusing on low aspect ratio microchannels and derived the defocusing features in spiral microchannels[209]. A 1 mL/min flow rate can separate 15 µm from 10 µm particles using differential migration as a proof-of-

principle for high-resolution particle separation, which has only been previously shown in inertial microfluidics. The 10 μm and 15 μm particles were separated with 98% and 97% efficiency, respectively[214].

2.2.2 Biochemical marker-based separation

Labeled sorting

Affinity-based isolation, which is widely used, is now a viable option for CTC counting. This technique uses an antigen pattern specific to CTCs. This technique of CTC count is based on the unique antigens generated by CTC depending on their tissue origin that are not shared with other normal blood components[221,222]. Negative enrichment may also be achieved by using antigens not found on CTCs but other blood cells that selectively collect normal blood cells surrounding CTCs using the CD45 antigen. Negative enrichment techniques are preferable to positive enrichment methods in terms of purity since label-free CTCs can be collected independent of specific antigen expression[222-224]. One of the most common examples of positive enrichment is EpCAM (Epithelial cancer adhesion molecule) for CTC collection in epithelial carcinoma types. EpCAM, a transmembrane glycoprotein absent in normal cells, is found in epithelial cancers. Antibodies against EpCAM can isolate epithelial CTCs from peripheral blood[153,225-228].

CellSearch[52,229] is the CTC industry standard. This is the first and only FDA-approved technology for performing CTC testing on patients with metastatic prostate, breast, and colorectal cancers. Magnetic field-based cell sorting identifies CTCs utilizing ferrofluid nanoparticles functionalized with anti-EpCAM antibodies. The cells are then separated using a magnetic field. To summarize, plasma and buffer are aspirated after blood and buffer are mixed and centrifuged. Ferrofluid nanoparticles are used to enrich EpCAM-expressing CTCs. Cytokeratin such as Cytokeratin 8,18,19-phycoerythrin is utilized to detect CTCs as epithelial markers following CTC enumeration. In the first landmark study with metastatic breast cancer patients, CellSearch technology discovered 5 CTCs per 7.5 mL blood sample[81]. Without centrifugation or lysis of red blood cells, MagSweeper[230] can separate CTCs from blood samples. Non-adhesive, ultrathin plastic sleeves less than 25 nanometers thick are used to catch and release CTCs from liquid samples, allowing for a large number of capture and release cycles and a high capture efficiency. A robotically

operated magnetic rod distinguishes CTCs by brushing through wells containing labeled samples. After the rod-sheath assembly has washed away contaminated unlabeled cells, an external magnetic field may release the tagged cells captured. MagSweeper can process 9 ml/h of blood with a single automated system and can easily be scaled up to process several samples simultaneously. Capture efficiency was 62% ± 7%, and purity was 51% ± 18% percent for this device's detection when tested on cancer cell lines.

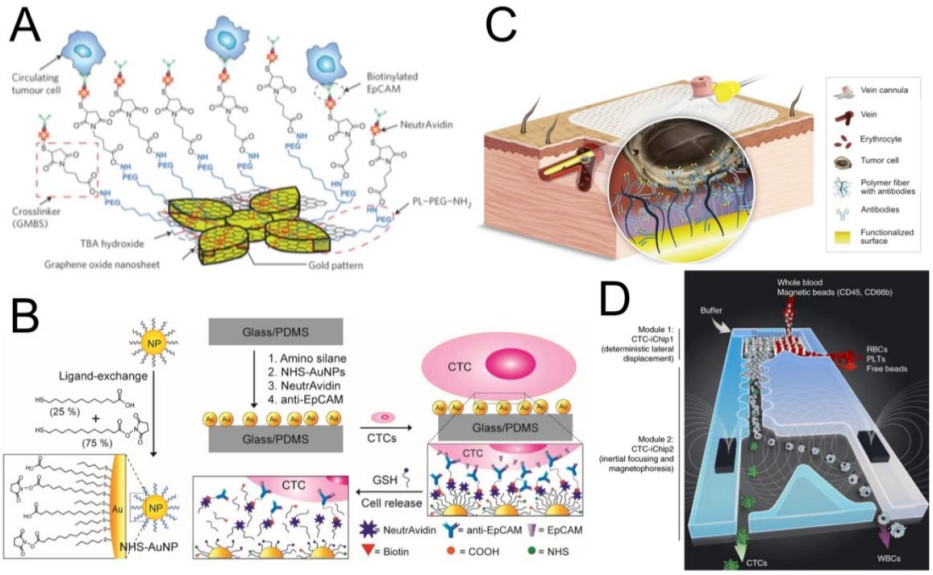

Figure 18: Technologies involved in labeled sorting of CTCs. A) Graphene oxide chip[231] B) NP-[HB]CTC-Chip[232] C) Gilupi CellCollector (reproduced from the official website) D) CTC-iChip[233]. Reproduced with permission from ref [231] [232] [233] under the terms of the Creative Commons Attribution License.

Microposts coated with anti-EpCAM antibodies are used in the CTC-Chip approach to capture CTCs[114]. In the initial generation of CTC-Chip, 78,000 microposts were put on a 970-mm² surface and coated with anti-EpCAM antibodies. One to two milliliters of blood was flowed per hour through the CTC-Chip to capture and identify CTCs. A total of just 2–3 mL of blood may be processed using the CTC-Chip technique. The standard blood sample is 7.5 mL in clinical settings, which might be a problem for CTC-Chip technique as it cannot process such as huge sample. HB-

Chip, the successor to the CTC-Chip, was designed with a Herringbone shape to disrupt blood flow and increase CTC collisions with antibody-functionalized chip walls. When using a new HB-chip design, there has been a significant increase in the number of CTC clusters recorded and the capacity to identify clinically substantial CTC clusters[234]. The CTC-iChip[233](Figure 18 (D)), the third version of the CTC-Chip, employs hydrodynamic size-based cell sorting to lower the number of small blood cells like red blood cells and platelets. The inertial focusing microfluidics inserts cells in a single cell line and applies a magnetic field to promote EpCAM positive CTCs or reduce CD45 positive leukocytes[235].

There is an increasing need for in-vivo CTC collection, and a novel approach, the Gilupi cell collector (Figure 18 (C)), attempts to address that demand. This technique uses an anti-EpCAM antibody-coated medical wire to extract CTCs from cancer patients' cubital veins. Compared to conventional ex-vivo CTC tests, this method allows for collecting CTCs from 1.5 to 3 L of blood[236]. A graphene oxide (GO) chip (Figure 18 (A)), a microfluidic device, is utilized to increase CTC capture sensitivity. Gold floral patterns absorb the gold nanosheets on the GO chip[231]. To harvest CTCs, EpCAM antibodies may be chemically functionalized on GO sheets. More than 80% of the EpCAM-expressing cells could be isolated. More than 65% of the spiked samples had cells expressing EpCAM. Many immunoaffinity-based techniques have a crucial problem in that it is challenging to remove live cells from the capturing surface. The GO chip is no different, but a thermoresponsive polymer was fabricated to overcome this problem, adjusting to temperature changes without affecting their structure. For cancer cells that express EpCAM, a higher capture efficiency of 84.93%-95.21% has been achieved. 95.21% and 91.56% of released cells were determined to be alive in buffer and blood experiments[237]. Another technique that focuses on releasing the captured cells is NP-^{HB}CTC-Chip (Figure 18 (B)). It relies on the ligand-exchange technique (AuNP-thiol exchange reaction) to release cells from AuNPs in this process[232,234]. Nonspecific binding was reduced by roughly 20%, while capture efficiency was increased by 96.4% $\pm$ 2.2%. This study indicated that CTC counts ranged from 6 to 12 cells per milliliter in patients with metastatic breast cancer. It takes around four hours to process three milliliters of whole blood.

Chapter 3: Biomaterials used in capturing CTCs

3.1 Surface modifications in microfluidic chips

As stated in this thesis, microfluidic devices have garnered considerable interest due to their competitive advantages. Microfluidic devices are often made of silicon, glass, polymers, or a mix of these materials[238-240]. Glass is a significantly more promising option because of its well-defined surface chemistries, favorable electroosmotic flow (EOF) properties, and better optical transparency[241,242]. However, when cost, time, and effort involved in fabrication and production are considered, polymers and elastomers become more desirable in microfluidic devices. Poly dimethyl siloxane (PDMS) is by far the most often used polymeric material in microfluidics. This is due to the material's numerous distinguishing characteristics, including its elastomeric properties, biocompatibility, gas permeability, optical transparency, ease of molding into micrometer features, ease of bonding to itself and glass, relatively high chemical inertia, and low manufacturing costs[243-246]. While PDMS offers several advantages, its hydrophobicity makes it difficult to introduce liquid into the microchannels of PDMS-based devices. Surface charges are necessary to effectively limit non-specific adsorption of hydrophobic substances, increase wettability, stabilize and improve EOF[247-250].

PDMS or glass surfaces may be modified in a variety of ways. Plasma is a partially ionized gas in which a fraction of electrons and ions are unbound from an atom or molecule, and radical species are abundant. Plasma surface modification is accomplished by dissociating and reacting with gases such as oxygen, nitrogen, and hydrogen on the substrate surface, forming chemical functional groups. This form of surface alteration is by far the most often utilized nowadays[248,251-256]. UV-treatment is roughly an order of magnitude slower than oxidizing PDMS with plasma in terms of time necessary to accomplish the same effect. However, the benefit of UV treatment techniques is that they allow for a considerably more profound change of the PDMS surface without causing cracking or mechanical weakness[256-258]. Surface silanization may be carried out on various substrates as long as they have hydroxyl groups on the surface that react with alkoxysilanes to generate covalent Si-O-Si bonds with the underlying substrate. Following surface oxidation, different functional head-groups may be added onto the surfaces using amine, thiol, or

carboxyl ended alkoxysilanes[248,259,260]. Within the last two decades, the advancement of nanotechnology has resulted in creating a diverse array of novel nano-scaled materials with a wide variety of uses. Due to the beneficial surface chemistry of nanomaterials and nanostructured substrates, such as a high surface-area-to-volume ratio and increased local topographical interactions, they play an increasingly essential role in detecting cancer components[261-266].

In microfluidics, layer-by-layer (LBL) deposition is a new approach for surface modification. The LBL assembly process is a broad term that refers to the alternating adsorption of polyanions and polycations on nearly any substrate surface to form polyelectrolyte multilayers. The LBL assembly approach has several benefits, including simplicity, efficiency, and nanoscale thickness control[267-271]. However, the structure, functionality, and stability of polyelectrolyte multilayers (PEM) are highly reliant on various parameters, including the ionic strength and concentration of the polyelectrolyte, the kind of solvent, the temperature, and pH of the solution, especially for weak polyelectrolytes[269,272]. Schmolke et al. employed an automated dipping robot to deposit PEMs of poly(diallyldi-methylammonium chloride)/poly(acrylic acid) (PDDA/PAAc) or poly(hydroxyethyl ammonium chloride)/poly(acrylic acid) (PAH/PAAc) on a PDMS surface prepared with HCl/H_2O_2. Following that, a top layer of custom-made PAAc-g-PEG was successfully grafted onto the PEMs, resulting in a hydrophilic surface[273]. The protein G-immobilized hydrogel chip was created by Sung et al. The PDMS surface was modified with PEMs (poly(ethyleneimine)/PAAc) in a microchannel using the LBL technique; photoinitiator (PI) was absorbed into the PEMs-modified PDMS microchannel; protein G was covalently attached to NHS-PEG-acrylate molecules for copolymerization with acrylamide/bisacrylamide, and a specific region in the PEMs-modified PDMS microchannel was exposed to UV. Hydrogel plugs with patterned surfaces were created inside PDMS microchannels[274]. Schrott et al. effectively coupled LBL deposition and protein adsorption to create multilayers of dextran sulfate/human IgG on a PDMS surface primed with IgG. The antibodies were then crosslinked with glutaraldehyde[275]. Wang et al. assembled LBL by first adding a polyelectrolyte (PDDA, linear polyethyleneimine (LPEI), poly(allylamine hydrochloride), or Chit) as a pre-layer. Later, gold nanoparticles stabilized with citrate were bonded to the polyelectrolyte modified PDMS surface[276].

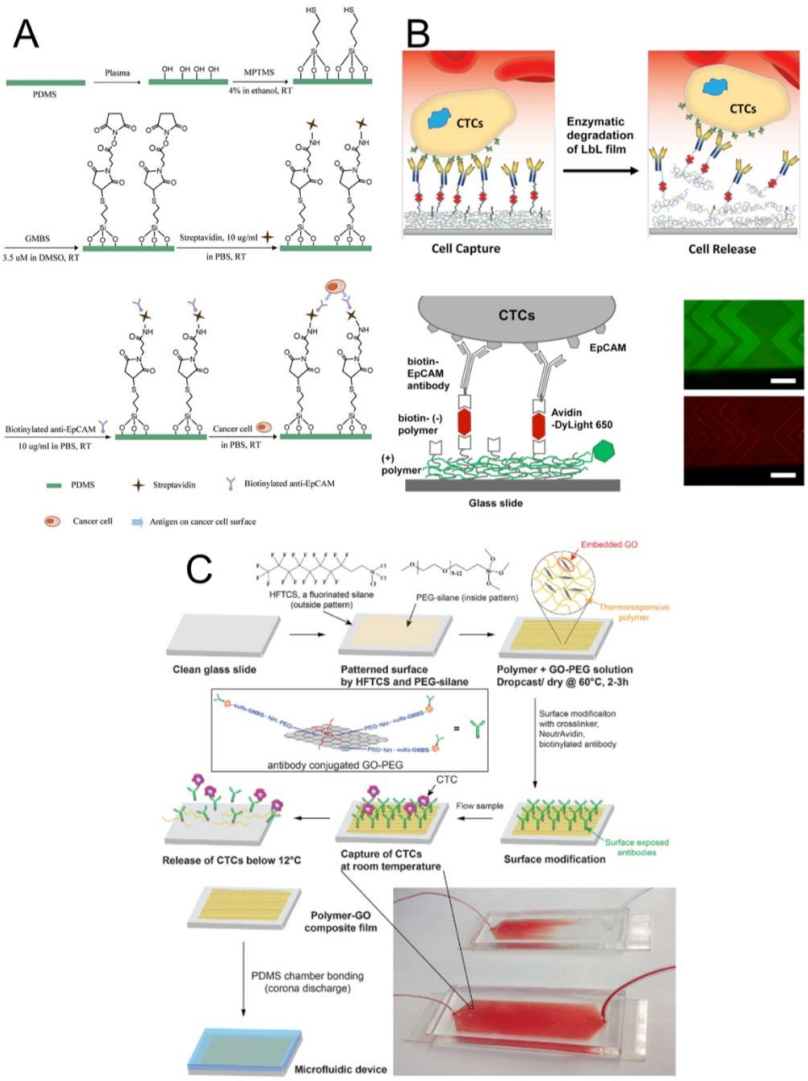

Figure 19: A) A classical bioconjugation of antibodies in microfluidics chips- (MPTMS-GMBS)[277] B) Alginate nano-film LBL for capture and release of CTCs[278] C) Thermo-responsive graphene oxide polymer[237]. Reproduced with permission from ref [267] [270] [237] under the terms of the Creative Commons Attribution License.

A microfluidic chip with a biodegradable nano-film covering may be utilized to catch and release cancer cell lines such as prostate and lung cancer non-invasively microfilter (Figure 19 (B)). An ultrathin coating of alginate was achieved using LbL assembly by Li et al. Prostate (PC-3, n = 3), and lung cancer (H1650 and H1975, n = 3) cancer cells spiked in whole blood were captured and released on ^{HB}CTC-chips modified with Polyallylyamine and Alginate (PAH/ALG). Around 79.2% for prostate and 78.9 % for lung cancer cells capture efficiency was observed, which is identical to the capture efficiency attained with non-degradable GMBS modified ^{HB}CTC-chips. After flushing the ^{HB}CTC-chip with an enzyme solution at a flow rate of 2.5 mL/h for 30 minutes, more than 95% of the collected cells were effectively freed[278]. In another approach by Yoon et al. [237]. Graphene oxide (GO) chip (Figure 19 (C)) was disseminated in a thermoresponsive polymer matrix with a lower critical solution temperature (LCST) of 13°C to cover the bottom substrate of the microfluidic device. The copolymer poly(N-acryloyl piperidine-co-N, N-diethyl acrylamide) was produced using free radical polymerization. At a flow rate of 1 mL per hour, blood samples were processed from 10 metastatic breast cancer patients and three pancreatic cancer patients. There were 2 to 20 CTCs per mL in samples from eight breast cancer patients and two pancreatic cancer patients. Both a thermally responsive (for bulk-population recovery at 37°C) and a mechanically sensitive (for single-cell recovery through frequency regulated microtip) gelatin nanostructure covering the surface was built for the release of CTCs from peripheral blood. In another novel approach, Reátegui et al.[279] Reátegui et al. employed biotinylated gelatin coated with alternating layers of streptavidin on plasma activated PDMS surfaces. Polystyrene nanoparticles coated with streptavidin were affixed directly to the top surface of a gelatin nanocoating, increasing the local concentration of antibodies accessible for binding to the target cell. Capture effectiveness was 95.9% ± 1.5%. The nanocoating enabled around 93.2% and 88.3% cell recovery and viability, respectively, to capture spiking prostate cancer cells in whole blood. Cellulose nanofibrils are a biodegradable and versatile material that emerges due to their unique three-dimensional structure and high biomolecular surface density. Because of their high density, hydroxyl groups may easily be transformed into carboxyl, epoxy, or amine groups.

Cellulose Nanofibrils

Bio-based green polymer, cellulose, is the most prevalent, have the most significant impact on environmental sustainability. Modern nanocellulose-based materials, such as those used in the aerospace, automotive industries, food, paper industries, and cosmetics industries, have begun to displace synthetic nanofillers in a variety of structural applications[280-283]. There are several advantages to using cellulose nanofibers in place of traditional medical biomaterials. These advantages include high aspect ratio and low density of the nanofibers, excellent mechanical characteristics, high tensile strength, stability, and biocompatibility. There are numerous biomedical applications involving cellulose nanofibers include drug delivery[284,285], wound dressing[286,287] as well as neural regeneration, tissue engineering[284], bone tissue engineering, and blood vessel replacement, among others[283,288-290]. A novel approach of using cellulose nanofibrils to build multiple layers of a matrix where CTCs can be trapped and released with high viability in a microfluidic chip was presented for the first time in this thesis. A series of polyelectrolytes were used to build the layers. A microfluidic channel with up to five alternating CNF layers was built using the layer-by-layer method. A chemically modified surface was utilized to anchor anti-EpCAM antibodies on the surface of the microfluidic devices. As many platforms provide the capturing of CTCs, very few could release the captured CTCs for further downstream analysis. In this case, a harmless chemical gently released the captured cells with an efficiency of 80% with high viability of more than 97% in less than 30 minutes[291]. This platform provides a promising device that could be scaled up and potentially applied in a clinical setting.

Chapter 4: Present investigation

4.1 Paper 1: 'High throughput viscoelastic particle focusing and separation in spiral microchannels'

In paper 1, we present the fundamental physics of particle focusing and separation at higher Reynolds number in a viscoelastic fluid, where particles are flowing through a rectangular curved microchannel. For the first time, we present particle focusing in a rectangular curved microfluidic channel at two order magnitude higher flow rate than previously reported in elasto inertial microfluidics. Figure 4.1 a) shows the principle behind elasto inertial microfluidics. Due to the balance between forces such as Dean force (F_D), Elastic force (F_E), Shear induced lift force (F_{LS}), and wall induced lift force (F_W), the particle settles in an equilibrium (position 3- Figure 4.1 a). Dean force increases with increased flow rate, changing the equilibrium of the focused particle and eventually the particles will be defocused. Figure 4.1 b) shows the difference between inertial and elasto inertial microfluidics, in the case of inertial microfluidics, the particles focus on the inner wall at a high flow rate of 1 ml/min in a curved microchannel, while in using a viscoelastic fluid, PEO (Polyethyleneoxide), at a concentration of 500 PPM, the particle completely shifts and focus to the outer wall. Different parameters, such as flow rates (Re), spiral curvature (De), aspect ratio (fixed width and different heights of the channel) and PEO concentrations were extensively characterized to investigate and optimize the particle focusing. While keeping the width constant at 500 μm, four different heights were tested (50,100,150 and 200 μm). A the height increases, particle defocusing was observed. Particle's equilibrium positions were changed as we increased the PEO concentrations from 500 PPM to 5000 PPM. As the viscosity increases, the particles moved closer to the center of the microfluidic channel as expected. Based on the optimized geometry and flow conditions, as a proof of principle, particle separation was demonstrated using a two-turn spiral microfluidic design (figure 4.2 a). 10 μm and 15 μm polystyrene fluorescent particles was suspended in 500 PPM (PEO) and pumped through the inner inlet while a sheath buffer of 500 PPM (PEO), was pumped through the outer inlet. At a flow rate of 50 μL/min for the sample and 950 μL/min for the sheath, a separation efficiency of 97% for 15 μm and 98% for 10 μm was achieved. However, despite very high separation efficiency, the system suffered from low sample throughput. To overcome this, we designed a novel integrated spiral microfluidic

chip, that circumvents the need for a sheath buffer (see figure 4.3 a). The system integrated two spirals where the first one is used to pre-focus particles above a certain size and the second spiral is used to differentially migrate particles based on size. In this setup, the sample is pushed into the chip at a flow rate of 1 ml/min. We separated 10 and 15 μm particles at a flow rate of 1 mL/min with an efficiency of 89% for the 10 μm particles and 99% for the 15μm particles. In summary, we demonstrated a high throughput elasto inertial microfluidics for the particle focusing, separation and volume reduction. It has several potential applications in rare cell separation that require the processing of large blood volumes, such as CTCs for cancer diagnostics and bacteria for sepsis diagnostics.

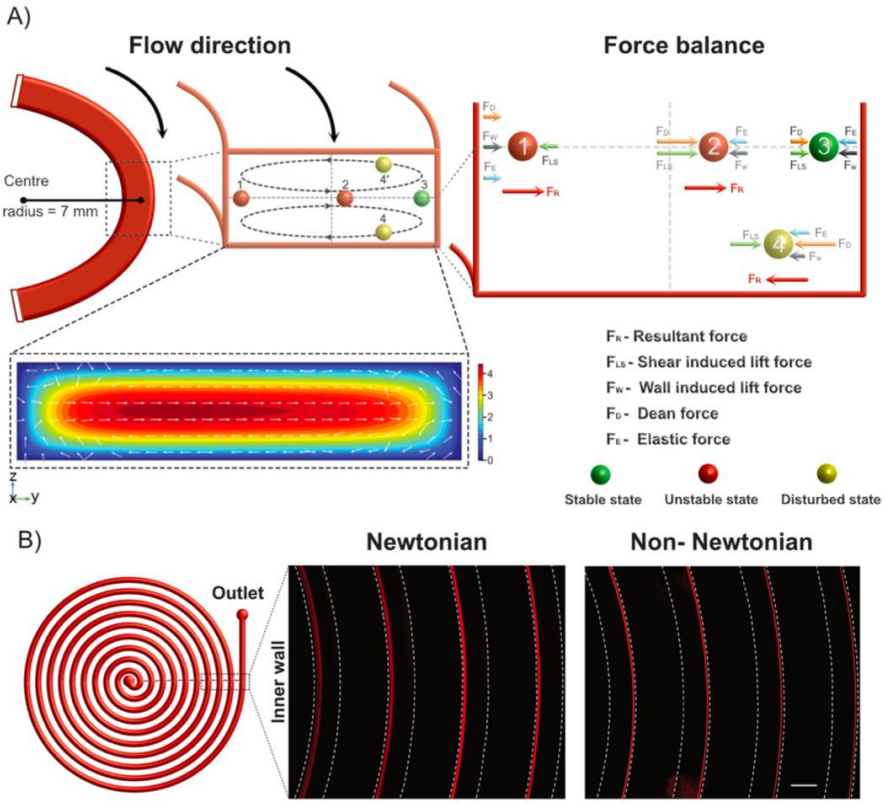

Figure 4.1: a) Overview of particle focusing principle in spiral microchannels. (**A**) Schematic illustration of particle focusing in elasto-inertial microfluidics. Under the influence of Dean drag forces (FD), particles migrate along the Dean vortices, and depending on the position the particles experience additional strong inertial lift forces (FLS and FW) and elastic forces (FE). How these forces acting on a particle focused in a distinct point (positions 1–4) are highlighted. Note, there are vertical lift and viscoelastic forces acting on the particles but are negligible at the center line. Inset, COMSOL simulation showing a of a skewed mean flow (contours) and cross-sectional flow (arrows). (**B**) Inertial and elasto-inertial particle focusing. Fluorescence image of 15 µm particles flowing through the spiral in Newtonian (left) and non-Newtonian (right) fluid using PEO as elasticity enhancer. In a Newtonian fluid, the particles are focused at the inner wall and for Non-Newtonian fluid at the outer wall. Scale bar: 500 µm.

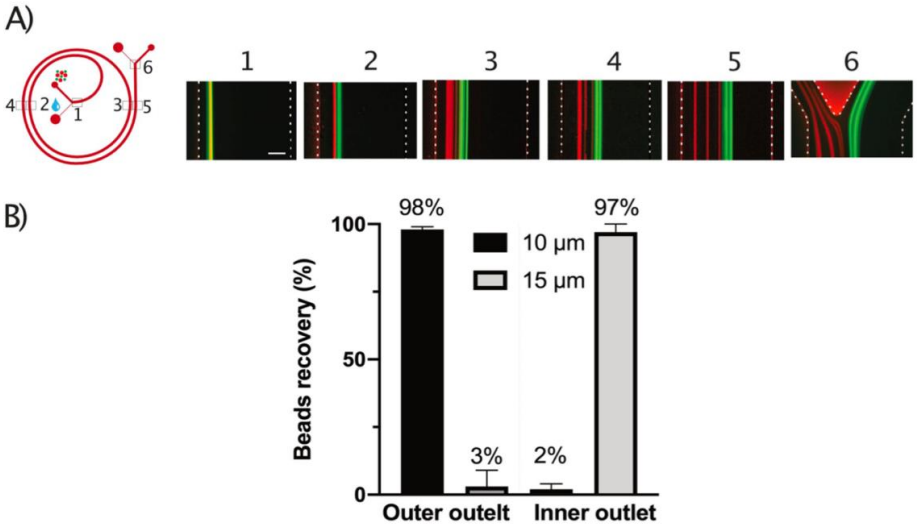

Figure 4.2: Sheath-based flow for particle separation. (**A**) Differential migration of 10 µm (green) 15 µm particles (red) from the inner wall. Particle position at the different regions (position 1–6) are shown, clearly indicating that the smaller 10 µm particles migrate first towards the outer wall. (**B**) Particle counting results, indicating high separation efficiency where 98% of 10 µm particles were collected at outer outlet and 97% of 15 µm particles at the inner outlet. The total flow rate was 1 mL/min (sheath: 950 µL/min and sample: 50 µL/min).

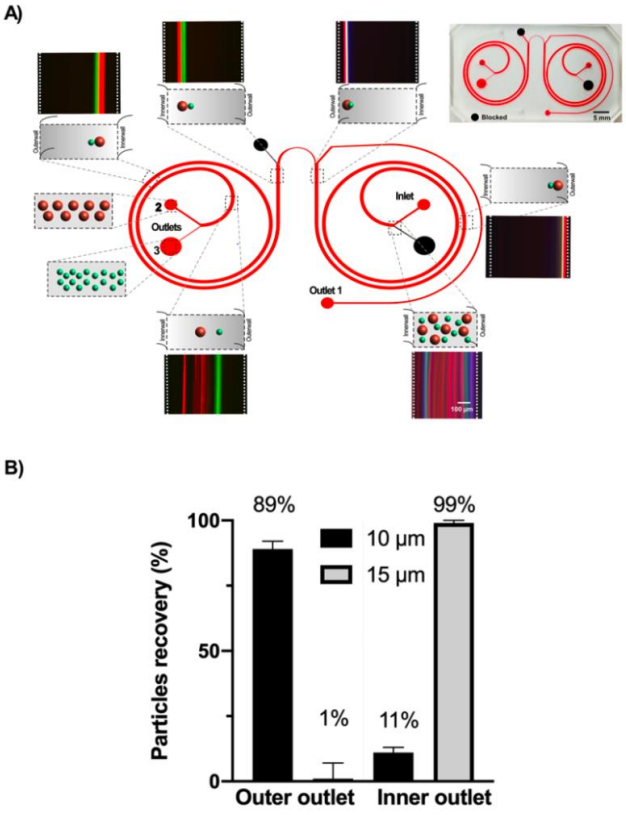

Figure 4.3: Sheath-less flow for high throughput particle separation using integrated spiral. Experimental results of two integrated spiral. (**A**) Particle size with 10 and 15 µm introduced at the inlet, where 10 and 15 µm particles are pre-focused in the first spiral and follows to the next spiral, where the 15 µm particles remains at the inner wall, while the 10 µm particles moves towards the outer wall of the channel. (**B**) Separation of particle 10 and 15 µm at a high flow rate of 1 ml/min, indicating a separation efficiency of 89% for 10 µm particles at the outer outlet and 99% for 15 µm particles at the inner outlet.

4.2 Paper 2: 'Analogue tuning of particle focusing in elasto-inertial flow.'

In paper 2, we studied particle focusing in weak viscoelastic flows theoretically and experimentally. Here, we used circular cross-sections and due to its uniformity in shape, the behavior of particles was very different but predictable compared to a rectangular channel. In order to understand the fundamental behavior of the particles, we started with Newtonian fluid, as shown in figure 4.4 a). The particles were spread across the channel and reached an equilibrium position at 0.6 radius from the center, as expected. In contrast, particles suspended in a non-Newtonian fluid (PEO) behaved differently. As shown in figure 4.4 b-d), the particle focusing position shifts towards the center with increased PEO concentration. In order to understand this behavior in detail, we applied numerical simulation and used FENE-P model to represent non-Newtonian fluids and Immersed Boundary Method (IBM) for the particles. FENE-P model allows us to reach higher Weissenberg number (Wi) compare to other viscoelastic flow model such as Oldroyd-B. While, IBM provides particle velocities and trajectories. As can be seen in figure 4.5 a, at a fixed Reynolds number (denoting flow rate) of 300 with different Weissenberg number (denotes the elasticity of the fluid) of 0, 1, 2 and 3 particles released at a fixed position (0.3 R) will gradually move towards the center. At the same time, particles released at different positions, such as 0.3R and 0.7R, will eventually end up at the same point, as seen in figure 4.5 b), indicative of fixed final equilibrium position. In both these cases, Wi = 0 (Newtonian) reached the equilibrium at 0.6R of the capillary. In summary, we show that particles can be focused at dynamic focusing positions in weakly viscoelastic fluids. This can have implications in the development of different techniques such as flow cytometry that require high resolution focusing and various biomedical applications.

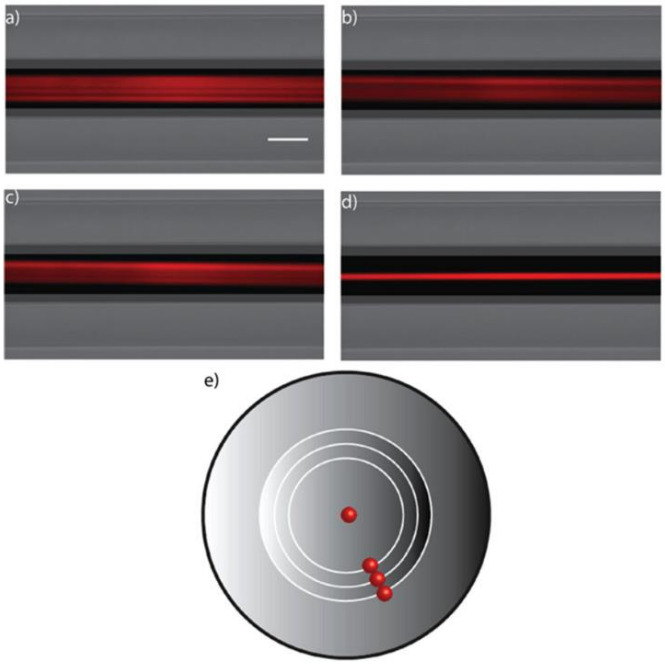

Figure 4.4: Different particle focusing equilibrium positions for concentrations of PEO solution ranging from 0 to 500ppm and for flow rates in the range from 5 till 180 µL/min. **a** Top view of capillary for Newtonian case, the particles reach equilibrium position at 0:6R from the center at F=0:6D. Scalebar:50 µm. **b** F=0:5D, Non-Newtonian fluid at 10 ppm: the behavior is similar to the one reported for a Newtonian fluid, except that the particles never reach a 0:6R distance but focus on a narrower bandwidth (F = 0:5D vs. 0:6D at 180 µL/min). c) F =0:4D, Non-Newtonian fluid at 50 ppm: the particles move even closer to the center than for 5 ppm (F=0.4D vs 0.6D at 180µL/min). **d** F=0 case for Non-Newtonian fluid at 500ppm, where particles achieve centerline focusing at low Reynolds number (Re<1, Wi = 0.1 at 20 µL/min)). **e** Cross sectional view of the four cases **a–d**

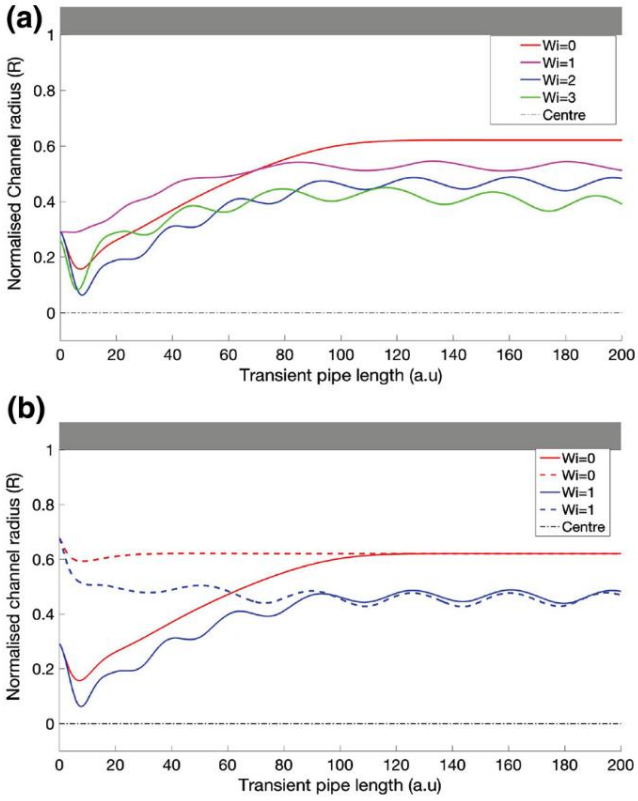

Figure 4.5: a Particle trajectories at Re 300 for different Weissenberg numbers. The particles progressively focus closer to the centre as Wi increases. b Particles introduced from different starting positions converge to the same final equilibrium position for both the Newtonian (Wi=0) and Non-Newtonian fluid (Wi=1); the two different starting position are 0.3 R and 0:7R

4.3 Paper 3: 'High performance micro-flow cytometer based on optical fibers'

In paper 3, we developed a portable, miniaturized microflow cytometry and demonstrated a high throughput elasto inertial particle focusing in a circular cross section. We combined the elasto inertial microfluidics to fiberoptic capillaries to achieve a compact optofluidic platform capable of focusing particles and counting. As shown in figure 4.6 a,c, and d), a combination of capillaries and fibers were used to fabricate the portable flow cytometer. A capillary carrying the focused particles was arranged opposite to the double cladding fiber, which was used for detection. After detection of each particle, the sample was collected in an output capillary aligned next to the detection capillary. The fourth capillary fiber (figure 4.6 (c)) was there to maintain the alignment. To achieve focusing and detection, various parameters were characterized such as different capillary diameter, particle size and the concentration of PEO. Using different diameter of micro-capillaries, we were able to focus a single stream of particles at a high flow rate of maximum of 800 μL/min, as shown in figure 4.7 b). Also, in increasing the concentration of PEO from 500 PPM to 2000 and 5000 PPM, we observed a good focusing even at lower flow rates (below 200 μL/min). However, at the same time, the higher viscoelastic fluid increased the pressure build-up in the capillaries leading to reduced throughput (figure 4.7 c). After characterizing the focusing behavior of different sized particles in microcapillaries, we detected the fluorescence and scattering of each particle. A 99% match was achieved between the fluorescent and scattering signals. We were able to count 2500 particles per second combining elasto inertial microfluidics and a portable optical system. After successfully demonstrating the capabilities of focusing of particles, we also focused and counted cancer cells (cell line HCT116) as a proof of concept at a flow rate of 400 μL/min (figure 4.8). In summary, we developed a portable microflow cytometer combining elasto inertial microfluidics and optical fibers. The developed platform can be possibly utilized in point-of-care diagnostic settings for cancer diagnostics and also in other areas where counting and detection of particles or cells are vital.

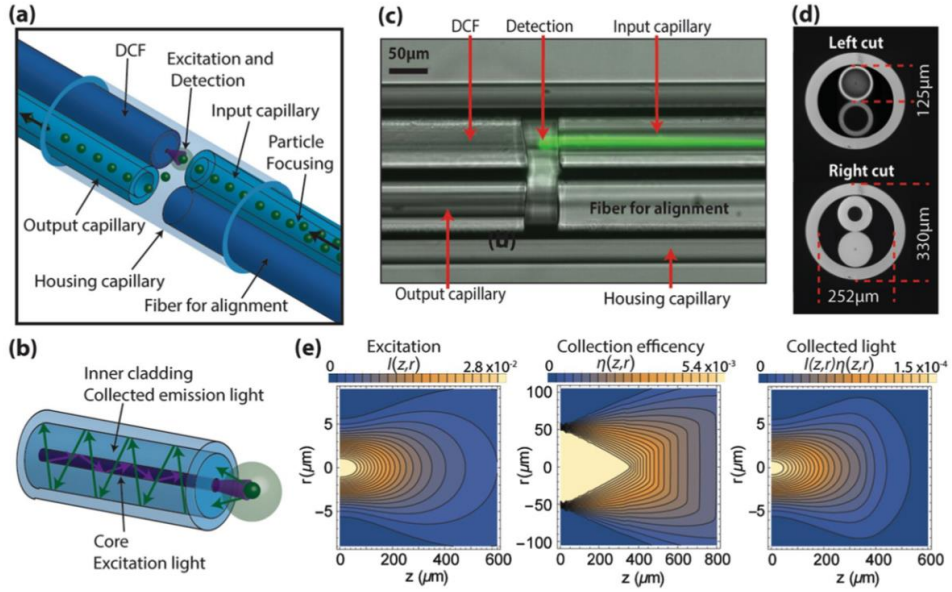

Figure 4.6: Fibre-based microflow cytometer. (**a**) Integrated detection micro-chamber; (**b**) Detection principle of the double-clad optical fibre (DCF); (**c**) Image of the micro-chamber during operation. The green light is fluorescence from particles flowing through the input capillary and excited by light from the DCF; (**d**) Cross- sectional views of the micro-chamber; (**e**) Simulated bi-dimensional map of: (left) excitation from the DCF core (9-*µm* diameter), (centre) collection efficiency of the DCF inner cladding (105-µm diameter and 0.2 NA), and (right) light collected by the DCF. An excitation wavelength 450 nm and a medium refractive index 1.33 (water) are used for the simulation.

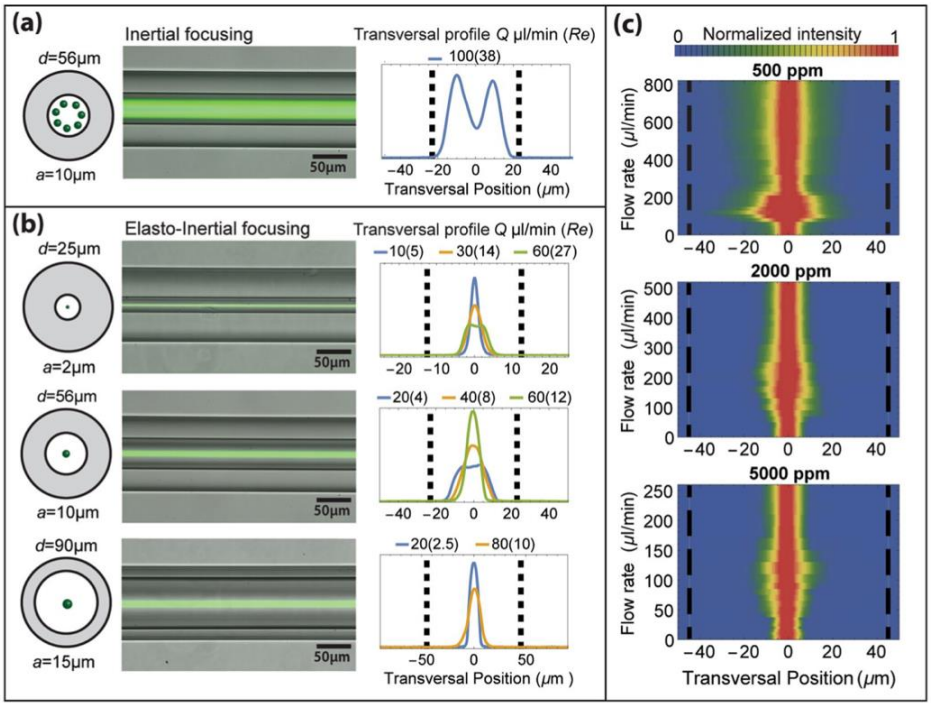

Figure 4.7: Particle focusing in capillary flow. (**a**) Inertial and (**b**) elasto-inertial focusing of particles of diameter *a* flowing in capillaries of diameter *d*. (left) schematic cross-section and long-exposure fluorescence microscopy image of focused particles, and (right) transversal profile obtained from fluorescence images indicating particle position for different flow rate (*Q*) and Reynold number (*Re*). Dashed black lines define the capillary walls; (**c**) Elasto-inertial focusing of 15-µm particles flowing in a 90-µm capillary at different flow rates for PEO concentrations of 500, 2000 and 5000 ppm. The figures consist of a contour plot made by stacking transversal profiles as a function of the flow rate.

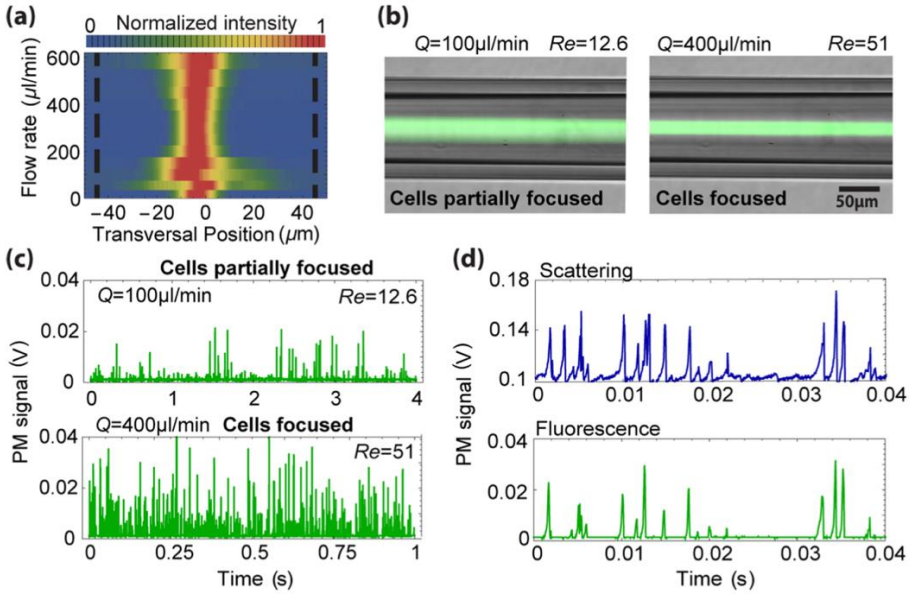

Figure 4.8: Detection of cells. (**a**) Focusing characterisation in a 90 μm capillary; (**b**) Long-exposure fluorescence microscope images of partially focused (left) and focused regimes (right); (**c**) Fluorescence signals corresponding to the images in (**b**); (**d**) Example of scattering and fluorescence over a 0.04 s interval. Data was obtained from a 1 minute recording with a total of 35484 fluorescence and 46101 scattering events.

4.4 Paper 4: 'Lab-in-a-fiber based particle separation and counting'

In paper 4, we present the integration of separation and detection of microparticles in a continuous flow all-fiber based capillary system. Here, elasto inertial microfluidics was combined with optics and mircocapillaries to first separate different sized particles followed by counting of the separated particles. A series of different capillary sizes were fused in sequence to achieve the separation and detection in a continuous flow system. We designed a five-hole microcapillary that carries the sheath in the center while the sample with the particles were kept at the four holes as shown in figure 4.9. This allowed to pre-position the particles away from the center to enable differential migration-based separation of particles based on sizes. To understand the differential migration behavior of a particle, different parameters were studied such as the flow rate needed to achieve differential migration, length of the separation capillary for the migration of particles to the center and different particle size. A sample mixture of 1 μm (red) and 10 μm (green) fluorescent particles were kept in the annular space (away from the center) of the capillary with the help of the sheath at the center, pushed at a higher flow rate compared to the sample. The bigger particles migrated towards the center, whereas the smaller particles were focused around the annulus of the capillary (Figure 4.10). Experimentally, we found that a minimum of 4 cm capillary length was required for the bigger particle to completely migrate to the center of the capillary while smaller particle were scattered close to the walls (away from the center) . The flow rate plays a crucial role in the migration of particles. A flow rate of the sheath (40 μL/min) at the center and sample (10 μL/min) from the side inlets allows the bigger particle to gradually migrate to the center. As shown in figure 4.11, it can be seen that the 10 μm particles were focused in the center while the 1 μm particles were away from the center. Separation efficiency of 100% for the 10 μm particles and 97% for the 1 μm particles was achieved, as shown in figure 4.12. The separated 10 μm particles were then counted in a continuous flow system, at a rate of 1400 particles/min as a proof of concept. The entire process from separation to detection was performed in a single step without any interventions. In summary, we introduced a Lab-in-a-fiber system, comprising of a single component, which is capable of separation with higher efficiency and detection of particle at the same time. To the best of our knowledge, this is the first time inertial microfluidics-based separation has been combined with

particle counting in an integrated system. This technology has greater potential in cancer cell isolation and detection.

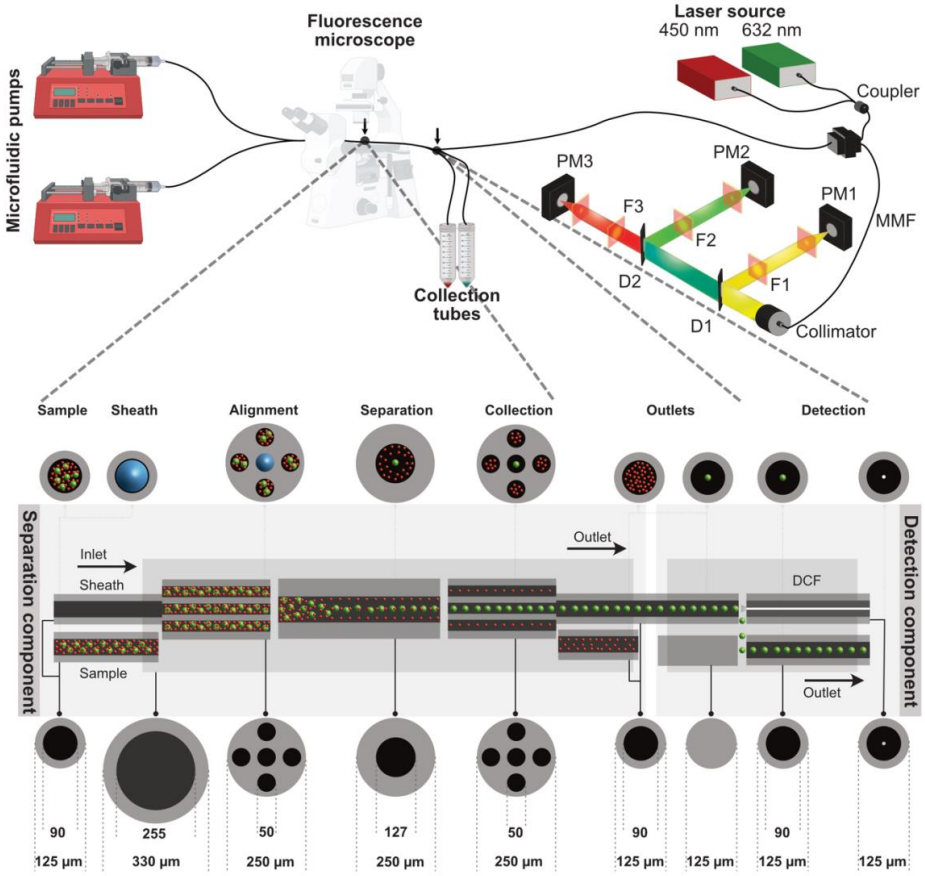

Figure 4.9: Experimental setup for separating the 10 µm green and 1 µm red fluorescent microparticles using an all-fiber separation component. The microfluidic pumps infuses visco-elastic fluid mixed with fluorescent microparticles. The separated particles exit the component in two distinct capillaries and the 10 µm fluorescent microparticles are counted. A fluorescence microscope is used for taking images of the microparticles at various intervals as they migrate through the all-fiber component.

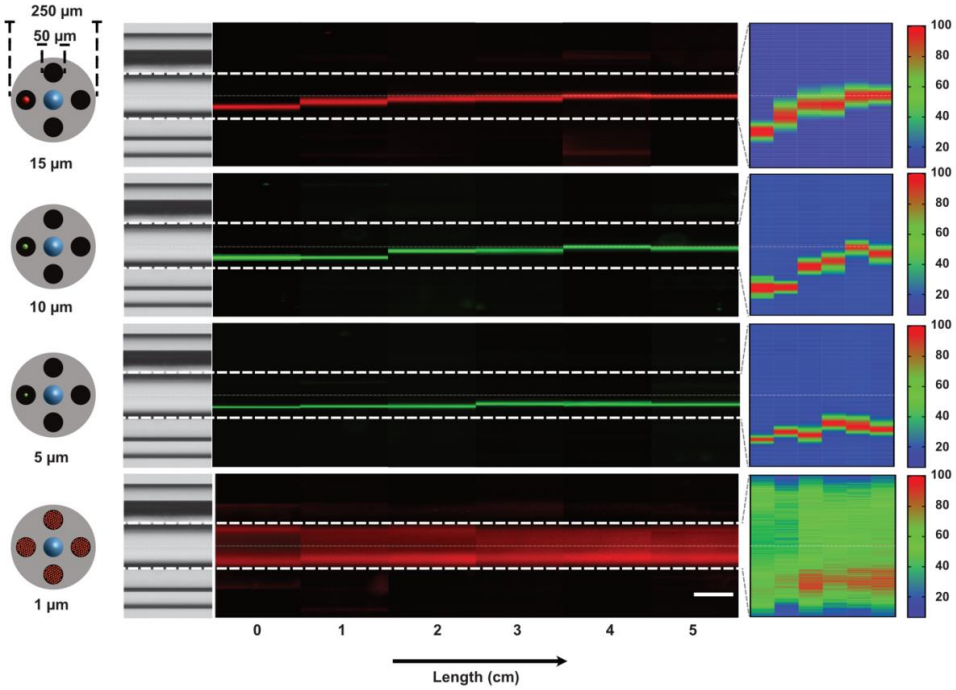

Figure 4.10: Fluorescent images of the separation channel taken from entrance up to 5 cm at an interval of 1 cm for identifying the migratory behavior of particles. The flow rates are 10 µL/min for sample and 40 µL/min for sheath. Larger particles enter the separation capillary pre-focussed whereas the 1 µm particle enters from all four holes of the 5-hole capillary. 15 µm particle at the top migrates to the center of the capillary within 3 cm from the entrance whereas the 1 µm particle remains unfocussed within 5 cm.

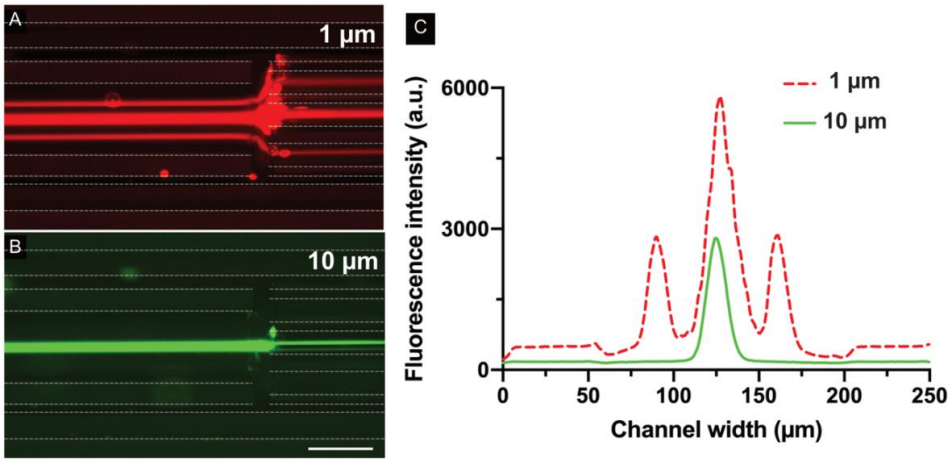

Figure 4.11: A) Fluorescent image of the end of separation capillary taken during separation where the 1 µm red particles are separated from the center and enter the outer four holes of the 5-hole fiber, B) fluorescent image of the same where the 10 µm green fluorescent particles are focused to the center and enter the central hole of 5-hole capillary. C) Normalized intensity graph of the cross-section at the end of the separation capillary showing focusing of the 10 µm particles (green).

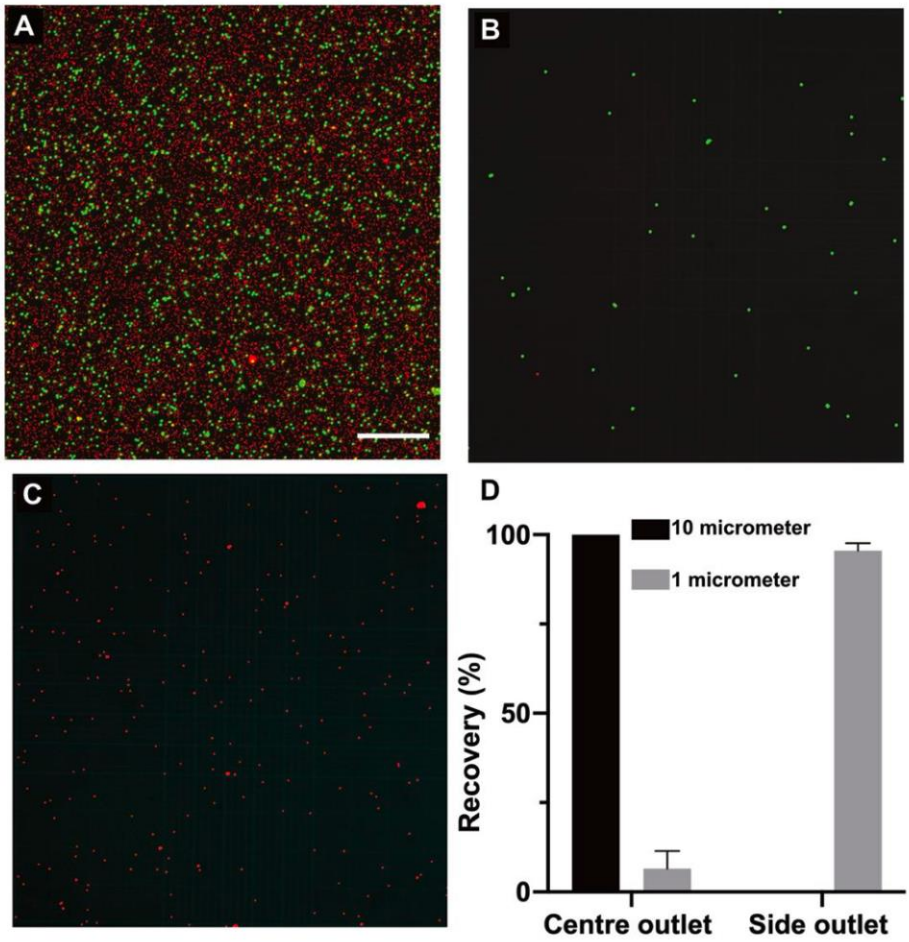

Figure 4.12: Enrichment analysis of separated particles. Results showing the separation efficiency of 1 and 10 µm particles calculated using a hemocytometer. A) Fluorescent images of 1 (red) and 10 (green) µm particles before separation, B and C) Fluorescent images after processing the sample through the separation device. D) The graph shows a 100% separation of 10 µm particle and 97% of 1 µm particles.

4.5 Paper 5: 'Multi-layer assembly of cellulose nanofibrils in a microfluidic device for the selective capture and release of viable tumor cells from whole blood'

In paper 5, we developed a novel technique for affinity-based capturing of cancer cells from whole blood followed by release for downstream analysis. A layer-by-layer (LBL) method was adopted to create a uniform layer of cellulose nanofibril (CNF) surface on microfluidic channel. By taking advantage of the polyelectrolyte polymers, alternating layers of cellulose nanofibrils, which are negatively charged, was built on top of positively charged polymers such as polyallylamine hydrochloride (PAH) and polyethyleneimine (PEI). Figure 4.13 shows the overall process of building the multiple layers of CNF, anchoring antibodies to capture CTCs, and finally releasing it. To achieve a uniform coating of CNF across the microfluidic device, different parameters were taken into consideration, such as the concentration of CNF and the incubation time required between each layer before building the next layer. A final concentration of 0.23 g/L with a 10 minutes incubation time was found to be sufficient to build each CNF layer. A minimum of 5 layers was built to achieve a uniform distribution of CNF to reduce the unspecific binding of antibodies and cells on the surface of the microfluidic chip. Viscozyme L cellulolytic enzyme mixture, which does not affect the cell viability, was used to digest the CNF layers, a process that takes only 30 minutes, as shown in figure 4.14. After successful optimization, we demonstrated the capturing and release of cancer cells spiked in whole blood, as shown in figure 4.15. A capture efficiency of 97% was achieved on the chip. The captured cancer cells were released with an efficiency of 80% from the microfluidic chip. Also, after releasing, 97% of the released cells were viable. The high releasing efficiency and high viability allows for further downstream analysis to be performed such as molecular studies including next-generation sequencing. In summary, a novel LBL based surface modification method was applied on microfluidic devices which enabled capturing and releasing cancer cells from whole blood. The possibility of releasing the cancer cells with high viability rate, opens several possibilities to interrogate the cancer cells, including culturing the primary cells and single cell “omics”. Access to the cells is going to be important to know more about the origin of the cancer, prognosis development, proteomic and genomic content to tailor the treatment and much more.

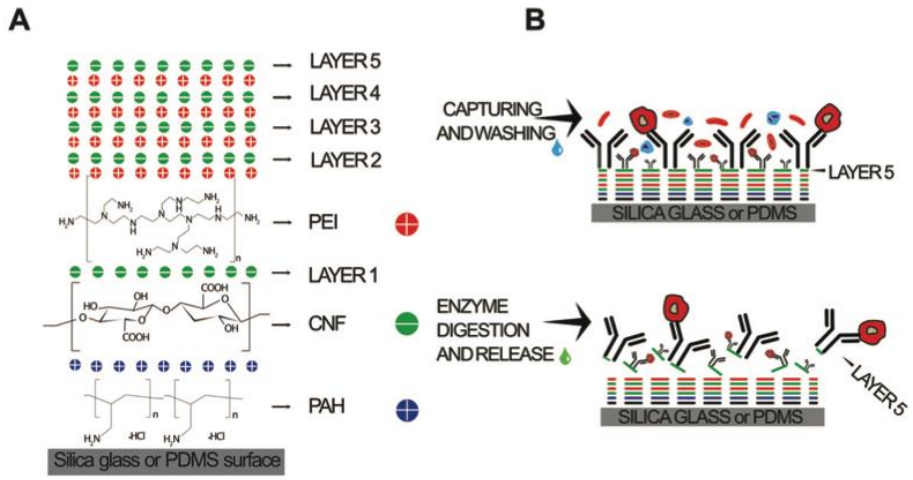

Figure 4.13: Schematics of LbL CNF assembly for affinity cell capture and enzymatic release and AFM characterization. (A) CNF LbL buildup at neutral pH on a surface modified with PAH. Both PEI and PAH have a global positive charge, while CNF has a global negative charge. (B) Affinity cell capture after conjugating anti-EpCAM antibodies on the upper layer of CNF (top), followed by digestion of the CNF layers using a cocktail of cellulolytic enzymes resulting in the release of trapped cells (bottom).

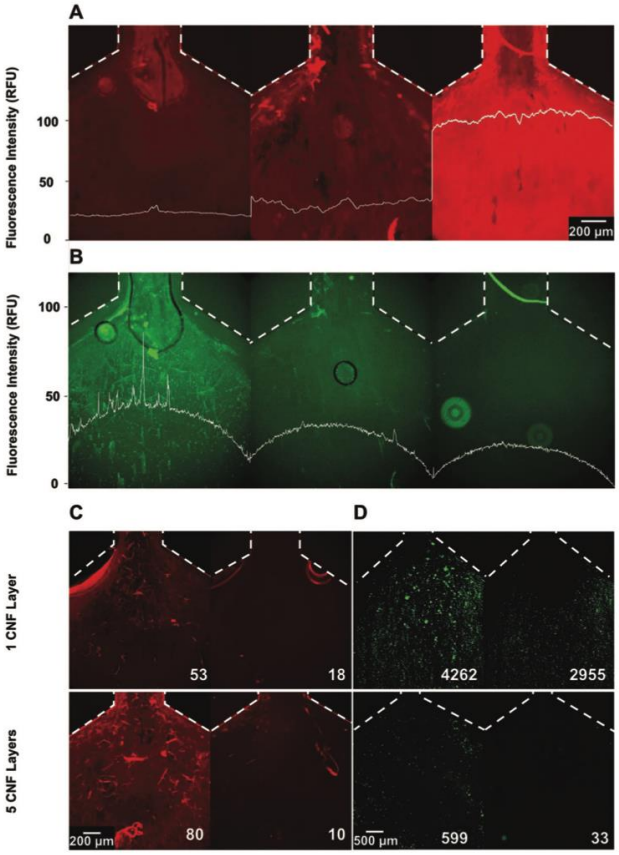

Figure 4.14: Effect of increasing numbers of CNF layers on CNF surface density, antibody immobilization, enzymatic CNF release and cell capture/release. Dotted lines indicate the border of the microchannel. The plots superimposed with the fluorescence microscopy images quantify the average lateral fluorescent intensity across the channel. (A) Cellulose surface density and homogeneity measured with CarbotraceTM 680 after coating 1, 3 or 5 CNF layers, from left to right, respectively. (B) Alexa 430 labeled anti-EpCAM antibody surface density with 1, 3 or 5 CNF layers from left to right, respectively. The results in A and B were measured in 3 independent devices, each coated with 1, 3 or 5 CNF layers. (C) Cellulose after coating (left) and after 30 min of enzyme digestion for 1 (top) and 5 (bottom) layers of CNF. The values indicate the background subtracted average fluorescence on the channel surface. (D) HCT 116 cell capture (left) and subsequent release (right) for 1 (top) and 5 (bottom) layers of CNF. The values indicate the total cell count in each image.

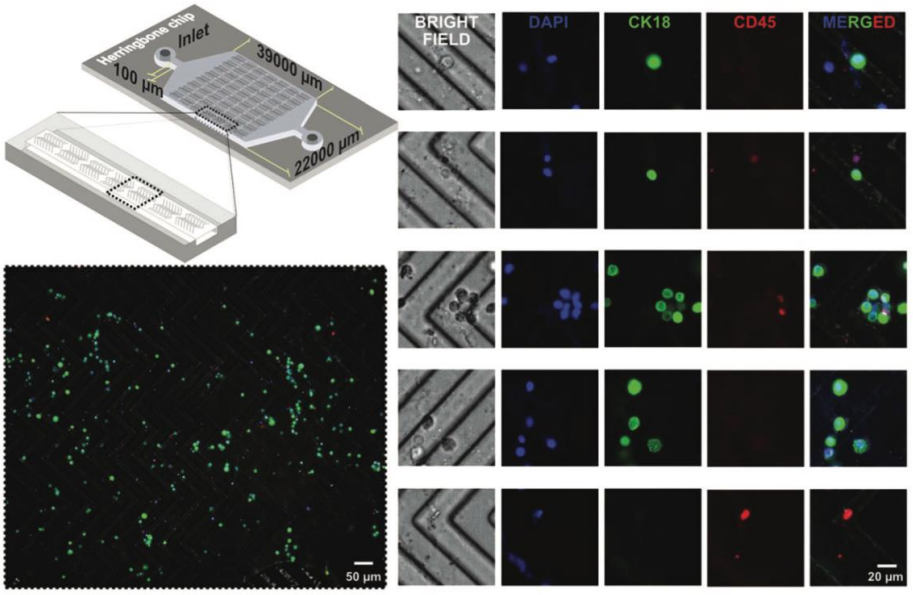

Figure 4.15: Schematics of the HB-Chip and HCT 116 cell capture directly from whole blood. On-chip immunocytochemistry was performed after cell capture. All images were acquired in a single device after flowing whole blood for 2 min at 41.25 µL min−1.

Chapter 5: Conclusion and outlook

This thesis focused at developing innovative methods to isolate rare CTCs from whole blood using different microfluidic approaches. The current gold standard in detecting cancer is primarily based on taking tissue biopsy, advanced imaging, and extensive invasive procedures. The current gold standard techniques available are often very invasive causing discomfort to the patient. Liquid biopsy is a new trend in cancer diagnostics, where non-invasive peripheral blood is used to look for biomarkers. It is a minimally invasive procedure and has the potential to provide a spectrum of information, such as CTCs originating from the tumor, tumor DNA/RNA released by the CTCs in the circulation, and exosomes which carry vital information about the cancer cells. Microfluidics is an enabling technology that has the potential to isolate and investigate cells and biomolecules in the blood. This thesis mainly focused on isolating CTCs from whole blood using microfluidics. We focused on two aspects of separation methods: biophysical and biochemical markers specific to cancer cells. The biophysical marker approach relies on the size of cancer cells compared to other cells present in the blood. On the other hand, the biochemical approach relies on the surface marker expressed on the surface, such as EpCAM, which is not found in other cells circulating in the blood. Due to heterogeneity of cancer cells, it is important to investigate several methods and find the best suited one. It is therefore important to pay attention to both approaches, because there is a high risk of missing CTCs because they are so rare in the complex biofluid.

We contributed some new findings to the rapidly evolving inertial microfluidic-based separation methods. Inertial microfluidics relies on the geometry of the microfluidic chip, hydrodynamic forces, and the size of the particle. In our work, we extensively studied the physics of viscoelastic fluid confined and flowing in a rectangular channel and circular microcapillaries. The physics of elasto inertial microfluidics at high Reynolds numbers, especially flow through curved channels, have been poorly understood. In this thesis work, we investigated this and demonstrated particle focusing in flow through curved, spiral, channels at throughputs previously only demonstrated in inertial microfluidics. Based on the fundamental understanding on particle focusing behaviour at high Reynolds numbers, the next steps will be to apply this technology to sort CTCs from whole blood for cancer diagnostics. While outside the focus on this thesis, current work in our group is focusing on this.

The fundamentals of particle behaviour in viscoelastic fluid flow was studied numerically and experimentally in flows through straight channels. Different concentrations of PEO were tested in a circular capillary. As the concentration of PEO increases, the microparticles experiences more elastic force which pushes the particles closer to the centre of the capillary. The possibility for analogue fine-tuning particle focusing position has the potential to open up applications in sorting and counting. Traditional lab-on-chip based devices often lack the integration of optical components to detect cells and particles in a continuous flow system. Towards this, we built lab-in-a-fiber based optofluidic device where the fluidics and optical detection are integrated. We developed an all silica microflow cytometer where we could focus different sized microparticles and cells in the capillary in viscoelastic fluid flow. We focused particles and cells at a high flow rate and detected both the fluorescent signal and scattering of the particle. In order to demonstrate the feasibility of a point-of-care device, we were able to identify a cancer cell line. Next, the capillary platform was further developed to combine separation and detection. Separation of different-sized particles and detection of the separated particle were accomplished in a continuous system by fusing a series of capillaries with various geometries. A higher throughput is still required even after successful separation and detection. As a result of the capillary setup's high resistance, it was unable to achieve a high flow rate. We can increase throughput by shortening the overall length and altering the general design. Finally, as an alternative approach, we also focused on the biochemical marker EpCAM, which is expressed on the surface of the CTCs. A novel Layer-by-Layer method was adapted to the microfluidic device using the naturally abundant material cellulose nanofibrils. CNF allowed us to capture cells and release them enzymatically in 30 minutes without harming the captured cells. This allowed for greater viability after release, which can be used for several downstream analyses.

This thesis provides an overview of integrating different technologies isolating cancer cells with greater efficiency. It is important to always consider the complex nature of the sample matrix and type of cancer and opt for different isolation techniques. While a single isolation technique can be attractive, integrating different techniques such as the biophysical and biochemical properties might result in improved CTC purity and yield. Also, CTC separation alone is not enough to provide information on what a physician might need. Accessing viable cells and doing further

downstream analysis, including next-generation sequencing and other omics analysis will provide improved cancer patient management. The isolation of CTCs is an essential sample preparation step that can analyse the sample in different ways to provide tailored treatment to the patient. I believe microfluidics will be a key enabler in cancer management in the future.

Acknowledgements

I want to thank my supervisor Aman Russom, who believed in me and allowed me to show my talents. I thank my co-supervisors, Fredrik Laurell and Gustaf Mårtensson, for their support throughout my education. I also thank Walter Margulis and my mentor Matthias Löhr for always cheering me up and providing a positive environment to work in. I thank all my past and present colleagues in the Nanobiotechnology division for making my days enjoyable at the workspace.

I would have never been where I am today if I had not been loved by the people mentioned below. I thank my grandmother Jayalakshmi and my grandfather Govindasamy who only showed their love and nothing else. I will forever be indebted to you both. My parents, Malarvizhi and Kumar, tried their best to provide what I wanted; thank you. My in-laws, Lakshmi Prabha and Ravisankar thank you for all the support and love you provided. My aunt and uncle, Selvakumarie and Kanapathy, are the most important people in my life. You both were always there for me during good and bad times. Your generosity is what my life is made of! I will make sure to give that back to the one who needs it.

Last but not least, my wife, Sharulatha. We will complete ten years together when I defend this thesis. Thank you for being there for me always as a friend, wife, and now as a mother to our child! I do not think I will be complete without you. Finally, a warm welcome to our baby Sara into this world. You will be here to watch me defend my thesis. I cannot wait to spend the rest of my life with the most beautiful two ladies in my life! I love you both.

Spread love and be nice to everyone!

Bibliography

1 KA, S. The cell cycle- A review. *Veterinary Pathology* **35(6)**, 461-478, doi:10.1177/030098589803500601 (1998).

2 Pardee, A. B. A restriction point for control of normal animal cell proliferation. *Proc Natl Acad Sci U S A* **71**, 1286-1290, doi:10.1073/pnas.71.4.1286 (1974).

3 Hartwell, L. H., Culotti, J., Pringle, J. R. & Reid, B. J. Genetic Control of the Cell Division Cycle in Yeast. *Science* **183**, 46-51, doi:doi:10.1126/science.183.4120.46 (1974).

4 Johnson, D. G. & Walker, C. L. CYCLINS AND CELL CYCLE CHECKPOINTS. *Annual Review of Pharmacology and Toxicology* **39**, 295-312, doi:10.1146/annurev.pharmtox.39.1.295 (1999).

5 Elledge, S. J. Cell Cycle Checkpoints: Preventing an Identity Crisis. *Science* **274**, 1664-1672, doi:doi:10.1126/science.274.5293.1664 (1996).

6 Hartwell, L. H. & Weinert, T. A. Checkpoints: controls that ensure the order of cell cycle events. *Science* **246**, 629-634, doi:10.1126/science.2683079 (1989).

7 Wang, Z. Regulation of Cell Cycle Progression by Growth Factor-Induced Cell Signaling. *Cells* **10**, doi:10.3390/cells10123327 (2021).

8 Froelich-Ammon, S. J. & Osheroff, N. Topoisomerase poisons: harnessing the dark side of enzyme mechanism. *J Biol Chem* **270**, 21429-21432, doi:10.1074/jbc.270.37.21429 (1995).

9 Branzei, D. & Foiani, M. Regulation of DNA repair throughout the cell cycle. *Nature Reviews Molecular Cell Biology* **9**, 297-308, doi:10.1038/nrm2351 (2008).

10 Lonati, L., Barbieri, S., Guardamagna, I., Ottolenghi, A. & Baiocco, G. Radiation-induced cell cycle perturbations: a computational tool validated with flow-cytometry data. *Scientific Reports* **11**, 925, doi:10.1038/s41598-020-79934-3 (2021).

11 Hustedt, N. & Durocher, D. The control of DNA repair by the cell cycle. *Nature Cell Biology* **19**, 1-9, doi:10.1038/ncb3452 (2017).

12 De Falco, M. & De Felice, M. Take a Break to Repair: A Dip in the World of Double-Strand Break Repair Mechanisms Pointing the Gaze on Archaea. *Int J Mol Sci* **22**, doi:10.3390/ijms222413296 (2021).
13 Kastan, M., Bartek. Cell-cycle checkpoints and cancer. *Nature* **432**, 316–323, doi:https://doi.org/10.1038/nature03097 (2004).
14 Carusillo, A. & Mussolino, C. DNA Damage: From Threat to Treatment. *Cells* **9**, doi:10.3390/cells9071665 (2020).
15 Lord, C. J. & Ashworth, A. The DNA damage response and cancer therapy. *Nature* **481**, 287-294, doi:10.1038/nature10760 (2012).
16 Siegel, R. L., Miller, K. D., Fuchs, H. E. & Jemal, A. Cancer Statistics, 2021. *CA: A Cancer Journal for Clinicians* **71**, 7-33, doi:https://doi.org/10.3322/caac.21654 (2021).
17 Roy, P. S. & Saikia, B. J. Cancer and cure: A critical analysis. *Indian J Cancer* **53**, 441-442, doi:10.4103/0019-509x.200658 (2016).
18 Quail, D. F. & Joyce, J. A. Microenvironmental regulation of tumor progression and metastasis. *Nat Med* **19**, 1423-1437, doi:10.1038/nm.3394 (2013).
19 Duesberg, P., Li, R., Fabarius, A. & Hehlmann, R. The Chromosomal Basis of Cancer. *Cellular Oncology* **27**, 951598, doi:10.1155/2005/951598 (2005).
20 Tufail, A. B. *et al.* Deep Learning in Cancer Diagnosis and Prognosis Prediction: A Minireview on Challenges, Recent Trends, and Future Directions. *Comput Math Methods Med* **2021**, 9025470, doi:10.1155/2021/9025470 (2021).
21 Torre, L. A., Siegel, R. L., Ward, E. M. & Jemal, A. Global Cancer Incidence and Mortality Rates and Trends--An Update. *Cancer Epidemiol Biomarkers Prev* **25**, 16-27, doi:10.1158/1055-9965.Epi-15-0578 (2016).
22 Cairns, J. *Cancer: Science and Society*. (W. H. Freeman, 1978).
23 Vogelstein, B. & Kinzler, K. W. The multistep nature of cancer. *Trends Genet* **9**, 138-141, doi:10.1016/0168-9525(93)90209-z (1993).
24 Weinberg, R. A. How cancer arises. *Sci Am* **275**, 62-70, doi:10.1038/scientificamerican0996-62 (1996).
25 O'Connor, M. J. Targeting the DNA Damage Response in Cancer. *Mol Cell* **60**, 547-560, doi:10.1016/j.molcel.2015.10.040 (2015).
26 Basu, B., Yap, T. A., Molife, L. R. & de Bono, J. S. Targeting the DNA damage response in oncology: past, present and future perspectives. *Curr Opin Oncol* **24**, 316-324, doi:10.1097/CCO.0b013e32835280c6 (2012).

27 Liang, Y., Lin, S. Y., Brunicardi, F. C., Goss, J. & Li, K. DNA damage response pathways in tumor suppression and cancer treatment. *World J Surg* **33**, 661-666, doi:10.1007/s00268-008-9840-1 (2009).
28 Hanahan, D. & Weinberg, R. A. Hallmarks of cancer: the next generation. *Cell* **144**, 646-674, doi:10.1016/j.cell.2011.02.013 (2011).
29 Holm, J. B., Rosendahl, A. H. & Borgquist, S. Local Biomarkers Involved in the Interplay between Obesity and Breast Cancer. *Cancers (Basel)* **13**, doi:10.3390/cancers13246286 (2021).
30 Fouad, Y. A. & Aanei, C. Revisiting the hallmarks of cancer. *Am J Cancer Res* **7**, 1016-1036 (2017).
31 Dai, X., Xiang, L., Li, T. & Bai, Z. Cancer Hallmarks, Biomarkers and Breast Cancer Molecular Subtypes. *J Cancer* **7**, 1281-1294, doi:10.7150/jca.13141 (2016).
32 Suhail, Y. *et al.* Systems Biology of Cancer Metastasis. *Cell Syst* **9**, 109-127, doi:10.1016/j.cels.2019.07.003 (2019).
33 Clarke, R. *et al.* A systems biology approach to discovering pathway signaling dysregulation in metastasis. *Cancer Metastasis Rev* **39**, 903-918, doi:10.1007/s10555-020-09921-7 (2020).
34 Zeeshan, R. & Mutahir, Z. Cancer metastasis - tricks of the trade. *Bosn J Basic Med Sci* **17**, 172-182, doi:10.17305/bjbms.2017.1908 (2017).
35 Li, F., Tiede, B., Massagué, J. & Kang, Y. Beyond tumorigenesis: cancer stem cells in metastasis. *Cell Res* **17**, 3-14, doi:10.1038/sj.cr.7310118 (2007).
36 Bernstein, L. R. & Liotta, L. A. Molecular mediators of interactions with extracellular matrix components in metastasis and angiogenesis. *Curr Opin Oncol* **6**, 106-113, doi:10.1097/00001622-199401000-00015 (1994).
37 Klein, C. A. Cancer progression and the invisible phase of metastatic colonization. *Nat Rev Cancer* **20**, 681-694, doi:10.1038/s41568-020-00300-6 (2020).
38 Lorusso, G. & Rüegg, C. New insights into the mechanisms of organ-specific breast cancer metastasis. *Semin Cancer Biol* **22**, 226-233, doi:10.1016/j.semcancer.2012.03.007 (2012).
39 Chung, L. W., Baseman, A., Assikis, V. & Zhau, H. E. Molecular insights into prostate cancer progression: the missing link of tumor microenvironment. *J Urol* **173**, 10-20, doi:10.1097/01.ju.0000141582.15218.10 (2005).

40 Kauffman, E. C., Robinson, V. L., Stadler, W. M., Sokoloff, M. H. & Rinker-Schaeffer, C. W. Metastasis suppression: the evolving role of metastasis suppressor genes for regulating cancer cell growth at the secondary site. *J Urol* **169**, 1122-1133, doi:10.1097/01.ju.0000051580.89109.4b (2003).

41 Géraud, C., Koch, P. S., Damm, F., Schledzewski, K. & Goerdt, S. The metastatic cycle: metastatic niches and cancer cell dissemination. *J Dtsch Dermatol Ges* **12**, 1012-1019, doi:10.1111/ddg.12451 (2014).

42 Kath, R. & Schmidt, C. G. [Tumor progression and metastasis]. *Zentralbl Chir* **115**, 785-792 (1990).

43 Haraldsdottir, S., Einarsdottir, H. M., Smaradottir, A., Gunnlaugsson, A. & Halfdanarson, T. R. [Colorectal cancer - review]. *Laeknabladid* **100**, 75-82, doi:10.17992/lbl.2014.02.531 (2014).

44 Qiu, Z. *et al.* A Pharmacogenomic Landscape in Human Liver Cancers. *Cancer Cell* **36**, 179-193.e111, doi:10.1016/j.ccell.2019.07.001 (2019).

45 Ferguson, J. L. & Turner, S. P. Bone Cancer: Diagnosis and Treatment Principles. *Am Fam Physician* **98**, 205-213 (2018).

46 Paoletti, C. & Hayes, D. F. Circulating Tumor Cells. *Adv Exp Med Biol* **882**, 235-258, doi:10.1007/978-3-319-22909-6_10 (2016).

47 Zhong, X. *et al.* Circulating tumor cells in cancer patients: developments and clinical applications for immunotherapy. *Mol Cancer* **19**, 15, doi:10.1186/s12943-020-1141-9 (2020).

48 Ruoslahti, E. & Reed, J. C. Anchorage dependence, integrins, and apoptosis. *Cell* **77**, 477-478, doi:10.1016/0092-8674(94)90209-7 (1994).

49 Diamantopoulou, Z., Castro-Giner, F. & Aceto, N. Circulating tumor cells: Ready for translation? *J Exp Med* **217**, doi:10.1084/jem.20200356 (2020).

50 Micalizzi, D. S., Maheswaran, S. & Haber, D. A. A conduit to metastasis: circulating tumor cell biology. *Genes Dev* **31**, 1827-1840, doi:10.1101/gad.305805.117 (2017).

51 Cristofanilli, M. *et al.* Circulating tumor cells, disease progression, and survival in metastatic breast cancer. *N Engl J Med* **351**, 781-791, doi:10.1056/NEJMoa040766 (2004).

52 Allard, W. J. *et al.* Tumor cells circulate in the peripheral blood of all major carcinomas but not in healthy subjects or patients with nonmalignant diseases. *Clin Cancer Res* **10**, 6897-6904, doi:10.1158/1078-0432.Ccr-04-0378 (2004).

53 Krebs, M. G. *et al.* Molecular analysis of circulating tumour cells-biology and biomarkers. *Nat Rev Clin Oncol* **11**, 129-144, doi:10.1038/nrclinonc.2013.253 (2014).
54 Follain, G. *et al.* Hemodynamic Forces Tune the Arrest, Adhesion, and Extravasation of Circulating Tumor Cells. *Dev Cell* **45**, 33-52.e12, doi:10.1016/j.devcel.2018.02.015 (2018).
55 Pantel, K. & Alix-Panabières, C. The clinical significance of circulating tumor cells. *Nature Clinical Practice Oncology* **4**, 62-63, doi:10.1038/ncponc0737 (2007).
56 Schlange, T. & Pantel, K. Potential of circulating tumor cells as blood-based biomarkers in cancer liquid biopsy. *Pharmacogenomics* **17**, 183-186, doi:10.2217/pgs.15.163 (2016).
57 Aceto, N. *et al.* Circulating tumor cell clusters are oligoclonal precursors of breast cancer metastasis. *Cell* **158**, 1110-1122, doi:10.1016/j.cell.2014.07.013 (2014).
58 Martin-Harris, B. *et al.* Best Practices in Modified Barium Swallow Studies. *Am J Speech Lang Pathol* **29**, 1078-1093, doi:10.1044/2020_ajslp-19-00189 (2020).
59 Furlow, B. Barium swallow. *Radiol Technol* **76**, 49-58; quiz 59-61 (2004).
60 Prevrhal, S. [Absorptiometry]. *Radiologe* **46**, 847-860, doi:10.1007/s00117-006-1414-3 (2006).
61 Clasey, J. L. *et al.* Body composition by DEXA in older adults: accuracy and influence of scan mode. *Med Sci Sports Exerc* **29**, 560-567, doi:10.1097/00005768-199704000-00020 (1997).
62 Partovi, S. *et al.* Fast MRI breast cancer screening - Ready for prime time. *Clin Imaging* **60**, 160-168, doi:10.1016/j.clinimag.2019.10.013 (2020).
63 Zugni, F. *et al.* Whole-body magnetic resonance imaging (WB-MRI) for cancer screening in asymptomatic subjects of the general population: review and recommendations. *Cancer Imaging* **20**, 34, doi:10.1186/s40644-020-00315-0 (2020).
64 Niell, B. L., Freer, P. E., Weinfurtner, R. J., Arleo, E. K. & Drukteinis, J. S. Screening for Breast Cancer. *Radiol Clin North Am* **55**, 1145-1162, doi:10.1016/j.rcl.2017.06.004 (2017).
65 Coleman, C. Early Detection and Screening for Breast Cancer. *Semin Oncol Nurs* **33**, 141-155, doi:10.1016/j.soncn.2017.02.009 (2017).

66 de Leon, A. *et al.* Ultrasound Contrast Agents and Delivery Systems in Cancer Detection and Therapy. *Adv Cancer Res* **139**, 57-84, doi:10.1016/bs.acr.2018.04.002 (2018).
67 Deshpande, N., Pysz, M. A. & Willmann, J. K. Molecular ultrasound assessment of tumor angiogenesis. *Angiogenesis* **13**, 175-188, doi:10.1007/s10456-010-9175-z (2010).
68 Foley, R. W. *et al.* Chest X-ray in suspected lung cancer is harmful. *Eur Radiol* **31**, 6269-6274, doi:10.1007/s00330-021-07708-0 (2021).
69 Miyahara, R., Furukawa, K. & Hirooka, Y. [X-ray screening for gastric cancer]. *Nihon Shokakibyo Gakkai Zasshi* **117**, 463-468, doi:10.11405/nisshoshi.117.463 (2020).
70 London, S., Hoilat, G. J. & Tichauer, M. B. in *StatPearls* (StatPearls Publishing Copyright © 2021, StatPearls Publishing LLC., 2021).
71 Cho, S. D., Groves, E. & Lao, V. V. History of High-Resolution Anoscopy. *Clin Colon Rectal Surg* **31**, 336-346, doi:10.1055/s-0038-1668103 (2018).
72 Millien, V. O. & Mansour, N. M. Bowel Preparation for Colonoscopy in 2020: A Look at the Past, Present, and Future. *Curr Gastroenterol Rep* **22**, 28, doi:10.1007/s11894-020-00764-4 (2020).
73 Bodilsen, J. *et al.* Association of Lumbar Puncture With Spinal Hematoma in Patients With and Without Coagulopathy. *Jama* **324**, 1419-1428, doi:10.1001/jama.2020.14895 (2020).
74 Marton, K. I. & Gean, A. D. The spinal tap: a new look at an old test. *Ann Intern Med* **104**, 840-848, doi:10.7326/0003-4819-104-6-840 (1986).
75 DeVita, V. T., Lawrence, T. S. & Rosenberg, S. A. *DeVita, Hellman, and Rosenberg's cancer: principles & practice of oncology*. Vol. 2 (Lippincott Williams & Wilkins, 2008).
76 Filippini, S. E. & Vega, A. Breast cancer genes: beyond BRCA1 and BRCA2. *Front Biosci (Landmark Ed)* **18**, 1358-1372, doi:10.2741/4185 (2013).
77 Saleem, M. *et al.* The BRCA1 and BRCA2 Genes in Early-Onset Breast Cancer Patients. *Adv Exp Med Biol* **1292**, 1-12, doi:10.1007/5584_2018_147 (2020).
78 Hellman, S. & Vokes, E. E. Advancing Current Treatments for Cancer. *Scientific American* **275**, 118-123 (1996).
79 Sidransky, D. Advances in Cancer Detection. *Scientific American* **275**, 104-109 (1996).

80 Cristofanilli, M. *et al.* Circulating Tumor Cells, Disease Progression, and Survival in Metastatic Breast Cancer. *New England Journal of Medicine* **351**, 781-791, doi:10.1056/NEJMoa040766 (2004).
81 Cohen, S. J. *et al.* Relationship of circulating tumor cells to tumor response, progression-free survival, and overall survival in patients with metastatic colorectal cancer. *J Clin Oncol* **26**, 3213-3221, doi:10.1200/jco.2007.15.8923 (2008).
82 Danila, D. C. *et al.* Circulating tumor cell number and prognosis in progressive castration-resistant prostate cancer. *Clin Cancer Res* **13**, 7053-7058, doi:10.1158/1078-0432.Ccr-07-1506 (2007).
83 Poulet, G., Massias, J. & Taly, V. Liquid Biopsy: General Concepts. *Acta Cytol* **63**, 449-455, doi:10.1159/000499337 (2019).
84 Kallergi, G. *et al.* Epithelial to mesenchymal transition markers expressed in circulating tumour cells of early and metastatic breast cancer patients. *Breast Cancer Res* **13**, R59, doi:10.1186/bcr2896 (2011).
85 Myung, J. H. & Hong, S. Microfluidic devices to enrich and isolate circulating tumor cells. *Lab Chip* **15**, 4500-4511, doi:10.1039/c5lc00947b (2015).
86 Banys-Paluchowski, M., Reinhardt, F. & Fehm, T. Disseminated Tumor Cells and Dormancy in Breast Cancer Progression. *Adv Exp Med Biol* **1220**, 35-43, doi:10.1007/978-3-030-35805-1_3 (2020).
87 Dasgupta, A., Lim, A. R. & Ghajar, C. M. Circulating and disseminated tumor cells: harbingers or initiators of metastasis? *Mol Oncol* **11**, 40-61, doi:10.1002/1878-0261.12022 (2017).
88 Lin, H., Balic, M., Zheng, S., Datar, R. & Cote, R. J. Disseminated and circulating tumor cells: Role in effective cancer management. *Crit Rev Oncol Hematol* **77**, 1-11, doi:10.1016/j.critrevonc.2010.04.008 (2011).
89 Balic, M. *et al.* Most early disseminated cancer cells detected in bone marrow of breast cancer patients have a putative breast cancer stem cell phenotype. *Clin Cancer Res* **12**, 5615-5621, doi:10.1158/1078-0432.Ccr-06-0169 (2006).
90 Gerber, B. *et al.* Simultaneous immunohistochemical detection of tumor cells in lymph nodes and bone marrow aspirates in breast cancer and its correlation with other prognostic factors. *J Clin Oncol* **19**, 960-971, doi:10.1200/jco.2001.19.4.960 (2001).
91 Schindlbeck, C. *et al.* Disseminated and circulating tumor cells in bone marrow and blood of breast cancer patients: properties, enrichment, and

potential targets. *J Cancer Res Clin Oncol* **142**, 1883-1895, doi:10.1007/s00432-016-2118-3 (2016).

92 Jin, C. *et al.* Technologies for label-free separation of circulating tumor cells: from historical foundations to recent developments. *Lab on a Chip* **14**, 32-44, doi:10.1039/C3LC50625H (2014).

93 Tsutsuyama, M. *et al.* Detection of circulating tumor cells in drainage venous blood from colorectal cancer patients using a new filtration and cytology-based automated platform. *PLOS ONE* **14**, e0212221, doi:10.1371/journal.pone.0212221 (2019).

94 Akgönüllü, S., Bakhshpour, M., Pişkin, A. K. & Denizli, A. Microfluidic Systems for Cancer Diagnosis and Applications. *Micromachines (Basel)* **12**, doi:10.3390/mi12111349 (2021).

95 Yang, L., Ye, T., Zhao, X., Hu, T. & Wei, Y. Design and Fabrication of a Microfluidic Chip for Particle Size-Exclusion and Enrichment. *Micromachines (Basel)* **12**, doi:10.3390/mi12101218 (2021).

96 Galvis, M. M., Romero, C. S., Bueno, T. O. & Teng, Y. Toward a New Era for the Management of Circulating Tumor Cells. *Adv Exp Med Biol* **1286**, 125-134, doi:10.1007/978-3-030-55035-6_9 (2021).

97 Sun, Y. F. *et al.* Circulating tumor cells: advances in detection methods, biological issues, and clinical relevance. *J Cancer Res Clin Oncol* **137**, 1151-1173, doi:10.1007/s00432-011-0988-y (2011).

98 Williams, A., Balic, M., Datar, R. & Cote, R. Size-based enrichment technologies for CTC detection and characterization. *Recent Results Cancer Res* **195**, 87-95, doi:10.1007/978-3-642-28160-0_8 (2012).

99 Bhagat, A. A. & Lim, C. T. Microfluidic technologies. *Recent Results Cancer Res* **195**, 59-67, doi:10.1007/978-3-642-28160-0_5 (2012).

100 Fleischer, R. L., Price, P. B. & Symes, E. M. Novel Filter for Biological Materials. *Science* **143**, 249-250, doi:10.1126/science.143.3603.249 (1964).

101 Kim, E. H. *et al.* Enrichment of cancer cells from whole blood using a microfabricated porous filter. *Anal Biochem* **440**, 114-116, doi:10.1016/j.ab.2013.05.016 (2013).

102 Ma, Y. C., Wang, L. & Yu, F. L. Recent advances and prospects in the isolation by size of epithelial tumor cells (ISET) methodology. *Technol Cancer Res Treat* **12**, 295-309, doi:10.7785/tcrt.2012.500328 (2013).

103 Liadov, V. K., Skrypnikova, M. A. & Popova, O. P. [Isolation of circulating tumor cells in blood by means of "Isolation by SizE of Tumor cells (ISET)"]. *Vopr Onkol* **60**, 548-552 (2014).
104 Henslee, E. A. Review: Dielectrophoresis in cell characterization. *Electrophoresis* **41**, 1915-1930, doi:10.1002/elps.202000034 (2020).
105 Qian, C. *et al.* Dielectrophoresis for bioparticle manipulation. *Int J Mol Sci* **15**, 18281-18309, doi:10.3390/ijms151018281 (2014).
106 Carey, T. R., Cotner, K. L., Li, B. & Sohn, L. L. Developments in label-free microfluidic methods for single-cell analysis and sorting. *Wiley Interdiscip Rev Nanomed Nanobiotechnol* **11**, e1529, doi:10.1002/wnan.1529 (2019).
107 Chiu, D. T. Cellular manipulations in microvortices. *Anal Bioanal Chem* **387**, 17-20, doi:10.1007/s00216-006-0611-2 (2007).
108 Hur, S. C., Mach, A. J. & Di Carlo, D. High-throughput size-based rare cell enrichment using microscale vortices. *Biomicrofluidics* **5**, 22206, doi:10.1063/1.3576780 (2011).
109 Suwannaphan, T. *et al.* Investigation of Leukocyte Viability and Damage in Spiral Microchannel and Contraction-Expansion Array. *Micromachines (Basel)* **10**, doi:10.3390/mi10110772 (2019).
110 Eyvazi, S. *et al.* Antibody Based EpCAM Targeted Therapy of Cancer, Review and Update. *Curr Cancer Drug Targets* **18**, 857-868, doi:10.2174/1568009618666180102102311 (2018).
111 Armstrong, A. & Eck, S. L. EpCAM: A new therapeutic target for an old cancer antigen. *Cancer Biol Ther* **2**, 320-326, doi:10.4161/cbt.2.4.451 (2003).
112 Riethdorf, S., O'Flaherty, L., Hille, C. & Pantel, K. Clinical applications of the CellSearch platform in cancer patients. *Adv Drug Deliv Rev* **125**, 102-121, doi:10.1016/j.addr.2018.01.011 (2018).
113 Wang, L. *et al.* Promise and limits of the CellSearch platform for evaluating pharmacodynamics in circulating tumor cells. *Semin Oncol* **43**, 464-475, doi:10.1053/j.seminoncol.2016.06.004 (2016).
114 Nagrath, S. *et al.* Isolation of rare circulating tumour cells in cancer patients by microchip technology. *Nature* **450**, 1235-1239, doi:10.1038/nature06385 (2007).
115 Sheng, W. *et al.* Capture, release and culture of circulating tumor cells from pancreatic cancer patients using an enhanced mixing chip. *Lab Chip* **14**, 89-98, doi:10.1039/c3lc51017d (2014).

116 Murlidhar, V. *et al.* A radial flow microfluidic device for ultra-high-throughput affinity-based isolation of circulating tumor cells. *Small* **10**, 4895-4904, doi:10.1002/smll.201400719 (2014).
117 Sackmann, E. K., Fulton, A. L. & Beebe, D. J. The present and future role of microfluidics in biomedical research. *Nature* **507**, 181-189, doi:10.1038/nature13118 (2014).
118 Elvira, K. S., Casadevall i Solvas, X., Wootton, R. C. & deMello, A. J. The past, present and potential for microfluidic reactor technology in chemical synthesis. *Nat Chem* **5**, 905-915, doi:10.1038/nchem.1753 (2013).
119 Jokerst, J. C., Emory, J. M. & Henry, C. S. Advances in microfluidics for environmental analysis. *Analyst* **137**, 24-34, doi:10.1039/c1an15368d (2012).
120 Salieb-Beugelaar, G. B., Simone, G., Arora, A., Philippi, A. & Manz, A. Latest developments in microfluidic cell biology and analysis systems. *Anal Chem* **82**, 4848-4864, doi:10.1021/ac1009707 (2010).
121 Becker, H. & Gärtner, C. Microfluidics and the life sciences. *Sci Prog* **95**, 175-198, doi:10.3184/003685012x13361524970266 (2012).
122 Ortseifen, V., Viefhues, M., Wobbe, L. & Grünberger, A. Microfluidics for Biotechnology: Bridging Gaps to Foster Microfluidic Applications. *Front Bioeng Biotechnol* **8**, 589074, doi:10.3389/fbioe.2020.589074 (2020).
123 Winkler, S., Grünberger, A. & Bahnemann, J. Microfluidics in Biotechnology: Quo Vadis. *Adv Biochem Eng Biotechnol*, doi:10.1007/10_2020_162 (2021).
124 Xu, J., Zhang, Y., Su, X., Zhang, S. & Ge, S. [Application of paper-based microfluidics in point-of-care testing]. *Sheng Wu Gong Cheng Xue Bao* **36**, 1283-1292, doi:10.13345/j.cjb.190518 (2020).
125 Pandey, C. M. *et al.* Microfluidics Based Point-of-Care Diagnostics. *Biotechnol J* **13**, doi:10.1002/biot.201700047 (2018).
126 Gao, D., Jin, F., Zhou, M. & Jiang, Y. Recent advances in single cell manipulation and biochemical analysis on microfluidics. *Analyst* **144**, 766-781, doi:10.1039/c8an01186a (2019).
127 Xiong, B. *et al.* Recent developments in microfluidics for cell studies. *Adv Mater* **26**, 5525-5532, doi:10.1002/adma.201305348 (2014).
128 Xu, X. *et al.* Microfluidic Single-Cell Omics Analysis. *Small* **16**, e1903905, doi:10.1002/smll.201903905 (2020).

129 Ben-Yakar, A. High-Content and High-Throughput In Vivo Drug Screening Platforms Using Microfluidics. *Assay Drug Dev Technol* **17**, 8-13, doi:10.1089/adt.2018.908 (2019).
130 Rienzo, M. *et al.* High-throughput screening for high-efficiency small-molecule biosynthesis. *Metab Eng* **63**, 102-125, doi:10.1016/j.ymben.2020.09.004 (2021).
131 Du, G., Fang, Q. & den Toonder, J. M. Microfluidics for cell-based high throughput screening platforms - A review. *Anal Chim Acta* **903**, 36-50, doi:10.1016/j.aca.2015.11.023 (2016).
132 Drese, K. S. [Lab on a Chip]. *Internist (Berl)* **60**, 339-344, doi:10.1007/s00108-018-0526-y (2019).
133 Sia, S. K. & Kricka, L. J. Microfluidics and point-of-care testing. *Lab Chip* **8**, 1982-1983, doi:10.1039/b817915h (2008).
134 Sorger, P. K. Microfluidics closes in on point-of-care assays. *Nat Biotechnol* **26**, 1345-1346, doi:10.1038/nbt1208-1345 (2008).
135 Priye, A. *et al.* Lab-on-a-Drone: Toward Pinpoint Deployment of Smartphone-Enabled Nucleic Acid-Based Diagnostics for Mobile Health Care. *Anal Chem* **88**, 4651-4660, doi:10.1021/acs.analchem.5b04153 (2016).
136 Priye, A. & Ugaz, V. M. Smartphone-Enabled Detection Strategies for Portable PCR-Based Diagnostics. *Methods Mol Biol* **1571**, 251-266, doi:10.1007/978-1-4939-6848-0_16 (2017).
137 Hu, J. *et al.* Portable microfluidic and smartphone-based devices for monitoring of cardiovascular diseases at the point of care. *Biotechnol Adv* **34**, 305-320, doi:10.1016/j.biotechadv.2016.02.008 (2016).
138 Liu, A. Q. & Yang, C. Optofluidics 2013. *Lab Chip* **13**, 2673-2674, doi:10.1039/c3lc90054a (2013).
139 Pang, L., Chen, H. M., Freeman, L. M. & Fainman, Y. Optofluidic devices and applications in photonics, sensing and imaging. *Lab Chip* **12**, 3543-3551, doi:10.1039/c2lc40467b (2012).
140 Ozcelik, D., Cai, H., Leake, K. D., Hawkins, A. R. & Schmidt, H. Optofluidic bioanalysis: fundamentals and applications. *Nanophotonics* **6**, 647-661, doi:10.1515/nanoph-2016-0156 (2017).
141 Lv, C. *et al.* Integrated optofluidic-microfluidic twin channels: toward diverse application of lab-on-a-chip systems. *Sci Rep* **6**, 19801, doi:10.1038/srep19801 (2016).

142 Sudirman, A., Etcheverry, S., Stjernström, M., Laurell, F. & Margulis, W. A fiber optic system for detection and collection of micrometer-size particles. *Opt Express* **22**, 21480-21487, doi:10.1364/oe.22.021480 (2014).
143 Etcheverry, S. *et al.* High performance micro-flow cytometer based on optical fibres. *Scientific Reports* **7**, doi:10.1038/s41598-017-05843-7 (2017).
144 Kumar, T. *et al.* Optofluidic Fiber Component for Separation and counting of Micron-Sized Particles. *bioRxiv*, 2021.2004.2013.439593, doi:10.1101/2021.04.13.439593 (2021).
145 Zhu, S., Jiang, F., Han, Y., Xiang, N. & Ni, Z. Microfluidics for label-free sorting of rare circulating tumor cells. *Analyst* **145**, 7103-7124, doi:10.1039/d0an01148g (2020).
146 Zhang, X., Zhu, Z., Xiang, N., Long, F. & Ni, Z. Automated Microfluidic Instrument for Label-Free and High-Throughput Cell Separation. *Anal Chem* **90**, 4212-4220, doi:10.1021/acs.analchem.8b00539 (2018).
147 Gossett, D. R. *et al.* Label-free cell separation and sorting in microfluidic systems. *Anal Bioanal Chem* **397**, 3249-3267, doi:10.1007/s00216-010-3721-9 (2010).
148 Warkiani, M. E. *et al.* An ultra-high-throughput spiral microfluidic biochip for the enrichment of circulating tumor cells. *Analyst* **139**, 3245-3255, doi:10.1039/c4an00355a (2014).
149 Volovetskiy, A. B. *et al.* Isolation of Circulating Tumor Cells from Peripheral Blood Samples of Cancer Patients Using Microfluidic Technology. *Sovrem Tekhnologii Med* **12**, 62-68, doi:10.17691/stm2020.12.6.08 (2021).
150 Cho, H. *et al.* Microfluidic technologies for circulating tumor cell isolation. *Analyst* **143**, 2936-2970, doi:10.1039/c7an01979c (2018).
151 Zhou, J., Mukherjee, P., Gao, H., Luan, Q. & Papautsky, I. Label-free microfluidic sorting of microparticles. *APL Bioeng* **3**, 041504, doi:10.1063/1.5120501 (2019).
152 Vaidyanathan, R., Yeo, T. & Lim, C. T. Microfluidics for cell sorting and single cell analysis from whole blood. *Methods Cell Biol* **147**, 151-173, doi:10.1016/bs.mcb.2018.06.011 (2018).
153 Bankó, P. *et al.* Technologies for circulating tumor cell separation from whole blood. *J Hematol Oncol* **12**, 48, doi:10.1186/s13045-019-0735-4 (2019).

154 Tian, C. *et al.* Development and Clinical Prospects of Techniques to Separate Circulating Tumor Cells from Peripheral Blood. *Cancer Manag Res* **12**, 7263-7275, doi:10.2147/cmar.S248380 (2020).
155 Harouaka, R. A. *et al.* Flexible micro spring array device for high-throughput enrichment of viable circulating tumor cells. *Clin Chem* **60**, 323-333, doi:10.1373/clinchem.2013.206805 (2014).
156 Harouaka, R. A. *et al.* Viable circulating tumor cell enrichment by flexible micro spring array. *Annu Int Conf IEEE Eng Med Biol Soc* **2012**, 6269-6272, doi:10.1109/embc.2012.6347427 (2012).
157 Yeh, Y. T., Harouaka, R. A. & Zheng, S. Y. Evaluating a novel dimensional reduction approach for mechanical fractionation of cells using a tandem flexible micro spring array (tFMSA). *Lab Chip* **17**, 691-701, doi:10.1039/c6lc01527a (2017).
158 Zhou, M. D. *et al.* Separable bilayer microfiltration device for viable label-free enrichment of circulating tumour cells. *Sci Rep* **4**, 7392, doi:10.1038/srep07392 (2014).
159 Choi, M. K. *et al.* Circulating tumor cells detected using fluid-assisted separation technique in esophageal squamous cell carcinoma. *J Gastroenterol Hepatol* **34**, 552-560, doi:10.1111/jgh.14543 (2019).
160 Baek, D. H. *et al.* Clinical Potential of Circulating Tumor Cells in Colorectal Cancer: A Prospective Study. *Clin Transl Gastroenterol* **10**, e00055, doi:10.14309/ctg.0000000000000055 (2019).
161 Kim, T. H. *et al.* FAST: Size-Selective, Clog-Free Isolation of Rare Cancer Cells from Whole Blood at a Liquid-Liquid Interface. *Anal Chem* **89**, 1155-1162, doi:10.1021/acs.analchem.6b03534 (2017).
162 Miller, M. C., Robinson, P. S., Wagner, C. & O'Shannessy, D. J. The Parsortix™ Cell Separation System-A versatile liquid biopsy platform. *Cytometry A* **93**, 1234-1239, doi:10.1002/cyto.a.23571 (2018).
163 Jin, X. *et al.* An efficient method for CTCs screening with excellent operability by integrating Parsortix™-like cell separation chip and selective size amplification. *Biomed Microdevices* **20**, 51, doi:10.1007/s10544-018-0293-5 (2018).
164 Hvichia, G. E. *et al.* A novel microfluidic platform for size and deformability based separation and the subsequent molecular characterization of viable

circulating tumor cells. *Int J Cancer* **138**, 2894-2904, doi:10.1002/ijc.30007 (2016).
165 Cohen, E. N. *et al.* Antigen-agnostic microfluidics-based circulating tumor cell enrichment and downstream molecular characterization. *PLoS One* **15**, e0241123, doi:10.1371/journal.pone.0241123 (2020).
166 Hosokawa, M. *et al.* Size-based isolation of circulating tumor cells in lung cancer patients using a microcavity array system. *PLoS One* **8**, e67466, doi:10.1371/journal.pone.0067466 (2013).
167 Negishi, R. *et al.* Development of the automated circulating tumor cell recovery system with microcavity array. *Biosens Bioelectron* **67**, 438-442, doi:10.1016/j.bios.2014.09.002 (2015).
168 Cohen, E. N. *et al.* Enumeration and molecular characterization of circulating tumor cells enriched by microcavity array from stage III non-small cell lung cancer patients. *Transl Lung Cancer Res* **9**, 1974-1985, doi:10.21037/tlcr-20-841 (2020).
169 Huang, L. R., Cox, E. C., Austin, R. H. & Sturm, J. C. Continuous particle separation through deterministic lateral displacement. *Science* **304**, 987-990, doi:10.1126/science.1094567 (2004).
170 McGrath, J., Jimenez, M. & Bridle, H. Deterministic lateral displacement for particle separation: a review. *Lab Chip* **14**, 4139-4158, doi:10.1039/c4lc00939h (2014).
171 Ranjan, S., Zeming, K. K., Jureen, R., Fisher, D. & Zhang, Y. DLD pillar shape design for efficient separation of spherical and non-spherical bioparticles. *Lab Chip* **14**, 4250-4262, doi:10.1039/c4lc00578c (2014).
172 Salafi, T., Zhang, Y. & Zhang, Y. A Review on Deterministic Lateral Displacement for Particle Separation and Detection. *Nanomicro Lett* **11**, 77, doi:10.1007/s40820-019-0308-7 (2019).
173 Beech, J. P., Jönsson, P. & Tegenfeldt, J. O. Tipping the balance of deterministic lateral displacement devices using dielectrophoresis. *Lab Chip* **9**, 2698-2706, doi:10.1039/b823275j (2009).
174 Au, S. H. *et al.* Microfluidic Isolation of Circulating Tumor Cell Clusters by Size and Asymmetry. *Sci Rep* **7**, 2433, doi:10.1038/s41598-017-01150-3 (2017).
175 Xavier, M. *et al.* Label-free enrichment of primary human skeletal progenitor cells using deterministic lateral displacement. *Lab Chip* **19**, 513-523, doi:10.1039/c8lc01154k (2019).

176 Liu, Z. *et al.* Integrated Microfluidic Chip for Efficient Isolation and Deformability Analysis of Circulating Tumor Cells. *Advanced Biosystems* **2**, 1800200, doi:https://doi.org/10.1002/adbi.201800200 (2018).
177 Tan, F., Wang, T., Wang, H. & Zheng, Y. Microfluidic techniques for tumor cell detection. *Electrophoresis*, doi:10.1002/elps.201800413 (2018).
178 Karthick, S., Pradeep, P. N., Kanchana, P. & Sen, A. K. Acoustic impedance-based size-independent isolation of circulating tumour cells from blood using acoustophoresis. *Lab Chip* **18**, 3802-3813, doi:10.1039/c8lc00921j (2018).
179 Li, P. *et al.* Acoustic separation of circulating tumor cells. *Proc Natl Acad Sci U S A* **112**, 4970-4975, doi:10.1073/pnas.1504484112 (2015).
180 Undvall Anand, E. *et al.* Two-Step Acoustophoresis Separation of Live Tumor Cells from Whole Blood. *Anal Chem* **93**, 17076-17085, doi:10.1021/acs.analchem.1c04050 (2021).
181 Augustsson, P., Magnusson, C., Nordin, M., Lilja, H. & Laurell, T. Microfluidic, label-free enrichment of prostate cancer cells in blood based on acoustophoresis. *Anal Chem* **84**, 7954-7962, doi:10.1021/ac301723s (2012).
182 Antfolk, M., Antfolk, C., Lilja, H., Laurell, T. & Augustsson, P. A single inlet two-stage acoustophoresis chip enabling tumor cell enrichment from white blood cells. *Lab Chip* **15**, 2102-2109, doi:10.1039/c5lc00078e (2015).
183 Laurell, T., Petersson, F. & Nilsson, A. Chip integrated strategies for acoustic separation and manipulation of cells and particles. *Chem Soc Rev* **36**, 492-506, doi:10.1039/b601326k (2007).
184 Ohlsson, P. *et al.* Integrated Acoustic Separation, Enrichment, and Microchip Polymerase Chain Reaction Detection of Bacteria from Blood for Rapid Sepsis Diagnostics. *Anal Chem* **88**, 9403-9411, doi:10.1021/acs.analchem.6b00323 (2016).
185 Wu, M. *et al.* High-throughput cell focusing and separation via acoustofluidic tweezers. *Lab Chip* **18**, 3003-3010, doi:10.1039/c8lc00434j (2018).
186 Urbansky, A., Olm, F., Scheding, S., Laurell, T. & Lenshof, A. Label-free separation of leukocyte subpopulations using high throughput multiplex acoustophoresis. *Lab Chip* **19**, 1406-1416, doi:10.1039/c9lc00181f (2019).
187 Ding, X. *et al.* Cell separation using tilted-angle standing surface acoustic waves. *Proc Natl Acad Sci U S A* **111**, 12992-12997, doi:10.1073/pnas.1413325111 (2014).

188 Alnaimat, F., Dagher, S., Mathew, B., Hilal-Alnqbi, A. & Khashan, S. Microfluidics Based Magnetophoresis: A Review. *Chem Rec* **18**, 1596-1612, doi:10.1002/tcr.201800018 (2018).
189 Munaz, A., Shiddiky, M. J. A. & Nguyen, N. T. Recent advances and current challenges in magnetophoresis based micro magnetofluidics. *Biomicrofluidics* **12**, 031501, doi:10.1063/1.5035388 (2018).
190 Xuan, X. Recent Advances in Continuous-Flow Particle Manipulations Using Magnetic Fluids. *Micromachines (Basel)* **10**, doi:10.3390/mi10110744 (2019).
191 Zhao, W., Cheng, R., Miller, J. R. & Mao, L. Label-Free Microfluidic Manipulation of Particles and Cells in Magnetic Liquids. *Adv Funct Mater* **26**, 3916-3932, doi:10.1002/adfm.201504178 (2016).
192 Zhao, W. *et al.* Label-free ferrohydrodynamic cell separation of circulating tumor cells. *Lab Chip* **17**, 3097-3111, doi:10.1039/c7lc00680b (2017).
193 Di Carlo, D. Inertial microfluidics. *Lab Chip* **9**, 3038-3046, doi:10.1039/b912547g (2009).
194 Kuntaegowdanahalli, S. S., Bhagat, A. A., Kumar, G. & Papautsky, I. Inertial microfluidics for continuous particle separation in spiral microchannels. *Lab Chip* **9**, 2973-2980, doi:10.1039/b908271a (2009).
195 Silberberg, G. S. A. Radial particle displacement in poiseuille flow of suspensions. *Nature* **189**, 209-210 (1961).
196 Huang, D., Man, J., Jiang, D., Zhao, J. & Xiang, N. Inertial microfluidics: Recent advances. *Electrophoresis*, doi:10.1002/elps.202000134 (2020).
197 Zhang, J. *et al.* Fundamentals and applications of inertial microfluidics: a review. *Lab Chip* **16**, 10-34, doi:10.1039/c5lc01159k (2016).
198 Zhou, Z. *et al.* Inertial microfluidics for high-throughput cell analysis and detection: a review. *Analyst* **146**, 6064-6083, doi:10.1039/d1an00983d (2021).
199 Nivedita, N. & Papautsky, I. Continuous separation of blood cells in spiral microfluidic devices. *Biomicrofluidics* **7**, 54101, doi:10.1063/1.4819275 (2013).
200 Huang, D. *et al.* Rapid separation of human breast cancer cells from blood using a simple spiral channel device. *Analytical Methods* **8**, 5940-5948, doi:10.1039/C6AY01077F (2016).

201 Sun, J. *et al.* Double spiral microchannel for label-free tumor cell separation and enrichment. *Lab on a Chip* **12**, 3952-3960, doi:10.1039/C2LC40679A (2012).
202 Warkiani, M. E. *et al.* Slanted spiral microfluidics for the ultra-fast, label-free isolation of circulating tumor cells. *Lab Chip* **14**, 128-137, doi:10.1039/c3lc50617g (2014).
203 Warkiani, M. E. *et al.* Ultra-fast, label-free isolation of circulating tumor cells from blood using spiral microfluidics. *Nat Protoc* **11**, 134-148, doi:10.1038/nprot.2016.003 (2016).
204 Di Carlo, D., Irimia, D., Tompkins, R. G. & Toner, M. Continuous inertial focusing, ordering, and separation of particles in microchannels. *Proc Natl Acad Sci U S A* **104**, 18892-18897, doi:10.1073/pnas.0704958104 (2007).
205 Wang, L. & Dandy, D. S. High-Throughput Inertial Focusing of Micrometer- and Sub-Micrometer-Sized Particles Separation. *Adv Sci (Weinh)* **4**, 1700153, doi:10.1002/advs.201700153 (2017).
206 Zhang, J. *et al.* Inertial particle separation by differential equilibrium positions in a symmetrical serpentine micro-channel. *Sci Rep* **4**, 4527, doi:10.1038/srep04527 (2014).
207 Renier, C. *et al.* Label-free isolation of prostate circulating tumor cells using Vortex microfluidic technology. *NPJ Precis Oncol* **1**, 15, doi:10.1038/s41698-017-0015-0 (2017).
208 Wang, X., Zhou, J. & Papautsky, I. Vortex-aided inertial microfluidic device for continuous particle separation with high size-selectivity, efficiency, and purity. *Biomicrofluidics* **7**, 44119, doi:10.1063/1.4818906 (2013).
209 Xiang, N. *et al.* Fundamentals of elasto-inertial particle focusing in curved microfluidic channels. *Lab on a Chip* **16**, 2626-2635, doi:10.1039/c6lc00376a (2016).
210 Yang, S., Kim, J. Y., Lee, S. J., Lee, S. S. & Kim, J. M. Sheathless elasto-inertial particle focusing and continuous separation in a straight rectangular microchannel. *Lab Chip* **11**, 266-273, doi:10.1039/c0lc00102c (2011).
211 Lee, D. J., Brenner, H., Youn, J. R. & Song, Y. S. Multiplex particle focusing via hydrodynamic force in viscoelastic fluids. *Sci Rep* **3**, 3258, doi:10.1038/srep03258 (2013).

212 Song, H. Y., Lee, S. H., Salehiyan, R. & Hyun, K. Relationship between particle focusing and dimensionless numbers in elasto-inertial focusing. *Rheologica Acta* **55**, 889-900, doi:10.1007/s00397-016-0962-3 (2016).
213 Xiang, N. *et al.* Fundamentals of elasto-inertial particle focusing in curved microfluidic channels. *Lab Chip* **16**, 2626-2635, doi:10.1039/c6lc00376a (2016).
214 Kumar, T. *et al.* High throughput viscoelastic particle focusing and separation in spiral microchannels. *Sci Rep* **11**, 8467, doi:10.1038/s41598-021-88047-4 (2021).
215 Yuan, D. *et al.* Recent progress of particle migration in viscoelastic fluids. *Lab Chip* **18**, 551-567, doi:10.1039/c7lc01076a (2018).
216 Zhang, J. *et al.* Three-dimensional particle focusing under viscoelastic flow based on dean-flow-coupled elasto-inertial effects. *SEVENTH INTERNATIONAL SYMPOSIUM ON PRECISION MECHANICAL MEASUREMENTS* **9903**, 99030K, doi:10.1117/12.2211265 info:doi/10.1117/12.2211265 (2016).
217 Lu, X. & Xuan, X. Elasto-Inertial Pinched Flow Fractionation for Continuous Shape-Based Particle Separation. *Anal Chem* **87**, 11523-11530, doi:10.1021/acs.analchem.5b03321 (2015).
218 Cha, S. *et al.* Hoop stress-assisted three-dimensional particle focusing under viscoelastic flow. *Rheologica Acta* **53**, 927-933, doi:10.1007/s00397-014-0808-9 (2014).
219 Yuan, D. *et al.* Dean-flow-coupled elasto-inertial three-dimensional particle focusing under viscoelastic flow in a straight channel with asymmetrical expansion-contraction cavity arrays. *Biomicrofluidics* **9**, 044108, doi:10.1063/1.4927494 (2015).
220 Zhou, Y., Ma, Z. & Ai, Y. Dynamically tunable elasto-inertial particle focusing and sorting in microfluidics. *Lab Chip* **20**, 568-581, doi:10.1039/c9lc01071h (2020).
221 Murlidhar, V., Rivera-Báez, L. & Nagrath, S. Affinity Versus Label-Free Isolation of Circulating Tumor Cells: Who Wins? *Small* **12**, 4450-4463, doi:10.1002/smll.201601394 (2016).
222 Hu, X., Zang, X. & Lv, Y. Detection of circulating tumor cells: Advances and critical concerns. *Oncol Lett* **21**, 422, doi:10.3892/ol.2021.12683 (2021).

223 Shahneh, F. Z. Sensitive antibody-based CTCs detection from peripheral blood. *Hum Antibodies* **22**, 51-54, doi:10.3233/hab-130270 (2013).
224 Liu, Z. *et al.* Negative enrichment by immunomagnetic nanobeads for unbiased characterization of circulating tumor cells from peripheral blood of cancer patients. *J Transl Med* **9**, 70, doi:10.1186/1479-5876-9-70 (2011).
225 Königsberg, R. *et al.* Detection of EpCAM positive and negative circulating tumor cells in metastatic breast cancer patients. *Acta Oncol* **50**, 700-710, doi:10.3109/0284186x.2010.549151 (2011).
226 Deng, G. *et al.* Enrichment with anti-cytokeratin alone or combined with anti-EpCAM antibodies significantly increases the sensitivity for circulating tumor cell detection in metastatic breast cancer patients. *Breast Cancer Res* **10**, R69, doi:10.1186/bcr2131 (2008).
227 Alix-Panabières, C. & Pantel, K. Technologies for detection of circulating tumor cells: facts and vision. *Lab Chip* **14**, 57-62, doi:10.1039/c3lc50644d (2014).
228 Ao, Z., Cote, R. J. & Datar, R. H. in *Circulating Tumor Cells* (eds Richard J. Cote & Ram H. Datar) 17-28 (Springer New York, 2016).
229 Rostami, P. *et al.* Novel approaches in cancer management with circulating tumor cell clusters. *Journal of Science: Advanced Materials and Devices* **4**, 1-18, doi:https://doi.org/10.1016/j.jsamd.2019.01.006 (2019).
230 Talasaz, A. H. *et al.* Isolating highly enriched populations of circulating epithelial cells and other rare cells from blood using a magnetic sweeper device. *Proc Natl Acad Sci U S A* **106**, 3970-3975, doi:10.1073/pnas.0813188106 (2009).
231 Yoon, H. J. *et al.* Sensitive capture of circulating tumour cells by functionalized graphene oxide nanosheets. *Nature Nanotechnology* **8**, 735-741, doi:10.1038/nnano.2013.194 (2013).
232 Park, M. H. *et al.* Enhanced Isolation and Release of Circulating Tumor Cells Using Nanoparticle Binding and Ligand Exchange in a Microfluidic Chip. *J Am Chem Soc* **139**, 2741-2749, doi:10.1021/jacs.6b12236 (2017).
233 Karabacak, N. M. *et al.* Microfluidic, marker-free isolation of circulating tumor cells from blood samples. *Nature Protocols* **9**, 694-710, doi:10.1038/nprot.2014.044 (2014).

234 Stott, S. L. *et al.* Isolation of circulating tumor cells using a microvortex-generating herringbone-chip. *Proc Natl Acad Sci U S A* **107**, 18392-18397, doi:10.1073/pnas.1012539107 (2010).
235 Ozkumur, E. *et al.* Inertial focusing for tumor antigen-dependent and -independent sorting of rare circulating tumor cells. *Sci Transl Med* **5**, 179ra147, doi:10.1126/scitranslmed.3005616 (2013).
236 Saucedo-Zeni, N. *et al.* A novel method for the in vivo isolation of circulating tumor cells from peripheral blood of cancer patients using a functionalized and structured medical wire. *Int J Oncol* **41**, 1241-1250, doi:10.3892/ijo.2012.1557 (2012).
237 Yoon, H. J. *et al.* Tunable Thermal-Sensitive Polymer-Graphene Oxide Composite for Efficient Capture and Release of Viable Circulating Tumor Cells. *Adv Mater* **28**, 4891-4897, doi:10.1002/adma.201600658 (2016).
238 Pattanayak, P. *et al.* Microfluidic chips: recent advances, critical strategies in design, applications and future perspectives. *Microfluid Nanofluidics* **25**, 99, doi:10.1007/s10404-021-02502-2 (2021).
239 Wang, T., Chen, J., Zhou, T. & Song, L. Fabricating Microstructures on Glass for Microfluidic Chips by Glass Molding Process. *Micromachines (Basel)* **9**, doi:10.3390/mi9060269 (2018).
240 Gao, K., Liu, J., Fan, Y. & Zhang, Y. Ultra-low-cost fabrication of polymer-based microfluidic devices with diode laser ablation. *Biomed Microdevices* **21**, 83, doi:10.1007/s10544-019-0433-6 (2019).
241 Nielsen, J. B. *et al.* Microfluidics: Innovations in Materials and Their Fabrication and Functionalization. *Anal Chem* **92**, 150-168, doi:10.1021/acs.analchem.9b04986 (2020).
242 Yuen, P. K. & Goral, V. N. Low-Cost Rapid Prototyping of Whole-Glass Microfluidic Devices. *Journal of Chemical Education* **89**, 1288-1292, doi:10.1021/ed3000292 (2012).
243 Duffy, D. C., McDonald, J. C., Schueller, O. J. & Whitesides, G. M. Rapid Prototyping of Microfluidic Systems in Poly(dimethylsiloxane). *Anal Chem* **70**, 4974-4984, doi:10.1021/ac980656z (1998).
244 McDonald, J. C. *et al.* Fabrication of microfluidic systems in poly(dimethylsiloxane). *Electrophoresis* **21**, 27-40, doi:10.1002/(sici)1522-2683(20000101)21:1<27::Aid-elps27>3.0.Co;2-c (2000).

245 Sia, S. K. & Whitesides, G. M. Microfluidic devices fabricated in poly(dimethylsiloxane) for biological studies. *Electrophoresis* **24**, 3563-3576, doi:10.1002/elps.200305584 (2003).
246 Ariati, R., Sales, F., Souza, A., Lima, R. A. & Ribeiro, J. Polydimethylsiloxane Composites Characterization and Its Applications: A Review. *Polymers (Basel)* **13**, doi:10.3390/polym13234258 (2021).
247 Kuncová-Kallio, J. & Kallio, P. J. PDMS and its suitability for analytical microfluidic devices. *Conf Proc IEEE Eng Med Biol Soc* **2006**, 2486-2489, doi:10.1109/iembs.2006.260465 (2006).
248 Zhou, J., Ellis, A. V. & Voelcker, N. H. Recent developments in PDMS surface modification for microfluidic devices. *Electrophoresis* **31**, 2-16, doi:10.1002/elps.200900475 (2010).
249 Zhou, J., Khodakov, D. A., Ellis, A. V. & Voelcker, N. H. Surface modification for PDMS-based microfluidic devices. *Electrophoresis* **33**, 89-104, doi:10.1002/elps.201100482 (2012).
250 Makamba, H., Kim, J. H., Lim, K., Park, N. & Hahn, J. H. Surface modification of poly(dimethylsiloxane) microchannels. *Electrophoresis* **24**, 3607-3619, doi:10.1002/elps.200305627 (2003).
251 Pinto, S. *et al.* Poly(dimethyl siloxane) surface modification by low pressure plasma to improve its characteristics towards biomedical applications. *Colloids Surf B Biointerfaces* **81**, 20-26, doi:10.1016/j.colsurfb.2010.06.014 (2010).
252 Kim, S. C., Sukovich, D. J. & Abate, A. R. Patterning microfluidic device wettability with spatially-controlled plasma oxidation. *Lab Chip* **15**, 3163-3169, doi:10.1039/c5lc00626k (2015).
253 Zhou, J., Ellis, A. V. & Voelcker, N. H. Poly(dimethylsiloxane) surface modification by plasma treatment for DNA hybridization applications. *J Nanosci Nanotechnol* **10**, 7266-7270, doi:10.1166/jnn.2010.2826 (2010).
254 Kaneda, S. *et al.* Modification of the glass surface property in PDMS-glass hybrid microfluidic devices. *Anal Sci* **28**, 39-44, doi:10.2116/analsci.28.39 (2012).
255 Waters, L. J., Finch, C. V., Bhuiyan, A., Hemming, K. & Mitchell, J. C. Effect of plasma surface treatment of poly(dimethylsiloxane) on the permeation of pharmaceutical compounds. *J Pharm Anal* **7**, 338-342, doi:10.1016/j.jpha.2017.05.003 (2017).

256 Borók, A., Laboda, K. & Bonyár, A. PDMS Bonding Technologies for Microfluidic Applications: A Review. *Biosensors (Basel)* **11**, doi:10.3390/bios11080292 (2021).
257 Efimenko, K., Wallace, W. E. & Genzer, J. Surface modification of Sylgard-184 poly(dimethyl siloxane) networks by ultraviolet and ultraviolet/ozone treatment. *J Colloid Interface Sci* **254**, 306-315, doi:10.1006/jcis.2002.8594 (2002).
258 Fu, Y. J. *et al.* Effect of UV-ozone treatment on poly(dimethylsiloxane) membranes: surface characterization and gas separation performance. *Langmuir* **26**, 4392-4399, doi:10.1021/la903445x (2010).
259 Zargar, R., Nourmohammadi, J. & Amoabediny, G. Preparation, characterization, and silanization of 3D microporous PDMS structure with properly sized pores for endothelial cell culture. *Biotechnol Appl Biochem* **63**, 190-199, doi:10.1002/bab.1371 (2016).
260 Ahangaran, F. & Navarchian, A. H. Recent advances in chemical surface modification of metal oxide nanoparticles with silane coupling agents: A review. *Adv Colloid Interface Sci* **286**, 102298, doi:10.1016/j.cis.2020.102298 (2020).
261 Lu, Y. T. *et al.* NanoVelcro Chip for CTC enumeration in prostate cancer patients. *Methods* **64**, 144-152, doi:10.1016/j.ymeth.2013.06.019 (2013).
262 Diéguez, L., Winter, M. A., Pocock, K. J., Bremmell, K. E. & Thierry, B. Efficient microfluidic negative enrichment of circulating tumor cells in blood using roughened PDMS. *Analyst* **140**, 3565-3572, doi:10.1039/c4an01768d (2015).
263 Cui, H. *et al.* ZnO nanowire-integrated bio-microchips for specific capture and non-destructive release of circulating tumor cells. *Nanoscale* **12**, 1455-1463, doi:10.1039/c9nr07349c (2020).
264 Lin, M. *et al.* Nanostructure embedded microchips for detection, isolation, and characterization of circulating tumor cells. *Acc Chem Res* **47**, 2941-2950, doi:10.1021/ar5001617 (2014).
265 Chen, W. *et al.* Nanoroughened adhesion-based capture of circulating tumor cells with heterogeneous expression and metastatic characteristics. *BMC Cancer* **16**, 614, doi:10.1186/s12885-016-2638-x (2016).

266 Zhao, M. *et al.* State-of-the-art nanotechnologies for the detection, recovery, analysis and elimination of liquid biopsy components in cancer. *Nano Today* **42**, 101361, doi:https://doi.org/10.1016/j.nantod.2021.101361 (2022).
267 Ariga, K., Ahn, E., Park, M. & Kim, B. S. Layer-by-Layer Assembly: Recent Progress from Layered Assemblies to Layered Nanoarchitectonics. *Chem Asian J* **14**, 2553-2566, doi:10.1002/asia.201900627 (2019).
268 Petrila, L. M., Bucatariu, F., Mihai, M. & Teodosiu, C. Polyelectrolyte Multilayers: An Overview on Fabrication, Properties, and Biomedical and Environmental Applications. *Materials (Basel)* **14**, doi:10.3390/ma14154152 (2021).
269 Das, B. P. & Tsianou, M. From polyelectrolyte complexes to polyelectrolyte multilayers: Electrostatic assembly, nanostructure, dynamics, and functional properties. *Adv Colloid Interface Sci* **244**, 71-89, doi:10.1016/j.cis.2016.12.004 (2017).
270 Wu, T. & Farnood, R. Cellulose fibre networks reinforced with carboxymethyl cellulose/chitosan complex layer-by-layer. *Carbohydr Polym* **114**, 500-505, doi:10.1016/j.carbpol.2014.08.053 (2014).
271 Tong, W., Song, X. & Gao, C. Layer-by-layer assembly of microcapsules and their biomedical applications. *Chem Soc Rev* **41**, 6103-6124, doi:10.1039/c2cs35088b (2012).
272 Eivazi, A., Medronho, B., Lindman, B. & Norgren, M. On the Development of All-Cellulose Capsules by Vesicle-Templated Layer-by-Layer Assembly. *Polymers (Basel)* **13**, doi:10.3390/polym13040589 (2021).
273 Schmolke, H. *et al.* Polyelectrolyte multilayer surface functionalization of poly(dimethylsiloxane) (PDMS) for reduction of yeast cell adhesion in microfluidic devices. *Biomicrofluidics* **4**, 44113, doi:10.1063/1.3523059 (2010).
274 Sung, W. C., Chen, H. H., Makamba, H. & Chen, S. H. Functionalized 3D-hydrogel plugs covalently patterned inside hydrophilic poly(dimethylsiloxane) microchannels for flow-through immunoassays. *Anal Chem* **81**, 7967-7973, doi:10.1021/ac901138w (2009).
275 Schrott, W., Nebyla, M., Přibyl, M. & Snita, D. Detection of immunoglobulins in a laser induced fluorescence system utilizing polydimethysiloxane microchips with advanced surface and optical properties. *Biomicrofluidics* **5**, 14101, doi:10.1063/1.3553006 (2011).

276 Wang, A. J., Xu, J. J., Zhang, Q. & Chen, H. Y. The use of poly(dimethylsiloxane) surface modification with gold nanoparticles for the microchip electrophoresis. *Talanta* **69**, 210-215, doi:10.1016/j.talanta.2005.09.029 (2006).
277 Xiao, J. *et al.* PDMS micropillar-based microchip for efficient cancer cell capture. *RSC Advances* **5**, 52161-52166, doi:10.1039/C5RA04353K (2015).
278 Li, W. *et al.* Biodegradable nano-films for capture and non-invasive release of circulating tumor cells. *Biomaterials* **65**, 93-102, doi:10.1016/j.biomaterials.2015.06.036 (2015).
279 Reátegui, E. *et al.* Tunable nanostructured coating for the capture and selective release of viable circulating tumor cells. *Adv Mater* **27**, 1593-1599, doi:10.1002/adma.201404677 (2015).
280 Dai, L. & Si, C. Recent Advances on Cellulose-Based Nano-Drug Delivery Systems: Design of Prodrugs and Nanoparticles. *Curr Med Chem* **26**, 2410-2429, doi:10.2174/0929867324666170711131353 (2019).
281 Ahmed, J., Gultekinoglu, M. & Edirisinghe, M. Bacterial cellulose micro-nano fibres for wound healing applications. *Biotechnol Adv* **41**, 107549, doi:10.1016/j.biotechadv.2020.107549 (2020).
282 Chang, M. *et al.* Cellulose-based Biosensor for Bio-molecules Detection in Medical Diagnosis: A Mini-Review. *Curr Med Chem* **27**, 4593-4612, doi:10.2174/0929867327666200221145543 (2020).
283 Kamel, S. & T, A. K. Recent Advances in Cellulose-Based Biosensors for Medical Diagnosis. *Biosensors (Basel)* **10**, doi:10.3390/bios10060067 (2020).
284 Patil, T. V. *et al.* Nanocellulose, a versatile platform: From the delivery of active molecules to tissue engineering applications. *Bioact Mater* **9**, 566-589, doi:10.1016/j.bioactmat.2021.07.006 (2022).
285 Sun, B. *et al.* Applications of Cellulose-based Materials in Sustained Drug Delivery Systems. *Curr Med Chem* **26**, 2485-2501, doi:10.2174/0929867324666170705143308 (2019).
286 Alven, S. & Aderibigbe, B. A. Chitosan and Cellulose-Based Hydrogels for Wound Management. *Int J Mol Sci* **21**, doi:10.3390/ijms21249656 (2020).
287 He, W. *et al.* Bacterial Cellulose: Functional Modification and Wound Healing Applications. *Adv Wound Care (New Rochelle)* **10**, 623-640, doi:10.1089/wound.2020.1219 (2021).

288 Du, H. *et al.* Cellulose nanocrystals and cellulose nanofibrils based hydrogels for biomedical applications. *Carbohydr Polym* **209**, 130-144, doi:10.1016/j.carbpol.2019.01.020 (2019).
289 Pandey, A. Pharmaceutical and biomedical applications of cellulose nanofibers: a review. *Environmental Chemistry Letters* **19**, 2043-2055, doi:10.1007/s10311-021-01182-2 (2021).
290 Nagarajan, K. J. *et al.* A comprehensive review on cellulose nanocrystals and cellulose nanofibers: Pretreatment, preparation, and characterization. *Polymer Composites* **42**, 1588-1630, doi:https://doi.org/10.1002/pc.25929 (2021).
291 Kumar, T. *et al.* Multi-layer assembly of cellulose nanofibrils in a microfluidic device for the selective capture and release of viable tumor cells from whole blood. *Nanoscale* **12**, 21788-21797, doi:10.1039/d0nr05375a (2020).

Paper Reprints